NASA CR 72807
AMS 963

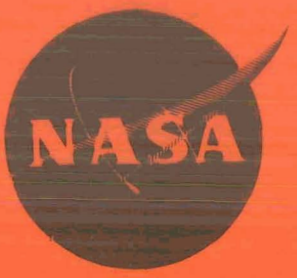

Fluid Mechanics Approach To Acoustic Liner Design

by

T. S. Tonon, W. A. Sirignano
and D. T. Harrje

PRINCETON UNIVERSITY

prepared for

NATIONAL AERONAUTICS AND SPACE ADMINISTRATION

NASA Lewis Research Center
Grant NGL 31-001-155
Marcus Heidmann, Project Manager
Chemical Rockets Division

Requests for copies of this report should be referred to

National Aeronautics and Space Administration
Office of Scientific and Technical Information
Attention: AFSS-A
Washington, D.C. 20546

NASA CR 72807
AMS 963

FLUID MECHANICS APPROACH TO ACOUSTIC LINER DESIGN

by

T. S. Tonon, W. A. Sirignano
and D. T. Harrje

PRINCETON UNIVERSITY
DEPARTMENT OF AEROSPACE AND MECHANICAL SCIENCES
Princeton, New Jersey 08540

prepared for

NATIONAL AERONAUTICS AND SPACE ADMINISTRATION

December, 1970

GRANT NGL 31-001-155

NASA Lewis Research Center
Cleveland, Ohio
Marcus Heidmann, Project Manager
Chemical Rockets Division

ABSTRACT

The purpose of this report is to serve as a working guide in the construction of acoustic liners for the suppression of combustion instability in liquid propellant rocket motors with chamber geometries most often occurring in practice. The geometry of the liners may consist of Helmholtz resonators, quarter-wave (or some multiple) tubes, or half-wave (or some multiple) tubes. Certain optional design procedures are developed - optional in the sense that the space occupied by the liner is minimized, subject to various constraints. A method for the evaluation of the stabilizing effectiveness of a given design is also presented. Among the effects considered in these procedures are the following: high amplitude chamber pressure oscillations, both mean and oscillatory chamber flows, a liner-mean-through flow, a flow in the liner backing volume (for Helmholtz geometries), and differences between the mean temperatures, molecular weights, and ratio of specific heats between the liner backing volume and the local environment in the combustion chamber (again for Helmholtz geometries).

TABLE OF CONTENTS

NOMENCLATURE

A	= orifice cross-sectional area (dimensional)
A_j	= constant depending upon j, defined by Eq. (2.3-11)
$A_{m,n}$	= constants defined in Appendix B
A_w	= chamber wall area (dimensional)
a	= defined by Eq. (2.1-2)
B	= constant
B^*	= defined by Eq. (3.2-12)
$B_{m,n}$	= constants defined in Appendix B
C	= constant
C_D	= coefficient of discharge for the orifice
C_d	= drag coefficient
$\overline{C}_p$	= average jet pressure coefficient
C_1, C_2	= design coefficients accounting for environmental factors. See paragraph after Eq. (3.2-12)
c	= speed of sound (dimensional)
c_v	= specific heat at constant volume (dimensional)
D	= orifice diameter (dimensional)
d_L	= diameter of a spherical liquid drop (dimensional)
$\mathcal{E}$	= nozzle admittance (non-dimensional)
e	= defined by Eq. (2.1-7)
$F(x)$	= function defined by Eq. (3.2-11)
F_i	= constants defined in Appendix B
f	= instability frequency (dimensional)

f_L = fraction of chamber wall area occupied by a partial liner

G = constant defined by Eq. (3.2-13)

g = defined by Eq. (2.1-7)

h = chamber height for rectangular combustors (non-dimensional), also enthalpy (dimensional)

J_ν = standardized Bessel function of the first kind

J_1, J_2 = constants defined in Appendix B

j = integer that gives longitudinal character of stability mode

k = droplet drag parameter (non-dimensional)

$\mathfrak{k}$ = constant defined by Eq. (B-30)

$\mathfrak{k}'$ = constant defined by Eq. (A-19) or Eq. (A-39)

L = orifice length (dimensional)

$\mathfrak{L}$ = liner admittance coefficient (non-dimensional)

ℓ = integer

M = defined by Eq. (2.2-5)

$\overline{M}$ = chamber steady flow Mach number

$\mathfrak{m}$ = molecular weight (dimensional)

m* = see Eq. (A-10)

m = mass flux (dimensional)

N = defined by Eq. (2.2-5)

n = interaction index (non-dimensional)

n* = see (Eq. (A-11)

O = symbol for "of the order of"

P = amplitude coefficient

p = pressure (non-dimensional, or dimensional where noted)

Q = amplitude coefficient

R = defined by Eq. (2.2-11)

R_e = Reynolds number

r = radial distance in chamber (non-dimensional)

r_i = inner chamber radius for annular-cylindrical chamber (non-dimensional)

r_I = chamber radius at the injector for conical chamber (non-dimensional)

r_o = chamber radius for circular-cylindrical chamber, or outer chamber radius for annular-cylindrical chambers (dimensional)

S = surface of integration

$S^*_{\nu\eta}$ = eigenvalue describing instability mode. See Tables (A-1, 2)

s = non-dimensional distance from pressure anti-node

T = temperature (dimensional)

t = time (non-dimensional)

U = gas velocity (non-dimensional)

U_L = mass-averaged liquid velocity (non-dimensional)

u = orifice gas velocity (non-dimensional), or chamber velocity in Appendix A (dimensional)

V = cavity volume for Helmholtz resonators (dimensional), or volume of integration

v = chamber velocity in Appendix A (dimensional)

w = chamber width (dimensional), or chamber velocity in Appendix A (dimensional)

X = length of combustion or chamber length, whichever is smaller (non-dimensional)

x = distance from injector along chamber axis (non-dimensional)

x_e = chamber length to nozzle contraction section (non-dimensional)

Y_ν = standardized Bessel function of the second kind

y = distance along chamber width for rectangular chambers (non-dimensional)

z = distance along chamber height for rectangular chambers (non-dimensional)

α = growth coefficient for acoustic disturbances

$\bar{\alpha}$ = $(\bar{P}_{II}\ \bar{\rho}_I/\bar{P}_I\ \bar{\rho}_{II} - 1)/\epsilon$

α_m = constants defined in Appendix B

β = parameter AL/V

β_m = constants defined in Appendix B

γ = ratio of specific heats

$\Delta\tau_1$, $\Delta\tau_2$ = particle transit times within orifice. Important only when $\bar{u} \neq 0$. (non-dimensional)

δ_j = defined by Eq. (3.2-14)

δ_L = density of a liquid droplet

δ_m = constants defined in Appendix B

ϵ = square-root of the non-dimensional chamber pressure oscillations

ζ = ratio of the chamber height to the chamber width for rectangular chambers

η = integer giving the radial character of the mode. See Tables (A-1, 2)

$\bar{\eta}_T$ = $(\bar{T}_{II}/\bar{T}_I - 1)/\epsilon$

θ = circumferential angle for cylindrical chambers

$\varkappa$ = parameter $(A\lambda/V)$

$\varkappa_1$ = defined by Eq. (2.3-17) (non-dimensional)

$\varkappa_2$ = defined by Eq. (2.3-18) (non-dimensional)

λ = wavelength (dimensional)

λ' = defined by Eq. (2.3-3), (2.3-6), or (2.3-8) (non-dimensional)

λ^* = defined by Eq. (2.3-2), (2.3-5), or (2.3-7) (non-dimensional)

μ = gas viscosity (dimensional)

ν = integer describing tangential character of mode. See Tables (A-1, 2)

ξ = ratio of r_i/r_o for annular-cylindrical chambers

ρ = density (non-dimensional or dimensional where noted)

ρ_L = liquid concentration in chamber (non-dimensional)

σ = percent open area ratio of actual (partial) liner

σ_f = percent oper area ratio of a full liner

τ^* = sensitive time lag (dimensional)

φ_m^n = constants defined in Appendix B

ψ = angle between direction of $\vec{\vec{U}}_I$ and $\vec{U}'_I$

$\psi_{\nu\eta}$ = function defined by Eqs. (A-29a or b)

Π_n = defined by Eq. (2.2-17)

Π_λ = defined by Eq. (2.2-14)

ω = 2π L/λ, ω^* = $2\pi f$

Subscripts

a = spatially averaged value

e = value at start of nozzle contraction section

f = denotes full liner

I = value at injecter, or imaginary part

in = component in phase with chamber pressure

ℓ = value in a region local to the liner surface

L = denotes liquid

m = integer

n = integer, or value at neutral point (M = 0)

out = component out of phase with chamber pressure

p = denotes partial liner

λ = resonant value

R = real part

0 = zeroth-order (mean) quantity

1 = first-order quantity

2 = second-order quantity

3 = third-order quantity

I = chamber value

II = value in cavity volume V

Superscripts

asterisk = dimensional value

arrow = vector quantity

bar = steady-state value

prime = perturbation, or oscillatory quantity

CHAPTER 1

Introductory Remarks

1.1 Introduction

The purpose of this report is to aid in the design and evaluation of acoustic liners for use in the suppression of high frequency combustion instability in liquid propellant rocket engines. The basis for the methods presented here is primarily theoretical analysis.

The geometry of such liners may consist of Helmholtz resonators, quarter-wave tubes, half-wave tubes, or some multiple lengths thereof. In the underlying theory, there is no distinction among such geometries; suggestions for comparison and freedom of choice are contained in the design procedures.

Chapter 3 contains perhaps the most important information in this report. In that chapter a design procedure is presented to select the optimum liner design - optimum in the sense that the total surface area occupied by the liner is minimized. Chapter 3 is written so that it is not absolutely necessary to read any other chapter in the report. A certain minimal amount of information, that is usually readily obtainable, is sufficient to provide the basis for a rather simple design. In most instances, this approach will closely approximate the optimum design. More accurate

calculations can be performed, but some additional information is required. Except for those cases in which an accurate calculation is required to provide for a liner-mean-through flow, all calculations can be performed by hand. These exceptional calculations require the use of a computer to solve simultaneous algebraic equations. A convenient computer program is provided in Appendix D.

Chapter 4 contains certain classes of problems that are likely to occur in practice. In general, the calculations suggested in that chapter are more difficult than those of Chapter 3. It is suggested that one understand Chapter 3 before attempting calculations in Chapter 4.

Chapter 2 contains the underlying reasoning that leads to the methods contained in the succeeding chapters as well as the definitions of a number of parameters. There are at least two reasons why this chapter appears in this report. The first is to serve as a justification for the methods in Chapters 3 and 4. For these methods, it is necessary that information from various analytic studies be brought together. It was felt desirable that this amassing be performed at one location in this report. The second and perhaps more important justification is that Chapters 3 and 4 do not contain <u>all</u> the useful information that can be derived from the analytical results. It is hoped that these two chapters cover virtually all problems of practical interest, but there may

be certain isolated problems that connot be handled by these chapters. Thus, an understanding of Chapter 2 may provide useful suggestions not contained in Chapters 3 and 4.

Appendix A contains the acoustic-mode solutions for rectangular, circular-cylindrical, and annular-cylindrical geometries. It is expected that this appendix will be most useful for finding the eigenvalue (and thus frequency) and other parameters that characterize a specific instability mode. The solutions for chamber pressure and velocity are also given, but such information will be seldom necessary in practice.

Appendix B contains the definition of certain constants as well as certain auxiliary equations needed when a liner-mean-through flow is present.

Appendix C contains a study much like that appearing in Ref. (11). The results contained in this appendix are useful for the developments in Chapter 2.

Appendix D contains a computer program that solves for the liner response, given appropriate inputs. A full description of and operating instructions for the program are also included. The use of such a program will be necessary when accurate calculations involving a liner-mean-through flow are necessary, and when certain problems described in Chapter 4 need solution.

1.2 Scope and Limitations

This report is intended to aid in problems dealing with specific instability modes. In practice, it very often happens

that a chamber encounters stability problems with more than one mode. Baffles can be used to suppress some modes and acoustic liners then used for other modes. Liners may also be designed for more than one mode. Analytical results presented in Chapter 2 suggest that liners become more effective as the tangential mode number increases, as the radial mode number decreases, and as the chamber Mach number decreases. Also liners should be more effective for spontaneous instability than for triggered instability, and the distribution of combustion helps stabilize the longitudinal modes. Other suggestions of such general nature can also be found in Chapter 2. Apart from these general guidelines, the decisions to be made in the choice of the particular modes to be suppressed by a liner are outside the immediate scope of this report, although the designer can utilize this report in his decision process.

In employing the design procedures contained in this report, consideration is given to the following effects influencing liner design: chamber pressure oscillations, a chamber mean flow, chamber velocity oscillations, a liner-mean-through flow, a mean flow in the backing volume, and differences in mean temperatures, ratio of specific heats, and molecular weight between the fluid in the combustion chamber and the fluid in the liner backing volume. There are no specific restrictions placed on the steady-state operating characteristics of the chamber, and any instability mode in rectangular , circular-cylindrical, annular-cylindrical, and conical chambers can be considered.

1.3 Physical Description of Suppression

The Helmholtz geometry is depicted in Fig. (1.3-1). Such a geometry consists essentially of an orifice connecting

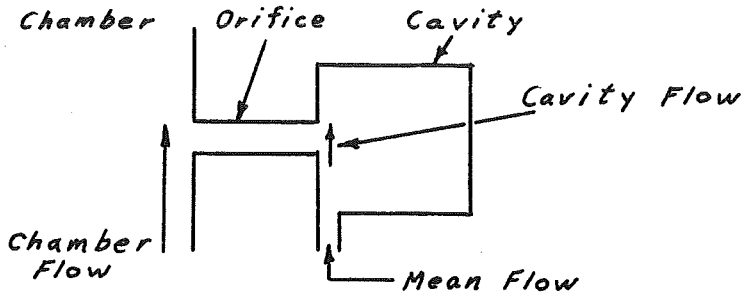

Fig. (1.3-1)

the chamber to a smaller volume called the cavity or backing volume.* Such a geometry is suitable for the discussion here; however, a more elaborate description is provided, when necessary, in a later section of this manual. The resonant-quarter-wave tube geometry occurs when the cavity volume is zero and the orifice length is one-quarter wavelength. The resonant-half-wave geometry occurs when the cavity volume is very large compared to the volume of the orifice and the orifice length is one-half wavelength.

Depicted here is a mean flow into the cavity and through the orifice, a chamber flow across one end of the orifice, and cavity flow across the other end. These are some of the effects considered in this report.

When such a geometry is in the unstable environment within a combustion chamber, oscillatory motion occurs within and near the orifice. The amplitudes are usually large enough (for a given frequency) that flow separation occurs when fluid

*In this report, the dimensionsof the cavity must be small compared to the wavelength of oscillation .

exits from the orifice; i.e., the orifice exit region is characterized by jet flow. The exit region alternates between the ends of the orifice and changes twice in one period (assuming one frequency dominates the motion). The kinetic energy in the jet is not recovered but is dissipated, and thus, such jet flow provides a mechanism by which energy from the ordered oscillations in the chamber is converted into a more random form. This is the nature of the suppression process.

The presence of a chamber flow (both mean and oscillatory), a mean cavity flow, and an orifice mean flow complicate the motion. These complications appear to be more theoretical than practical. References (1 to 5) should aid the interested reader in a more detailed understanding of the liner response and the resulting suppression mechanism.

CHAPTER 2

Design Considerations

2.1 Local Chamber Environment

In this section, we present the notation which is to represent the chamber environment in regions at or near the position of the liner (local environment). In Appendix A the acoustic mode solutions are given and these solutions are expressed in terms of the notation of this section. Thus, with the help of Appendix A, one could calculate, if necessary, the flow parameters defined here.

The local chamber static pressure is assumed in the following form:

$$P_{I\ell} \equiv P^*_{I\ell} / \bar{P}_{I\ell} \equiv 1 + \epsilon_\ell^2 \cos \omega t \qquad (2.1\text{-}1)$$

where subscript ℓ denotes local value, the symbol * denotes dimensional value, the bar denotes steady-state value, and subscript I denotes chamber conditions. Thus, ϵ_ℓ is the square root of the local nondimensional-chamber-pressure amplitude. This quantity can be further expressed by

$$\epsilon_\ell^2 \equiv a^2 \epsilon^2 \qquad (2.1\text{-}2)$$

where ϵ^2 is characteristic amplitude for the entire chamber, and a is a quantity that varies with position in the liner. These two quantities, a and ϵ, can be chosen so that

at pressure modes, $a = 0$, and at pressure antinodes $a = 1$.

The representation (2.1-1) is harmonic. In many cases, non-harmonic wave forms appear in actual chambers. It is a property of the liner that its response to certain harmonics is much greater than its response to others; the liner can be thought of as a mechanical filter. Thus, even in the presence of non-harmonic waves (e.g., shocks), the above representation is adequate in-so-far as the liner response in concerned. In such cases, one chooses ϵ_ℓ^a as the amplitude of the dominant harmonic present in the wave.

Throughout this manual, ω is defined as follows

$$\omega \equiv 2\pi L/\lambda \tag{2.1-3}$$

where L is the length of the liner orifice (thickness of the liner), and λ is the wavelength of oscillation. The non-dimensional time t is then

$$t \equiv t^* L/\bar{c}_{Ia} \tag{2.1-4}$$

where subscript a denotes an average over the chamber volume, and $\bar{c}_I$ is the steady-state speed of sound in the chamber.

The local chamber velocity is assumed in this form

$$\vec{U}_{I\ell} \equiv \vec{U}^*_{I\ell}/\bar{c}_{I\ell} \equiv \epsilon \vec{U}_{I\ell} \dotplus \epsilon \vec{U}'_{I\ell} \tag{2.1-5}$$

The symbol $\rightarrow$ denotes vector quantity and $\dotplus$ vector addition. The quantity $\vec{U}_{I\ell}$ is the steady-state mean flow and does not vary with time, but will, however, be a function of position within the chamber. $\vec{U}'_{I\ell}$ is made up of unsteady oscillations, and is a function of both time and space; furthermore,

$$| \vec{U}_{x\ell} | \equiv \bar{U}_{x\ell} \tag{2.1-6}$$

$$| \vec{U}'_{x\ell} | \equiv U'_{x\ell} \equiv e_\ell \cos \omega t + g_\ell \sin \omega t \tag{2.1-7}$$

where $| \ |$ denotes magnitude. The quantities e_ℓ and g_ℓ do not depend upon time, but may depend upon position in the chamber. Through the proper choice of these quantities, any phase difference between the chamber pressure and velocity can be considered. In particular, when $e_\ell \neq 0$ and $g_\ell = 0$, the pressure and velocity are in phase, and this corresponds to a tangential spinning mode. When $e_\ell = 0$ and $g_\ell \neq 0$, the pressure and velocity are 90° out of phase, and this corresponds to any standing mode (transverse, longitudinal, or mixed transverse-longitudinal) with no contribution from a tangential spinning factor. Any other particular values of e_ℓ and g_ℓ are permissible, although, in general, if e_ℓ and g_ℓ are both non-zero, the mode will contain both standing and (tangential) spinning contributions.

We let Ψ_ℓ represent the angle, less than or equal to 180°, between the direction of $\vec{\bar{U}}_{I\ell}$ and the direction of $\vec{U}'_{I\ell}$ when $U'_{I\ell}$, given by Eq. (2.1-7), is greater than zero (see Fig. 2.1-1).

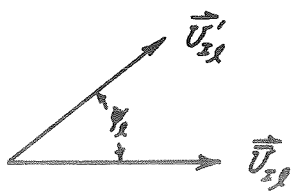

Figure 2.1-1

Thus, for purely transverse modes (tangential, radial, or mixed tangential-radial), the angle Ψ_ℓ is constant and is equal to 90°. For purely longitudinal modes, Ψ_ℓ is again constant, but is now equal to 0°. For mixed transverse-longitudinal modes, Ψ_ℓ may be a function of time.

2.2 Liner Response

In this section, we present the solution for the gas motion associated with a lined surface when it is placed in an environment described by the previous section.

Fig. (1.3-1) and the associated discussion describes the problem at hand. There are a few details that should be discussed here. In the solutions to be presented, any orifice-mean-flow and any cavity-mean-cross-flow are assumed to be constant in time. Such an assumption will be satisfied if the mean flow into the cavity is choked and is in the direction as shown. The effect of cross flows in the orifice jet is represented by a mean pressure coefficient $\overline{C}_p$, one for the chamber side of the orifice $\overline{C}_{pI}$, and one for the cavity side $\overline{C}_{pII}$. The following paragraph explains how $\overline{C}_p$ is defined.

Consider a reservoir at pressure p_o, discharging through an orifice into a moving stream where, at the orifice exit, there is pressure p_e and velocity u_e both averaged over the orifice exit cross-section. We define the average pressure coefficient here as

$$\bar{C}_p \equiv 2(p_e - p_\infty)/\rho_\infty U_\infty^2 \qquad (2.2\text{-}1)$$

where U is velocity and ∞ denotes value in the free-moving external stream. The value of this coefficient depends upon the ratio of the orifice momentum flux to that of the external stream[6]. Experimental results suggest that this quantity should not be greater than approximately -1, nor much less than about -2[6]. In an actual rocket chamber, since the above momentum ratio does vary in time, some averaged value must be chosen for quantitative results.

In the solution to be presented, there will also appear a coefficient of discharge C_D for the liner orifices. Such a coefficient allows for the consideration of certain real effects when the orifice motion is quasi-steady. Quasi-steady-orifice motion occurs when the particle stay time in the orifice is negligibly small compared to the period of oscillation, or

$$L \bar{c}_{za} / \lambda u^* \ll 1 \qquad (2.2\text{-}2)$$

where u^* is the (dimensional) orifice velocity. When this condition is fulfilled, one can use handbook values for C_D. If not, one should make $C_D = 1$. It is difficult to determine when condition (2.2-3) will be fulfilled in practice because of the variable nature of u*. However, it is known (from the results to be presented) that, when $C_D < 1$ (the only physically realizable case), liner performance is hindered. Thus, we can obtain a conservative criterion when Condition (2.2-2) is fulfilled. If the orifice flow does not go quasi-steady for the largest amplitudes, then it can't go quasi-

steady at all. Taking the largest pressure amplitudes (ϵ^2) as near 0.5, the solution to be presented suggests that $u^*/\overline{c}_I = O\left[\sqrt{0.5}\right]$, or conservatively, near unity. Thus, if L/λ is less than about 0.1, one should assume that the orifice motion will be quasi-steady in operation, or for C_D, if

$$L/\lambda = \begin{cases} < \text{ about } 0.1, \text{ use handbook value for } C_D \\ > \text{ about } 0.1, \text{ use } C_D = 1.0 \end{cases} \qquad (2.2\text{-}3)$$

For orifices with small L/D, $C_D \approx 0.615$ for large Reynolds number.

The normal gas velocity on the chamber side of the liner (at a surface slightly removed from the liner) is first represented by

$$u_\ell \equiv \sigma_\ell u_\ell^* / \bar{c}_{x\ell} \equiv \sigma_\ell \epsilon (\bar{u}_\ell + u'_\ell) \qquad (2.2\text{-}4)$$

where σ_ℓ is the local percent open area ratio of the liner, and $\epsilon\, \bar{u}_\ell$ is the local-mean flow velocity through the orifices in the local region.* The quantity $\epsilon\, u'_\ell$ is the local-oscillatory-orifice velocity and is further expressed as

$$u'_\ell \equiv M_\ell \cos \omega t - N_\ell \sin \omega t \qquad (2.2\text{-}5)$$

All that remains is to evaluate the constants M_ℓ and N_ℓ as a function of $\bar{u}_\ell$ and the parameters in the previous section. Generally speaking, these constants can be obtained as the result of a simultaneous solution of algebraic equations. These equations will first be written for a case which is quite general, although complex. We will then simplify these

*Note that ϵ is not a local value, but is a characteristic amplitude for the chamber.

equations to a form that will maintain generality in practice. Thus, for a specific liner geometry, a given mean flow through the liner, and a given chamber environment as described in the previous section, one can calculate the normal gas velocity on the chamber side of the liner from the following set of equations.* For convenience, we omit the subscript ℓ here.

$$\epsilon B_{2,1} \cos\omega + (\varkappa \cos\omega/2\pi - \sin\omega) M \cos\omega + \epsilon \bar{u} N \sin^2\omega - \epsilon B_{1,1} = 0 \tag{2.2-6}$$

$$\epsilon A_{2,1} \cos\omega + (\varkappa \cos\omega/2\pi - \sin\omega) N \cos\omega - \epsilon \bar{u} M \sin^2\omega - \epsilon A_{1,1} = 0 \tag{2.2-7}$$

where

$$\varkappa \equiv A\lambda/V \tag{2.2-8}$$

The above two equations help to determine the quantities M and N. Certain auxiliary equations are needed since the quantities $A_{i,j}$ and $B_{i,j}$ depend upon both M and N in a complicated way. These other equations, as well as the definitions of $A_{i,j}$ and $B_{i,j}$, are given in Appendix B.

Special Case: no liner-mean-through flow, $\bar{u} = 0$.

If there is no liner-mean-through flow, the above set of equations, including all auxiliary equations, can be simplified considerably. In this special case, the following two simultaneous algebraic equations can be numerically solved to determine both M and N.

---

*We note that this solution applies to near-resonance oscillations. Oscillations far from resonance are of no practical concern here.

$$2\epsilon\left(1+|\cos^3\omega|\right)NR/3C_D^2 - \epsilon N F_1/R + \epsilon\left(3N/2R - N^3/R^3\right)F_2 + \epsilon M^3 F_3/R^3 + \epsilon F_4 - \left(\pi\cos\omega/2 - \pi\sin\omega\right)M\cos\omega = 0 \qquad (2.2\text{-}9)$$

$$2\epsilon\left(1+|\cos^3\omega|\right)MR/3C_D^2 - \epsilon M F_1/R - \epsilon\left(3M/2R - M^3/R^3\right)F_2 + \epsilon N^3 F_3/R^3 - \epsilon F_5 - \epsilon a^2\pi/\gamma_I + \left(\pi\cos\omega/2 - \pi\sin\omega\right)N\cos\omega = 0 \qquad (2.2\text{-}10)$$

where the sign $|\ |$ denotes absolute value, and

$$R = \left(M^2 + N^2\right)^{1/2} \qquad (2.2\text{-}11)$$

The quantities F_i do not depend upon M or N, but merely depend upon the chamber velocity terms $\bar{U}_I$, e, and g. When the chamber velocity equals zero (both mean and oscillatory), all F_i likewise equal zero. The quantities F_i are defined in Appendix B.

Special Case: resonance with no liner-mean-through flow, $\underline{N = 0 \text{ and } \bar{u} = 0}$

Equations (2.2-9,10) can be simplified further, and a result obtained that is extremely useful in design considerations. From Eqs. (2.1-1, 2.2-5), one can see that, when N = 0, the orifice oscillatory velocity will be in phase with the chamber pressure. We call this condition resonance, and the optimum design will operate at (or very near) this condition. Setting N = 0 in Eqs. (2.2-9,10) gives one expression for the resulting velocity amplitude (obtained from M), and

another expression that determines the liner geometry under which this condition is satisfied (resonant geometry). Both of these expressions are given below, and this special case is denoted by the subscript r for resonance.

$$M_r = \{ 3C_D^2 [\alpha^2 \pi/\gamma_I + (\bar{U}_I^2 + 2e^2/3 + q^2/3)(1 - \bar{C}_{pI}) + \pi \bar{U}_I e \cos\psi (\bar{C}_{pI} + 1)/2 + \bar{U}_{II}^2 |\cos\omega_r| (1 - \bar{C}_{pII})]/2(1 + |\cos^3\omega_r|) \}^{1/2} \quad (2.2\text{-}12)$$

$$\gamma_r = 2\pi \tan\omega_r + 2\pi\epsilon \tilde{\Omega}_r / M_r \cos^2\omega_r \quad (2.2\text{-}13)$$

where

$$\tilde{\Omega}_r = 2eq(1 - \bar{C}_{pI})/3\pi + \bar{U}_I q \cos\psi (\bar{C}_{pI} + 1)/2 \quad (2.2\text{-}14)$$

Note that this solution is explicit and no numerical computation is necessary. In these expressions, three additional quantities appear which have not appeared explicitly before; namely, C_D, $\bar{C}_p$, and $\bar{U}_{II}$. The first of these is the coefficient of discharge for the liner orifices, the second of these is a mean pressure coefficient that describes the interaction of a jet with a cross-flow, and the third of these is a mean-cross-flow on the cavity side of the orifice. These quantities have already been discussed at the beginning of this section.

It can be proved that, if $\bar{C}_{pI} < 0$ (which is the only physically realistic range), the magnitude of M_r can only be increased by the contributions from $\bar{U}_I$, e and g. Thus, a chamber flow can only increase M_r.

Eq. (2.2-13) is extremely useful in design considerations. When this expression is satisfied, and when there is no liner-

mean-through flow, the liner geometry will be the resonant geometry. This expression contains the effects of a chamber flow on the resonant geometry. Note the very important result that, when $\tilde{\Omega}_{\mathcal{R}} = 0$, the resonant geometry only depends upon the frequency of the instability mode, and not upon the amplitudes of the chamber pressure and velocity encountered by the liner. From Eq. (2.2-14) we then conclude that, for no liner-mean-through flow, the resonant geometry does not depend upon the instability amplitude when any of the following conditions are satisfied. In the following list, any reference to chamber pressure and velocity concerns only those local values in the vicinity of where the liner is placed.

A-1) $g = 0$; or the chamber pressure is in phase with the chamber oscillatory velocity. Such a condition occurs for all purely spinning tangential modes.

A-2) $e = 0$ and $\cos \psi = 0$; or the chamber pressure is 90° out of phase with the chamber oscillatory velocity, and the direction of the chamber oscillatory velocity is at right angles to the direction of the chamber mean flow. Such a condition occurs in all transverse standing modes of circular-cylindrical and annular-cylindrical combustors.

A-3) $\bar{U}_I = 0$ and either $e = 0$ or $g = 0$; or the chamber mean flow is zero with the chamber oscillatory pressure either in phase or 90° out of phase with the chamber oscillatory velocity. Such a condition is satisfied for any purely spinning or any purely standing mode in regions close to the injector.

A-4) $\sin \omega_r \gg \epsilon \tilde{\Omega}_{\mathcal{R}}/M_r \cos \omega_r$, or both $\sin \omega_r$ and $\epsilon \tilde{\Omega}_{\mathcal{R}}/M_r \cos \omega_r$ are small, or $\cos \omega_r = 0$. At least one of these will occur when ω is not near $\mathcal{R}\pi/2$, $\mathcal{R} = 0, 1, 2 \ldots$, the chamber velocity is relatively small (near a pressure antinode - because of the ordering involved, U_I, e and g will be small or zero), or, because of the ordering involved, any mode that has a spinning tangential component, or $\omega = \mathcal{R}\pi/2$, $\mathcal{R}$ odd.

Conditions (A-1,2,3,4) include most cases of transverse instability in rectangular, circular-cylindrical, and annular-cylindrical combustors. Conditions (3) and (4) include many cases of longitudinal and mixed transverse-longitudinal modes in such chambers. In applying these results to mixed transverse-longitudinal modes, strictly speaking, only those modes for which the angle ψ is constant should be admitted (see Sec. 2.1); however, if condition (4) is satisfied, it is suggested that all mixed modes can be considered. Also, if Condition (4) is satisfied, it is suggested that conical chambers be included also.

At a later point in this chapter, we will see that, in order to provide for a liner design with optimum damping, certain requirements must be satisfied. It turns out that these requirements are such that Condition (4) will be satisfied. Thus, for optimum design, for any instability mode in rectangular, circular-cylindrical, annular-cylindrical, and conical chambers, the designer need not be concerned with the instability amplitudes (as long as they are small, i.e., $\epsilon \ll 1$.) in finding the resonant geometry.

Special Case: no liner mean-through flow, $\bar{u} = 0$, and $M = 0$

Another special case of Eqs. (2.2-9,10) occurs when $M = 0$. In the presence of a chamber flow, the real part of the liner admittance can be negative in regions not too for from resonance. Theoretical study, to date, has suggested that, in such negative regions, the liner may behave in a destabilizing

way. That is, the liner action may provide a mechanism whereby energy from the chamber velocity field does work on the chamber pressure field. When M = 0, the real part of the liner admittance will be zero, and this will provide for a neutral condition of stability (subscript m below). Thus,

$$N_m = \pm\left\{3C_D^2\left[-\pi\bar{U}_I q\cos\psi\,(\bar{C}_{pI}+1)/2 \pm (\bar{U}_I^2 + e^2/3 + 2q^2/3)(1-\bar{C}_{pI}) \pm \bar{U}_{II}^2|\cos\omega_m|(1-\bar{C}_{pII})\right]/2(1+|\cos^3\omega_m|)\right\}^{1/2} \tag{2.2-15}$$

$$\mathcal{K}_m = 2\pi\tan\omega_m + 2\pi\epsilon\tilde{\Omega}_m/N_m\cos^2\omega_m \tag{2.2-16}$$

where

$$\tilde{\Omega}_m = a^2/\gamma_I + \bar{U}_I e\cos\psi\,(\bar{C}_{pI}+1)/2 \mp 2eq(1-\bar{C}_{pI})/3\pi \tag{2.2-17}$$

Eq. (2.2-15) serves to determine the resulting orifice velocity amplitude. In general, two possible values of N_m can be obtained - one for $N_m > 0$ (say N_+) and the other for $N_m < 0$ (say N_-). In Eqs. (2.2-15,17), the upper signs are to be used for N_+, and the lower signs for N_-. Eq. (2.2-16) then serves to determine the liner geometries at which this condition will occur. Note that $\mathcal{K} = A\,\lambda/v$ can only be zero or positive, so that if a negative value is obtained for a specific value of N_m, this solution is physically unrealizable.* If $\mathcal{K} > \mathcal{K}_+$ (for N_+) or if $\mathcal{K} < \mathcal{K}_-$ (for N_-), the real part of the liner admittance will be negative. Positive values of the liner admittance occur for $\mathcal{K}_- < \mathcal{K} < \mathcal{K}_+$.

*This is true only for cavities with dimensions small compared to λ.

Pressure in the Backing Volume

The nondimensional pressure in the backing volume can be found from

$$P_{II_\ell} \equiv P^*_{II_\ell} / \bar{P}_{II_\ell} = 1 + \epsilon P'_{II_\ell} \tag{2.2-18}$$

where

$$P'_{II_\ell} = \gamma_I \left(N_\ell \cos \omega t + M_\ell \sin \omega t \right) \sin \omega \tag{2.2-19}$$

and where M_ℓ and N_ℓ can be found by the above methods.

Example Calculations

Figures (2.2-1 to 6) illustrate the solution of Eqs. (2.2-6 and 7) together with the auxiliary equations given in Appendix B. Such auxiliary equations are necessary only when $\bar{u} \neq 0$. Both the real and imaginary parts of the liner admittance are plotted versus K for particular values of ω. The real and imaginary parts of the admittance are given below in the notation of this section.

$$\mathcal{L}_{R_\ell} = \sigma_\ell M_\ell / a^2 \epsilon \tag{2.2-20}$$

$$\mathcal{L}_{I_\ell} = \sigma_\ell N_\ell / a^2 \epsilon \tag{2.2-21}$$

We will see in a later section that $\mathcal{L}_R$ is an important design parameter and that at any given position in the chamber, $\mathcal{L}_R$ should be maximized for optimum stability.

Figure (2.2-1) illustrates the liner behavior with flow effects absent. Higher amplitudes lower the peak values of $\mathcal{L}_R$ but increase the half-width. The increase of $\mathcal{L}_{R_\ell}$ with ω is due to the $(1 + | \cos^3 \omega_\ell |)$ term in the denominator

in Eq. (2.2-12). $(\mathcal{L}_R)_{\mathcal{R}}$ will become a maximum when $\omega = n\,\pi/2$ or $L/\lambda = n/4$, where n is an odd integer. Such a result has important implications on design.

Figure (2.2-2) illustrates the effect of a discharge coefficient less than unity. As mentioned at the beginning of this section, such a coefficient is proper only when the orifice motion is quasi-steady ($\omega \to 0.0$). Note that the peak value of $\mathcal{L}_R$ is decreased, the half-width is increased, and larger values of $\mathcal{L}_R$ are obtained not too far from resonance.

Figure (2.2-3) illustrates the effect of a chamber flow. As noted earlier, $M_{\mathcal{R}}$ (and consequently $\mathcal{L}_{R\mathcal{R}}$) is always increased by a chamber flow. Values of $\mathcal{K}$ for which $\mathcal{L}_R$ is negative should be avoided since, as mentioned earlier, this may lead to destabilizing operation. The external flow components $\overline{U}_I$, e, and g affect $\mathcal{L}_R$ in the same qualitative way, but the quantitative effects on the maximum and minimum values of $\mathcal{L}_R$ and the half-width do differ. Figure (2.2-3 e) illustrates that a particular flow configuration (and consequently the amplitudes) can change the resonant frequency (c.f. Eqs. 2.2-13 and 14). This figure also illustrates the asymmetrical character of Eq. (2.2-16), that an external flow can change the resonant frequency, but that $\mathcal{L}_R$ still peaks at its resonant value (this last statement has not yet been proven in general).

When there is no chamber flow, and the orifice flow is quasi-steady (small ω), the resonance condition can be satisfied only by a very large cavity volume.* In other words, in the limit $\omega \to 0.0$, the orifice fluid experiences no temporal

*In the theory presented here, the dimensions of the cavity volume should remain small compared to λ. This theory suggests

acceleration (inertia). Eqs. (2.2-13,14) show that, in the presence of particular chamber flows, the resonance condition can be satisfied in the quasi-steady case by smaller cavity volumes. (See Figures (2.2-1 and 3) for an illustration.) Thus, if any of Conditions A-1 to 4 of this section are satisfied, the resonance condition for the quasi-steady case can be obtained by making the orifice length as small as possible and the cavity volume as large as possible. The advantage in this procedure is that the desired condition is obtained in an asymtotic way so that sloppiness in the design and off-design operation is of no major consequence.

Figures (2.2-3 a and 3 c) illustrate that larger values of $(-\overline{C}_{pI})$ enhance the effects of a chamber flow. Such a result is expected since the aerodynamic "suction" caused by a cross-flow over the jet then becomes larger.

Figure (2.2-4) illustrates the effects of an orifice mean flow $\overline{u}$ and a cavity mean flow $\vec{\overline{U}}_{II}$. Since a cavity mean flow plays a similar role in the formulation as a chamber mean flow, it is not surprising that its effect is qualitatively the same as a chamber mean flow. Notice that the mean flow $\overline{u}$ does affect the geometry where $\mathcal{L}_R$ peaks, but that such a peak is still obtained at resonance (where N = 0). In the quasi-steady case (ω = 0.0), a contact surface always passes completely through the orifice (see Appendix B). In the unsteady

that, for ω very small, such dimensions must be at least of the order of the wavelength for resonance to occur.

case (ω = 0.1), the contact surface may not necessarily pass completely through the orifice. The dash-dot-dash lines were obtained through the use of Eqs. (B-31a, 32a). The solid lines were obtained through the use of Eq. (B-31b, 32b). As noted in Appendix B, when the solution can be obtained through the use of Eqs. (B-31a, 32a), it is the proper solution. If not, then one resorts to Eq. (B-31b, 32b) the dashed curves in Figure (2.2-4 b) thus indicate the expected behavior. For particular values of amplitude and frequency, either the set (B-31a, 32a) or (B-31b, 32b) can apply exclusively in the entire region.

Effects of Differences in Cavity and Chamber Environments

Among the important considerations in acoustic liner response are the effects of differences in mean temperatures ($\overline{T}$) and molecular weights ($\mathbb{m}$) between the fluid in the combustion chamber and the fluid in the liner backing volume. These effects have been studied numerically in Ref. (7), and some of those results are reported here.

A number of cases were considered in the calculations. The quantity β = AL/V was chosen to be 0.1 and 0.01. The chamber pressure amplitude (ϵ^2) was chosen as 0.1 and 0.25. Note that these are moderate and very high amplitudes. The ratio ($\mathbb{m}_I \overline{T}_{II}/\mathbb{m}_{II}\overline{T}_I$) was chosen to be 1.0, 0.20, and 0.08. Here, subscript I denotes chamber, and II denotes backing

volume (cavity). For all possible combinations of these cases, the results can be summarized as follows.

The speed of sound in the chamber can be used as the pertinent quantity in evaluating liner response. The above variations in $(m_I \bar{T}_{II}/m_{II}\bar{T}_I)$ do not appreciably affect the geometry at which the orifice velocity peaks (although the geometry at which the cavity pressure peaks is greatly affected). The orifice velocity near the maximum value (i.e., resonance) is largest when $(m_I \bar{T}_{II}/m_{II}\bar{T}_I)$ is unity, and monotonically decreases by no more than 35% when $(m_I \bar{T}_{II}/m_{II}\bar{T}_I)$ becomes 0.08.

From the above results, we can include such differences in cavity and chamber environments by a design factor which allows for a 35% drop in the orifice velocity amplitude near resonance. In the notation of this section,

$$(M)_{design} = C_1 (M)_{\substack{\bar{T}_I = \bar{T}_{II} \\ m_I = m_{II}}} \tag{2.2-22}$$

with

$$C_1 \approx 0.65 \tag{2.2-23}$$

Another important consideration concerning liner response involves differences in the ratio of specific heats (γ) between the cavity and chamber. The effect of such a difference has an influence on both the governing equation for the orifice motion and the boundary conditions on the two sides of the orifice. The effect on the boundary conditions has been studied analytically. Those results suggest

that such a difference affects both the orifice velocity amplitude at resonance and the resonant geometry. This effect on the orifice velocity resonant amplitude and the resonant geometry can be written as follows

$$M_r' = -\frac{J_2}{2J_1} + \sqrt{J_2^2/4J_1^2 + M_r^2} \qquad (2.2\text{-}24)$$

$$\mathcal{K}_r' = \mathcal{K}_r + 2\tan\omega_r[(\pi - \Delta\tau_2)/2 + \sin 2\Delta\tau_2](1 - \gamma_{II}/\gamma_I) \qquad (2.2\text{-}25)$$

where

$$J_1 = 2(1 + |\cos^3\omega_r|)/3\pi \qquad (2.2\text{-}26)$$

$$J_2 = (1 - \cos 2\Delta\tau_2)(1 - \gamma_{II}/\gamma_I)\sin\omega_r/\epsilon 4\pi \qquad (2.2\text{-}27)$$

These expressions do not contain the effect of an orifice mean through flow. The quantities M_r and $\mathcal{K}_r$ are those calculated by means of Eqs. (2.2-12,13). The quantity $\Delta\tau_2$ is the particle transit time from the chamber side of the orifice to the cavity side of the orifice. In the quasi-steady case, both ω and $\Delta\tau_2$ become very small, so that M_r' and $\mathcal{K}_r'$ approach M_r and $\mathcal{K}_r$. In the general case, $0 \leq \Delta\tau_2 \leq \pi$, so that such an effect can be significant. For instance, if we consider $J_1 \approx 0.5$, $J_2 \approx 1$, $M_r \approx 1$, we obtain $M_r' \approx 0.4$. Thus, a 60% reduction in the value of M_r is obtained. Since the resonant geometry is affected by a difference in γ, a design based upon $\mathcal{K}_r$ would result in a drop of M which is greater than 60%. For larger ϵ, in the above example, the actual M experience may be only one-half of 0.4.

Eqs. (2.2-24, 25) would be quite complicated to utilize in practice. For this reason, and since these equations consider only the effect of a difference in γ on the boundary conditions, such a result should be regarded as only a very general guide in design. From these considerations, it is suggested that, if in the design problem, $\gamma_I \neq \gamma_{II}$, one should assume, in a conservative way, that the actual M obtained be about one-fifth the value calculated without consideration of this effect when ω is not small:

$$(M)_{design} = C_2 (M)_{\gamma_I = \gamma_{II}} \tag{2.2-22}$$

with

$$C_2 \approx \begin{matrix} 1 \text{ , } L/\lambda < \text{about } 0.1 \\ 0.2, \; L/\lambda > \text{about } 0.1 \end{matrix} \tag{2.2-23}$$

2.3 Chamber Stability and Design Criteria

In this section are presented the results of certain analyses that consider the effect of a lined surface on the stability of a combustion chamber.

Sufficient Damping with Full-length Liners

Sirignano[8] has studied the effect of a full-length liner with uniform liner admittance on combustion chambers with rectangular, circular-cylindrical, and annular-cylindrical geometries.* No liner-mean-through flow was considered in this analysis. The result that gives the expression for

*This study only considered the explicit dependence of the liner admittance on the stability, also, the conditions of uniform admittance is satisfied only in special cases. The developments proceeding from Eq. (2.3-21) will supply some justification for the use of these results for partial-length liners.

the growth coefficient of acoustic disturbances (α) is given below. For rectangular chambers, the reference length is the chamber width (see Figure A-1). For circular-cylindrical and annular-cylindrical chambers, the reference length is the outer chamber radius (Figure A-2). Velocity is non-dimensionalized with respect to the mean chamber speed of sound, and thermodynamic properties with respect to their mean static values.

$$
\begin{aligned}
\alpha \;=\; & -\lambda^{*}\lambda' \mathcal{L}_{fR}(\gamma_I + 1)\bar{M}_e / A_j \kappa_e \tilde{\omega} \\
& + \left[\gamma_I \int_0^{\kappa_e} \frac{d}{d\kappa}\bar{U}_I(\kappa)\, m\,(1 - \cos\omega^{*}\tau^{*})\cos j\pi\frac{\kappa}{\kappa_e}\, d\kappa\right] / A_j \kappa_e \\
& + \mathcal{E}_R / A_j \kappa_e \\
& - \left[\int_0^{\kappa_e} K(\kappa)\bar{p}_L(\kappa)\left(1 + \cos 2j\pi\frac{\kappa}{\kappa_e}\right) d\kappa\right] / A_j \kappa_e \qquad (2.3\text{-}1) \\
& + \left(\frac{j\pi}{\tilde{\omega}\kappa_e}\right)^2 \bar{M}_e / A_j \kappa_e \\
& - \left\{\frac{j\pi}{\kappa_e}\left[\gamma_I - 2\left(\frac{j\pi}{\tilde{\omega}\kappa_e}\right)^2\right]\int_0^{\kappa_e} \bar{U}_I(\kappa)\sin 2j\pi\frac{\kappa}{\kappa_e}\, d\kappa\right\} / A_j \kappa_e
\end{aligned}
$$

where for

(1) rectangular chambers

$$\lambda^{*} = (m^{*2} + n^{*2})^{1/2} \qquad (2.3\text{-}2)$$

$$\lambda' = \frac{2\gamma_I \tilde{\omega}}{(m^{*2} + n^{*2})^{1/2}}\left(\frac{1 + \ell_\ell}{\ell_\ell}\right) \qquad (2.3\text{-}3)$$

ℓ_ℓ = chamber height/chamber width (2.3-4)

(2) circular-cylindrical chambers

$$\lambda^* = S^*_{\nu\eta} \tag{2.3-5}$$

$$\lambda' = \frac{\gamma_I \tilde{\omega}}{S^*_{\nu\eta}} \frac{1}{1 - \left(\frac{\nu}{S^*_{\nu\eta}}\right)^2} \tag{2.3-6}$$

(3) annular-cylindrical chambers

$$\lambda^* = S^*_{\nu\eta} \tag{2.3-7}$$

$$\lambda' = \frac{\gamma_I \tilde{\omega}}{S^*_{\nu\eta}} \frac{F(S^*_{\nu\eta}) - F(S^*_{\nu\eta}\,\xi)}{\left[\left(\frac{\nu}{S^*_{\nu\eta}}\right)^2 - 1\right] F(S^*_{\nu\eta}\,\xi) - \xi\left[\left(\frac{\nu}{S^*_{\nu\eta}}\right)^2 - 1\right] F(S^*_{\nu\eta})} \tag{2.3-8}$$

$$\xi = \text{chamber inner radius/chamber outer radius} \tag{2.3-9}$$

The quantity $\mathcal{L}_{fR}$ is the real part of the nozzle admittance for the full-liner and is expressed by

$$\mathcal{L}_{fR} = \sigma_f M/a^2 \epsilon \tag{2.3-10}$$

where σ_f is the percent open area ratio of the fully lined surface and M, a, and ϵ were defined in previous sections of this chapter. The quantity (M/a^2) must be considered as an average value over the lined surface. γ_I is the ratio of specific heats in the chamber, $\tilde{\omega}$ the nondimensional angular frequency of instability, ν an integer that describes the angular dependence of the instability mode (see Appendix A), $S^*_{\nu\eta}$ the eigenvalue that describes the instability mode (see Appendix A), $\bar{M}_e$ the steady-flow chamber Mach number at the nozzle entrance, $\varkappa_e$ the nondimensional chamber length (assuming combustion occurs throughout the chamber), n the interaction index incorporated in the Crocco n-τ theory, ω^* the

dimensional angular frequency of instability, τ^* the dimensional sensitive time lag in the same Crocco theory, $\mathcal{E}_R$ the real part of the nondimensional nozzle admittance, k a droplet drag coefficient (to be discussed shortly), $\bar{\rho}_L$ the nondimensional steady-state liquid concentration, and x nondimensional length measured along the chamber axis from the injector. The numbers m^* and n^* describe the type of mode in the rectangular case and are in turn described by Eqs. (A-10 and 11). The integer j is described by Eq. (A-9 or 27). $S^*_{\nu\eta}$ for the full cylinder can be found from Eq. (A-30b), and for the annular chamber, from Eq. (A-30a). The function $F(\beta)$ can be found from Eq. (3.2-11). The constant A_j has the following definition.

$$A_j = \begin{cases} 2 & , j = 0 \\ 1 & , j \neq 0 \end{cases} \qquad (2.3\text{-}11)$$

Since all acoustic quantities are proportional to $e^{\alpha t}$, any term on the right hand side of Eq. (2.3-1) that is positive (negative) must be interpreted as linearly destabilizing (stabilizing).

The first term of this expression represents the damping effect of the liner. With proper design, this term can have the dominant stabilizing effect. Note that this term becomes more dominant when the chamber-mean-flow Mach number ($\bar{M}_e$) becomes smaller, the liner length (x_e) becomes larger, the percent open area ratio (σ_f) becomes larger, and when the liner operates in a near-resonant condition - M then becomes larger.

Because of the occurrence of ϵ in the denominator, this term suggests that acoustic liners are more effective against spontaneous instability than against triggered instability. Also, in the circular-cylindrical case, since $\nu/S^*_{\nu\eta} \to 1$ as ν increases, but for a given ν, $S^*_{\nu\eta}$ increases as η increases, the higher the tangential mode number ν and the lower the radial mode number η (for a fixed ν), the more effective the liner will be. Thus baffles may be used for the modes for which liner effectiveness is less (in cases where the room for a liner is restricted).

For longitudinal modes of oscillations, $\tilde{\omega} = j\pi/x_e$, and the second and last two terms combine to yield the negative (stabilizing) quantity

$$-\left[\gamma_I \bar{M}_e + \tilde{\omega}(\gamma-2)\right]\int_0^{x_e} \bar{U}_I(x)\sin 2\tilde{\omega}x\,dx\Big]\Big/ x_e \qquad (2.2\text{-}12)$$

This implies that distribution of combustion tends to stabilize the longitudinal modes. For purely transverse modes, $j = 0$, and these terms are simply $-(\gamma_I + 1)\,\bar{M}_e/2x_e$ which is a stabilizing quantity due to the mean nozzle flow and is independent of the combustion distribution. In general, these terms are most important as stabilizing quantities; usually, only the acoustic liner term is more important.

The third term represents the driving mechanism provided by the combustion process (according to the sensitive time lag theory). Calculations that will aid the designer in evaluating n and τ^* can be found in Ref. (9).

The fourth term contains the real part of the nozzle admittance coefficient. Often, it is positive for first tangential mode oscillations, indicating that the nozzle has a destabilizing effect for that mode. Calculations indicate that ε_r/M_e can be of order unity in certain cases. In these cases, the effect of the nozzle will be important compared to the other effects present. In other cases, calculations show that this term is negligible compared to unity and has, therefore, negligible effects upon instability (except perhaps in marginal cases where α is very small). One cannot neglect the significant changes in the stability characteristics of an engine that can be achieved through modification of the nozzle design.

The fifth term describes the damping effect due to droplet drag. The drag parameter k is defined by

$$\frac{D}{Dt}\vec{U}_L \equiv K(\vec{U}_I - \vec{U}_L) \tag{2.3-13}$$

where $\vec{U}_L$ is the liquid velocity, and $\vec{U}_I$ the gas velocity in the chamber. An estimate of k can be made by considering the drag of a spherical body, which gives

$$K = 3\mu C_d R_e/4d_L^2\delta_L \tag{2.3-14}$$

where C_d is the drag coefficient, d_L is the sphere diameter, δ_L is the density of the liquid, μ is the gas viscosity, and R_e is the Reynolds number based upon the gas properties and the relative velocity. For purely transverse modes, j = 0, and the damping added by droplet drag becomes

$$\left[\int_0^{x_e} K \bar{\rho}_L \, dx\right] / 2 x_e \qquad (2.3\text{-}15)$$

On the other hand, for purely longitudinal or mixed longitudinal-transverse modes, with the combustion concentrated near the injector face, the damping will become exactly twice the above value. Axial spreading of the combustion zone tends to reduce the damping; however, this spreading may not be undesirable since the third term shows that such spreading also decreases the combustion response.

It is clear that the minimum amount of liner damping necessary is such that the right-hand-side of Eq. (2.3-1) be slightly negative.

Specializing to a Special Class of k(x), $\bar{U}_I(x)$, and $\bar{\rho}_L(x)$

The integrals appearing in Eq. (2.3-1) can be determined if the designer knows the steady-state axial variation of $\bar{U}_I(x)$, $\bar{\rho}_L(x)$, and k(x). For purposes of concreteness, we make the following assumptions concerning these functions.

$$K(x) = K, \quad \text{constant} \qquad (2.3\text{-}16)$$

$$\bar{U}_I(x) = \bar{M}_e \frac{1 - e^{-\alpha_1 x}}{1 - e^{-\alpha_1 x_e}} \qquad (2.3\text{-}17)$$

$$\bar{\rho}_L(x) = \frac{\bar{M}_e}{\bar{U}_{Ix}} \frac{e^{\alpha_2 (x_e - x)} - 1}{e^{\alpha_2 x_e} - 1} \qquad (2.3\text{-}18)$$

Here, subscript I denotes conditions at the injector , and subscript e denotes conditions at the nozzle entrance. The

constants $\mathcal{K}_i$ should be known for a particular application. Generally speaking, $\mathcal{K}_1$ should be around 1 or 2[10]. If there is nothing known by the designer about $\mathcal{K}_2$, then choosing $\mathcal{K}_2 = \mathcal{K}_1$ is probably not too bad in view of the uncertainties already present in k. The quantity $\bar{U}_{LI}$ is the steady-state mass averaged liquid propellant injection velocity divided by the average chamber speed of sound.

With these assumed functional forms, the condition for minimum liner damping becomes

$$\begin{aligned}
\lambda^* \lambda' / \tilde{\omega} \quad > \quad & -(\gamma_x + 1)/A_j \kappa_e \\
& + \frac{\gamma_x \bar{M}_e n (1 - \cos \omega^* \tau^*) \left[1 - (-1)^j e^{-\mathcal{K}_1 \kappa_e}\right]}{A_j \kappa_e \left(1 - e^{-\mathcal{K}_1 \kappa_e}\right)\left[1 + \left(\frac{j\pi}{\mathcal{K}_1 \kappa_e}\right)^2\right]} \\
& + E_R / A_j \kappa_e + \left(\frac{j\pi}{\tilde{\omega} \kappa_e}\right)^2 \bar{M}_e / A_j \kappa_e \\
& - \frac{K}{2 A_j \kappa_e} \frac{\bar{M}_e}{\mathcal{K}_2 \bar{U}_{LI} \left(e^{\mathcal{K}_2 \kappa_e} - 1\right)} \left\{ \left(e^{\mathcal{K}_2 \kappa_e} - 1\right)\left[1 + \frac{1}{1 + \left(\frac{2j\pi}{\mathcal{K}_2 \kappa_e}\right)^2}\right] \right. \\
& \left. - \mathcal{K}_2 \kappa_e (1 + \delta_j) \right\} \\
& - \frac{2\left(\frac{j\pi}{\kappa_e}\right)^2 \left[\gamma_x - 2\left(\frac{j\pi}{\tilde{\omega} \kappa_e}\right)^2\right] \bar{M}_e}{\left[A_j \kappa_e \mathcal{K}_1^2 + \left(\frac{2j\pi}{\kappa_e}\right)^2\right]}
\end{aligned} \tag{2.3-19}$$

where

$$\delta_j = \begin{cases} 1 , & j = 0 \\ 0 , & j \neq 0 \end{cases} \qquad (2.3\text{-}20)$$

Maximum Damping with Partial Liners

The above expression for minimum liner damping was based upon an analysis that assumed that the entire length of the chamber was lined and that the liner admittance was uniform. Only in rare cases would it be necessary to install a full liner, and even then, the liner admittance might not be uniform. It is thus necessary to understand effects that are local to the lined surface. With this in mind, we turn to the approach of Cantrell and Hart[11]. In Appendix C, a criterion for the maximum damping possible, at each point of the lined surface, is obtained, based upon a method developed in Ref. (11). The result obtained is the following

$$\iint_S ds \left\{ \sigma/\epsilon \left[a^2 M/\gamma_x + \bar{U}_x (Me - Ng) + \sigma^2 \bar{u} R^2 \right] \right\} = maximum \qquad (2.3\text{-}21)$$

All of the quantities within this surface integral, except for ϵ are local values. All quantities have been defined in previous sections of this chapter (see also the table of nomenclature). The maximum value of this integral must be positive for stability.

Clearly, the surface integral will be maximized when the integrand is maximized at every point on the surface. This, however, is not the proper approach to be taken here.

We are interested here in how to utilize a liner most efficiently, i.e., how to construct a liner that will produce maximum damping. More specifically, the question becomes: What is the optimim liner geometry and the optimum liner placement? The answer to this question lies in finding the specific liner geometry and the specific location in which the above integrand is maximized. The problem then becomes

$$\sigma\left[a^2 M/\gamma_z + \bar{U}_z(Me - Ng) + \sigma^2 \bar{u} R^2\right] = maximum \quad (2.3\text{-}22)$$

and the maximization (for positive values only) is to be achieved by finding the proper position in the chamber and the proper liner geometry.

In deriving the last expression, all of the quantities involved are considered to be of order unity or less. We now look into more detail as to the proper ordering. For any given position in the chamber, we know from the results of Sec. (2.2) that for some liner geometries, both M and N will be of order unity, and these are the largest magnitudes that they can obtain. For validity of the analysis presented in Sec. (2.2), $\bar{u}$ must be of order unity or less. In practice, $\sigma^2 << 1$. In order to consider the relative magnitudes of a, $\bar{U}_I$, e, and g, we separately consider first two cases that often occur in practice; namely, standing tangential and spinning tangential waves.

We first consider standing waves. In this case, we have in nondimensional form

$$p_I' = \epsilon^2 \cos\phi \cos\omega t = a^2\epsilon^2 \cos\omega t$$

$$\bar{M}_I = \bar{U}_I \epsilon$$

$$(U_I')_{in} = 0 = e\epsilon \cos\omega t$$

$$(U_I')_{out} = \epsilon^2 B \sin\phi \sin\omega t = q\epsilon \sin\omega t$$

where a prime denotes oscillatory component, subscript "in" denotes in phase component, subscript "out" denotes out of phase component, $\bar{M}_I$ is the chamber mean flow Mach number (which is of the order of the maximum pressure oscillation (ϵ^2)), and ϕ is distance from the point where the pressure oscillations are largest. The constant B is of order unity. We thus obtain

$$a = \sqrt{\cos\phi}$$

$$\bar{U}_I = O(\epsilon)$$

$$e = 0$$

$$q = \epsilon B \sin\phi$$

Expression (2.3-21) then becomes

$$\sigma\{O[\sqrt{\cos\phi}\, M] + O[\epsilon^2 B \sin\phi N] + O[\sigma^2 R^2]\} = \text{maximum} \qquad (2.3\text{-}22)$$

As ϕ is varied in this expression, only the first two terms change; the first of these becomes smaller, and the second becomes larger. Since $\epsilon \ll 1$, the optimum value of ϕ is

very near zero. Furthermore, since $\sigma^2 \ll 1$, the optimum geometry is such that M is maximized. The calculations presented in Sec. (2.2) show that, when the liner is placed near a pressure antinode (velocity effects are then small), the quantity M becomes maximum when the liner geometry is the resonant geometry.

For purely spinning (or travelling) waves, any given position in the chamber will experience both maximum pressure and velocity oscillations. The ordering now becomes

$$p_I' = \epsilon^2 \cos\omega t = a^2\epsilon^2 \cos\omega t$$

$$\bar{M}_I = \bar{U}_I \epsilon$$

$$(U_I')_{in} = \epsilon^2 C \cos\omega t = \epsilon e \cos\omega t$$

$$(U_I')_{out} = 0 = \epsilon g \sin\omega t$$

or

$$a = 1$$
$$\bar{U}_I = O(\epsilon)$$
$$e = O(\epsilon)$$
$$g = 0$$

Expression (2.3-21) then becomes

$$\sigma\left[O(M) + O(\epsilon^2 M) + O(\sigma^2 R^2)\right] = maximum \qquad (2.3\text{-}23)$$

So that, ideally speaking, liner placement is inconsequential, and M should be maximized. Calculations of Sec. (2.2) again show that for this ordering, M will be maximized when the liner geometry is the resonant geometry.

The above conclusions concerning liner placement can be stated more simply perhaps in words. It is known that, in a

combustion chamber, the maximum pressure oscillations are of the same order of magnitude as the maximum velocity oscillations. For standing modes, both maxima appear at different positions, whereas for spinning modes, any position experiences both maxima. The quantities $\overline{U}_I$, e, and g were defined in such a way that the chamber velocity would have to be an order of magnitude larger than the oscillatory pressure in order for these quantities to be of order unity; furthermore, only a product of these terms appears in Expression (2.3-21). Thus, the effect of a chamber velocity must be small compared to that of the pressure, and there is no benefit obtained in moving away from a region of maximum pressure oscillation towards that of a maximum velocity oscillation (or even maximum chamber mean flow velocity). Reasoning in this way, we would expect that, in actual combustors, no matter where an oscillatory pressure maximum occurs, this is where the liner should be placed. This conclusion is important since it is observed that axial variations in "maximum" pressure amplitude occur: the largest obtained being near the injector.

We note that the above conclusions were obtained independent of the angle ψ (see Sec. (2.1)). Thus, the above results are intended for any mode in rectangular, circular-cylindrical, annular-cylindrical, and conical chambers.

The main conclusion of this section is the following. For all cases of practical concern, the most efficient

operation of a liner can be achieved by constructing the liner such that its geometry is the resonant geometry, and that its placement is in the region where the oscillatory pressure amplitudes are the largest.

The above suggestion for optimum performance can be carried out only when there is sufficient freedom in the variables of liner geometry and liner placement. In some cases, one or both of these variables will be confined to certain limits. If the liner position is restricted, and the liner connot be placed in a region where the oscillatory pressure amplitudes are maximum, one must not conclude that the optimum geometry is the resonant geometry. Also, if the liner geometry is restricted, one should not conclude that the optimum placement is still as above. The most general approach to be taken is that Expression (2.3-21) be satisfied, whether or not constraints are imposed on the design. Chapter 3 considers the case where no essential constraints are imposed, and Chapter 4 considers special problems where constraints do exist.

2.4 Rationale for Design Procedures

The main ideas underlying any design procedure have been presented in the previous sections. There are, however, a few comments that need to be made.

In Section (2.3) a criterion was presented that is to give a measure of the minimum amount of liner damping necessary for chamber stability. This criterion was based on an

analysis that considered a full liner with uniform admittance in which there is no liner-mean-through flow. Since, in practical applications, it will usually not be necessary to fully line the chamber, we represent the percent open area ratio of the full liner (σ_f) by the following

$$\sigma_f = f_L \sigma \tag{2.4-1}$$

where f_L is the ratio of the lined-surface area divided by the chamber-wall area. The latter area is the area occupied by the full length liner in the analysis. The quantity σ is the percent open area ratio of the actual liner.

From Expression (2.3-21), it was found that, when optimization is desired, a mean flow through the liner does not have an explicitly significant result on damping since, in virtually all cases, $\sigma^2 << 1$. Thus, even though the minimum damping criterion (2.3-19) does not consider such a mean flow, this expression should be valid in optimization problems where $\bar{u} \neq 0$, as long as the implicit dependence of $\bar{u}$ on M is considered.

From the results concluded from Expression (2.3-21), the designer possesses a guideline as to the conditions under which partial-length liner damping is maximized. If this guideline is carried out, the partial-length liner will have locally uniform admittance with percent open area ratio σ. Then from the criterion of Sirignano (Sec. 2.3), writing $\sigma_f = f_L \sigma$, a measure as to the effectiveness of the optimum partial-length liner on stability can be evaluated. Thus,

a procedure for optimum design becomes evident, and this is presented in Chapter 3.

In some cases, an optimum design cannot be achieved. In these cases, an effective liner can still (usually) be constructed, and its effectiveness determined from the methods of Sec. (2.3). These latter cases are usually more difficult to handle, and techniques for the solution of a few most common of these problems are presented in Chapter 4.

The optimum design procedure will require that the liner operate in resonance. This means that the liner configuration should not change the frequency of the instability mode. However, for off-resonant designs (to be discussed in Chapter 4), such a modification must be considered.

CHAPTER 3

Optimal Design Procedure

The procedure suggested in this chapter is intended to provide a method for the selection of a liner that will supply a sufficient amount of damping in such a way that the total surface area occupied by the liner is minimized. This procedure consists of starting with certain known chamber parameters (chamber geometry, type of instability mode, etc.) and then determining requirements for the liner geometry and liner placement. More specifically, the procedure is to satisfy three conditions simultaneously. The first of these is a requirement placed on the liner geometry in such a way to assure that the liner operates in a resonant condition. The second is a requirement on the hole-area and total lined surface area in such a way to insure that the liner provides sufficient damping. The third is a requirement on liner position in the chamber.

From Sec. (2.2), it can be shown that the ¼-wave geometry ($L/\lambda = 1/4$, $V = 0$) contains the minimum volume for resonance. This usually means that the lined surface area is minimized for this geometry. Even so, because of other practical considerations, we maintain generality here by allowing Helmholtz resonators ($V \neq 0$) as well.

In certain special cases, the three conditions present cannot be satisfied simultaneously. Perhaps the most frequently occurring of such cases is when the design suffers

volume-limitations; i.e., there is not sufficient room in the chamber to provide enough backing volume as suggested in the procedure. In these latter cases, a liner design may still be found that utilizes the backing volume available and still provides a sufficient amount of damping. Such problems as these are considered in Chapter 4.

The outlined design procedure applies to any instability mode in any rectangular, circular-cylindrical, annular-cylindrical, and slightly conical (cone half-angle less than about 6°) combustion chambers. Other conical chambers can be handled by this method, but in a more approximate manner. There are no restrictions as to the type of liquid propellants, and to the particular steady-state operating characteristics.

3.1 Design Variables

The design variables are the following: f_L, L, A, V, σ, and liner position. f_L is the ratio of the total lined surface area (A_L) to the chamber wall area (A_w); $f_L = A_L/A_w$. For rectangular chambers, the chamber wall area is defined as follows:

$$A_w \equiv 2(w + h^*)X^*$$

where w is the chamber width, h^* the chamber height, and X* is the length along the chamber axis in which combustion occurs. The nozzle admittance condition should be applied at the end of this length. This length can usually be taken as the actual chamber length, i.e., the distance from the injector to where the nozzle contraction occurs. For circular-cylindrical and annular-cylindrical chambers, the wall area

is defined as follows:

$$A_w \equiv 2\pi r_o X^*$$

where r_o is the radius of the outer wall and X*is defined as above. For conical chambers,

$$A_w \equiv \pi(r_I^* + r_x^*)X^*$$

where X* is as defined above, r_I^* is the radius at the injector, and r_x^* is the radius at the axial distance X* from the injector. These definitions for A_w and f_L are independent of the position of the actual liner. L is the length of the liner orifices (liner thickness). In cases of a partitioned backing-volume, V is the volume of a partitioned section and A is the total orifice cross-sectional area associated with that section. For non-partitioned backing-volumes, where the orifices are evenly spaced on a local scale, A is the cross-sectional area of a single orifice, and V is the total backing-volume, in that local region, divided by the total number of orifices in that local region. Any cross-sectional geometry is allowable for the orifice holes, although the cross-sectional area should be constant with distances along the orifice axis. On a local scale, σ is the fraction of the total orifice hole area to the total liner surface area. The dimensions of the volume V must be small compared to the wavelength of oscillation.

3.2 Design Procedure: Case I, Small Liner-Mean-Through Flow

The procedure in this section is intended for those cases in which the liner-mean-through flow velocity is zero,

or sufficiently small. See Section (3.3) for suggestions as to what is meant by sufficiently small. The only difference between the procedure of this section and that of Section (3.3) is in the mechanics of certain calculations. The minimal amount of information necessary for this section is the following:

1. chamber geometry

2. type of instability mode
   a. the integer j that describes the longitudinal character of the mode (see Appendix A)
   b. for circular-cylindrical and annular cylindrical chambers, the integer ν that describes the tangential character of the mode, the integer η that describes the radial character of the mode, and the corresponding eigenvalue $S^*_{\nu\eta}$ (see Appendix A)
   c. for rectangular chambers, the numbers n* and m* that describe the transverse character of the mode (see Appendix A)

3. the position in the chamber where the maximum unstable pressure oscillations occur

4. the chamber steady-state speed of sound $\bar{c}_I$

5. the ratio of specific heats in the chamber γ_I

6. the steady-state Mach number of the flow at the nozzle entrance $\bar{M}_e$

7. for designs that result in short orifices; namely, those for which the orifice length to wavelength ratio is less than about 0.1, the coefficient of discharge for the orifices C_D

8. whether or not the molecular weight, the ratio of specific heats, or the mean temperature in the backing-volume will differ from the corresponding value in the chamber in the vicinity of where the liner is placed (which is at that position known from Item (3)).

The above information is usually available to the designer, and is sufficient for a calculation that will provide

for a fairly accurate design. For more accurate calculations, the following additional information is necessary:

9. exponent $\mathcal{K}_1$ that describes the steady-state Mach number variations, and the exponent $\mathcal{K}_2$ that describes the steady-state liquid concentration along the chamber axis. (see Eqs. (2.2-16,17)

10. the chamber interaction index n and the sensitive time lag τ^* (sec^{-1}) incorporated in the sensitive time lag theory of Crocco, or their equivalent

11. the real part of the nozzle admittance $\mathcal{E}_R$ (non-dimensional

12. an average droplet drag parameter k (non-dimensional)

13. the mass-averaged liquid injection velocity $\bar{U}_{LI}$ (nondimensional).

Since the steady-state values of the chamber speed of sound $\bar{c}_I$, and the ratio of specific heats γ_I vary along the chamber axis, the following discussions will contain these quantities with either of two subscripts, a and ℓ. Subscript a will denote a value averaged over the chamber volume, and subscript ℓ will denote a value in the region where the liner is placed.

The quantities j, ν, η, $S^*_{\nu\eta}$, m* and n* are discussed in Appendix A, and Tables (A.1, 2) should prove to be useful on this score.

The instability frequency f can be measured in firings of the test hardware and/or calculated from the knowledge of Items (1) and (2). For rectangular chambers, this calculation becomes*

*For a more accurate calculation of this frequency, see Eqs. (A-40, 41).

$$f = \bar{c}_{Ia} \sqrt{m^{*2} + n^{*2} + \pi^2 j^2 (1 - \bar{M}_e^2)^2 / \varkappa_e^2} \,/ 2\pi w \qquad (3.2\text{-}1)$$

where w is the chamber width, and $\varkappa_e$ is the actual chamber length plus two-thirds the nozzle contraction length all divided by w. In this equation and in what follows, any of the two transverse dimensions can be considered the chamber width, although consistency must be maintained. In general, m* and n* will depend upon this choice. For circular-cylindrical and annular-cylindrical geometries, the calculation is *

$$f = \bar{c}_{Ia} \sqrt{S_{\nu\eta}^{*2} + \pi^2 j^2 (1 - \bar{M}_e^2)^2 / \varkappa_e^2} \,/ 2\pi r_o \qquad (3.2\text{-}2)$$

where r_o is the outer chamber radius. The oscillatory wavelength λ can then be found from

$$\lambda = \bar{c}_{Ia} / f \qquad (3.2\text{-}3)$$

In this section, we have reserved comments on conical chambers until now. For such geometries, it is suggested that they be treated as circular-cylindrical geometries with radius $r_o = (r_I + r_x)/2$, where both r_I and r_x have been defined in the previous section. If the cone half-angle is less than about 6°, such a treatment should yield results with accuracy consistent with other aspects of the problem. For larger cone half angles, it would be desirable that the eigenvalue $S^*_{\nu\eta}$ be calculated from Eq. (3.2-2), where f is known from test firings. The quantity $\varkappa_e$ will then be the combustion length X* plus two thirds any remaining length

*For a more accurate calculation of this frequency, see Eqs. (A-40, 41).

to the minimum area (throat), all divided by the above r_o. The Mach number $\bar{M}_e$ should then be that value at station X. The numbers j, ν and η will always have the same meaning as in the circular-cylindrical case.

The constants $\mathcal{K}_1$ and $\mathcal{K}_2$ are defined in Eqs. (2.2-16, 17). Generally speaking, for hydrocarbon combustors, $\mathcal{K}_1$, should be in the range 1.0 - 2.0[10]. As already mentioned in Sec. (2.2), one might choose $\mathcal{K}_2 = \mathcal{K}_1$. One should consult Ref. (9) for the calculation of n and τ^*. Typical values for the real part of the nozzle admittance $\mathcal{E}_R$ and the droplet drag parameter k are discussed in Sec. (2.2).

The design procedure consists of satisfying the following three conditions simultaneously:

I-1) choose any value of A, L, and V such that*

$$A\lambda/V = 2\pi \tan(2\pi L/\lambda) \tag{3.2-4}$$

I-2) choose any value of L, f_L, and σ such that

a.) for rectangular chambers

$$f_L \sigma > \frac{\epsilon_o \bar{C}_{xl}}{2\gamma_{Ia}\bar{C}_{Ia} C_1 C_2 M} \frac{\mathcal{J}}{1+\mathcal{J}} G \tag{3.2-5}$$

where $\mathcal{J}$ = chamber height/chamber width (3.2-6)

b.) for circular-cylindrical chambers

$$f_L \sigma > \frac{\epsilon_o \bar{C}_{xl}}{\gamma_{Ia}\bar{C}_{Ia} C_1 C_2 M}\left[1 - \left(\frac{\nu}{S^*_{\nu 2}}\right)^2\right] G \tag{3.2-7}$$

*The dimensions of the cavity V (for Helmholtz resonators) must be small compared to the wavelength in order that the theory be applicable.

c.) for annular-cylindrical chambers

$$f_L \sigma > \frac{\epsilon_o \bar{c}_{zl}}{\gamma_{za} \bar{c}_{za} C_1 C_2 M} \frac{[F(S^*_{\nu_2}) - F(S^*_{\nu_2}\xi)]\, G}{\left[\left(\frac{\nu}{S^*_{\nu_2}}\right)^2 - 1\right] F(S^*_{\nu_2}\xi) - \xi\left[\left(\frac{\nu}{S^*_{\nu_2}}\right)^2 - 1\right] F(S^*_{\nu_2})} \quad (3.2\text{-}8)$$

where

$$\xi = \text{chamber inner radius/chamber outer radius} \quad (3.2\text{-}9)$$

In the above expressions

$$M = \left\{ 3 C_D^2 \pi / [2 \gamma_{zl} (1 + |\cos^3(2\pi L/\lambda)|)] \right\}^{1/2} \quad (3.2\text{-}10)$$

$$F(y) = \frac{d}{dr} Y_\nu(r)\Big|_{r=y} / [J_\nu(y) + B^* Y_\nu(y)] \quad (3.2\text{-}11)$$

and

$$B^* = -\frac{d}{dr} J_\nu(r)\Big|_{r = S^*_{\nu_2}\xi} \Big/ \frac{d}{dr} Y_\nu(r)\Big|_{r = S^*_{\nu_2}\xi} \quad (3.2\text{-}12)$$

where J_ν and Y_ν are the standardized Bessel functions. The coefficients C_1 and C_2 are defined as follows. If the mean temperature and/or the molecular weight in the backing volume differs from that in the local chamber environment, take $C_1 = 0.65$, otherwise, take $C_1 = 1.0$. If $L/\lambda <$ about 0.1, take $C_2 = 1.0$, otherwise choose C_2 from Fig. 3.1 below.

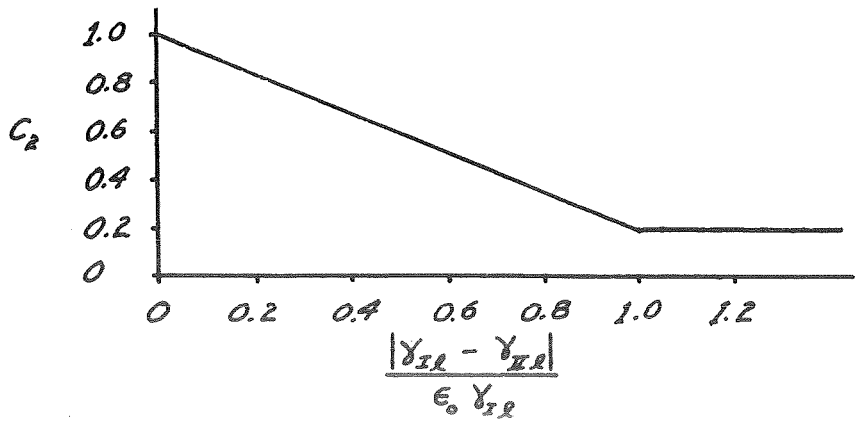

Figure 3.1

The quantity G is defined as follows:

$$G = -(\gamma_{Ia}+1)\bar{M}_e/A_j X + \varepsilon_R/A_j X + \left(\frac{j\pi}{\tilde{\omega}X}\right)^2 \bar{M}_e/A_j X$$
$$+ \frac{\gamma_{Ia}\bar{M}_e n(1-\cos\omega^*\tau^*)}{A_j X(1-e^{-\kappa_1 X})\left[1+\left(\frac{j\pi}{\kappa_1 X}\right)^2\right]}\left[1-(-1)^j e^{-\kappa_1 X}\right]$$
$$- \frac{\kappa\bar{M}_e}{2A_j X\bar{U}_{Ix}\kappa_2(e^{\kappa_2 X}-1)}\left\{(e^{\kappa_2 X}-1)\left[1+\frac{1}{1+\left(\frac{2j\pi}{\kappa_2 X}\right)^2}\right]-\kappa_2 X(1+\delta_j)\right\}$$
$$- \frac{2\left(\frac{j\pi}{X}\right)^2\left[\gamma_{Ia}-2\left(\frac{j\pi}{\tilde{\omega}X}\right)^2\right]\bar{M}_e}{A_j X\left[\kappa_1^2+\left(\frac{2j\pi}{X}\right)^2\right]} \qquad (3.2\text{-}13)$$

$$\delta_j = \begin{cases} 1, & j=0 \\ 0, & j\neq 0 \end{cases} \qquad (3.2\text{-}14)$$

$$A_j = \begin{cases} 2, & j=0 \\ 1, & j\neq 0 \end{cases} \qquad (3.2\text{-}15)$$

For rectangular chambers, X is the ratio of the quantity X* defined in the previous section to chamber width (w), and $\tilde{\omega} = \omega^* w/\bar{c}_{Ia}$. For circular-cylindrical and annular-cylindrical chambers, X is the ratio of X* to the chamber outside radius (r_o), and $\tilde{\omega} = \omega^* r_o/\bar{c}_{Ia}$. For designs with the shorter orifice lengths ($L/\lambda < 0.1$), C_D should assume the value of the steady flow discharge coefficient for the orifice; otherwise, C_D should be taken as unity.

The quantity ε_o in the above expressions is the square root of the non-dimensional spatially-maximum oscillatory pressure amplitude that occurs in the chamber, and to retain the validity of the underlying theory, should be small compared to unity. For spontaneous instability ε will be small whereas for triggered instability ε will be relatively large. Generally speaking, one should expect that $0 < \varepsilon_o \tilde{<} 0.3$. For a conservative estimate in this expression, one should choose the larger expected values of ε_o.

I-3) place any lined surface in areas at or very near the regions where the unstable pressure oscillations are largest.

3.3 Design Procedure: Case II, Non-Zero Liner-Mean-Through-Flow

The design procedure presented here is fundamentally the same as that appearing in Section 3.2. The only difference is that Eq. (3.2-4) cannot be used to precisely find the resonant geometry and Eq. (3.2-10) is no longer valid. If the alternate solution suggested here appears too difficult, one might still use the previous procedure even in the presence of a liner-mean-through flow. The calculations and figures provided in Sect. (2.2) suggest that such a simplification yields good results at least for mean flows that are not excessively large. If the quantity $\bar{u}$, calculated below, is less than about 0.3, the error in such a simplification appears to be less than about 10%. Values of ω are restricted here to $0 \leq \omega \lesssim 0.3$.

The alternate (more difficult) solution suggested here involves the numerical solution of simultaneous algebraic equations. In addition to the quantities listed in the previous section, the orifice mean flow velocity and a chamber pressure amplitude must be known. If $\bar{u}^*$ denotes the actual dimensional mean-flow-orifice velocity, one obtains

$$\bar{u} = \bar{u}^* / \epsilon \bar{c}_{\ell}$$

where $\bar{u}$ is the parameter to be used in the calculation and ϵ is the square root of the characteristic pressure amplitude for the chamber (see Eq. 2.1-2). To comply with the theory, ϵ should be a number much less than unity and $\bar{u}$ should be, at the largest, of order unity, but smaller than R cos ω.* For spontaneous instability ϵ will be small, and for triggered instability ϵ will be relatively large. One should perform the calculations in Condition (II-1) for a few specific values of ϵ and then choose the most reasonable value of ϵ that gives the smallest (conservative) value for M. Generally speaking, reasonable values for ϵ would be such that $0 < \epsilon \tilde{<} 0.3$. The design procedure then is to satisfy the following three conditions simultaneously:

II-1) The following set of algebraic equations must be solved simultaneously for the special case N = 0. Because of Conditions (II-3), the chamber flow terms in these equations can be neglected, i.e., $\vec{U}_I \approx \bar{U}_I \approx U_I' \approx e \approx g \approx 0$. This special case is denoted by $(\ )_o$.

$$\cos\omega(B_{2,1})_o + (\mathcal{R}\cos\omega/2\pi - \sin\omega)\cos\omega M/\epsilon - (B_{1,1})_o = 0 \qquad (3.3\text{-}1)$$

$$\cos\omega(A_{2,1})_o - \sin^2\omega\,\bar{u}M - (A_{2,1})_o = 0 \qquad (3.3\text{-}2)$$

The constants $A_{i,j}$ and $B_{i,j}$ are defined in Appendix B. There are certain other auxiliary relationships that must be

*Since the amplitude R is a function of $\bar{u}$, one does not know a priori whether or not $\bar{u}$ is greater than R. How this difficulty is treated in the computer program is explained in Appendix D.

satisfied together with the above two equations, and these are also presented in Appendix B. A suitable computer program is provided in Appendix D.

For any given value of the design variable L (which appears in $\omega = 2\pi L/\lambda$), the above two equations determine the design values of $\mathcal{K} = A\lambda/V$ and M. Thus, similar to Condition (I-1) of the previous section, this condition provides a relationship among the design variables A, L, and V. Any selection can be made for these variables, provided that the proper value of $\mathcal{K}$ (which depends upon L) be satisfied.*

II-2) The same as Condition (I-2) of the previous section, except that the quantity M is now that quantity calculated in the above step and not the quantity defined by Equation (3.2-10) in Condition (I-2).

III-2) The same as Condition (I-3) of the previous section.

3.4 Suggestive Comments

From Condition (I-2), one can see that the required lined area initially diminishes as the orifice length L becomes significant compared to the wavelength, and approaches a minimum when $\omega \approx n\pi/2$, or $L/\lambda \approx n/4$, with n = 1, 3, odd. The resonant geometry in such cases consists of quarter-wave or multiple-quarter-wave tubes. In reference to this fact, the designer should be aware of certain practical considerations. In general, as the orifice length approaches these optimum values, the liner response becomes more and more sensitive to the liner geometry. When the orifice length is very small

*See footnote on Page 47.

($L/\lambda \approx 0$), the liner response is virtually insensitive to the actual value of L.* Condition (I-1) then requires that the ratio $A\lambda/V \rightarrow 0$ or that the cavity volume is large in comparison to the area A. On the other hand, when $L/\lambda \approx 1/4$, the actual value of L/λ becomes very important. Thus, if there is considerable doubt in the value of the wavelength of oscillation, significant erosion occurs in the liner material altering the orifice dimensions, or if any other hard-to-define factor introduces considerable uncertainty in what the actual values of L/λ and $A\lambda/V$ will be, it is suggested that the designer not attempt to exploit this optimization for the larger values of L. In such cases it may be advisable to design for the cases where $L/\lambda \approx 0$ in that this results in a "safe" design, i.e., one that does not depend in a very sensitive way upon the actual liner geometry. Another alternative would be to select the proper design that would provide for any uncertainty in L, λ, etc. This alternative would, however, require more involved calculations to determine the limits of parameter variations, and this added complication must be justified by the amount the liner-surface area is reduced. In Chapter 4 suggestions are provided for accomplishing this alternate solution for designs with considerable uncertainty.

The above design procedures require that the lined surface be placed in regions where the unsteady pressure oscillations

*The resulting large bandwidth overshadows moderate variations in L.

are largest. For the case of spinning modes, it has been observed that such oscillations usually are maximized in the region close to the injector and at the chamber wall (injector-chamber interface). For longitudinal modes, regions near the injector will also experience the maximum pressure oscillations, although such oscillations will also occur in distinct regions along the chamber for the higher modes (see Appendix A). Some asymmetrical property of the combustion chamber is necessary in order that standing transverse modes exist. For instance, the presence of baffles or non-uniform mass distribution across the injector face might serve to establish a particular mode. In all cases, direct pressure measurements in the actual test hardware are necessary to establish the location of such pressure maximums. Knowledge of the acoustic solution (Appendix A) is highly desirable in locating oscillatory pressure maximums.

In many cases, the designer cannot, or does not want to accurately calculate the quantity G in Eq. (3.2-11). In such cases, it is useful to know that $G = b\,\bar{M}_e$, where b is a number that should not be much larger than approximately three.

As mentioned earlier, the above design procedures are intended to produce a design which will provide for a sufficient amount of damping with the minimum amount of liner-surface area. Conditions (I-2, II-2) serve to insure that the liner damping is sufficient, whereas Conditions (I-1, I-3, II-1, II-3) serve to minimize the lined-surface area. In some applications, minimization cannot be achieved. For instance,

because of geometrical constraints, it may occur that the liner can not be placed at the position where the pressure oscillations are largest, but instead, it must be placed in regions where chamber-velocity effects become important. Another example is in volume-limited situations, where, in order to provide for enough damping, the backing-volume will not be sufficient in order to satisfy Conditions (I-1 or II-1). In special cases such as these, a sufficient amount of liner damping may still be achieved, i.e., Conditions (I-2 or II-2) can still be fulfilled. One might then ask, given certain constraints, i.e., volume limitations, liner-placement restrictions, etc, what would be the liner design that would contain the optimized amount of lined-surface area. Another possibility is that the designer is not interested in optimization at all, and merely wants to evaluate the performance (determined whether or not the damping is sufficient) of a given liner with a given position in the chamber. Problems such as these are discussed in Chapter 4.

3.5 Example Problem

Problem: Design an optimum liner configuration for a circular-cylindrical chamber with radius r_o = 1 ft. The length of the cylindrical portion is 1 ft. and the contraction section has length ½ ft. The combustion length is equal to the length of the cylindrical portion. It is observed that a second tangential spinning instability occurs with the maximum pressure oscillations occurring at the injector-outer-wall corner. The average speed of sound in the chamber is

2,000 ft/sec, and the speed of sound near the injector is 1,500 ft/sec. The average ratio of specific heats is 1.2 and that near the injector is 1.3. The Mach number at the beginning of the nozzle contraction is 0.2. Assume the following values: $\mathcal{K}_1 = \mathcal{K}_2 = 2.0$, $n = 0.6$, $\tau^* = 5 \times 10^{-4}$ sec., $\mathcal{E}_r = 0.4$, $\mathcal{E}_I = 0.1$, $\bar{U}_{LI} = 0.1$, $k = 0.1$. Practical considerations require that the cavity environment will be cool so that values for the molecular weight and the ratio of specific heats in the cavity will differ from those in the chamber. Practical considerations also require that the orifice length be no smaller than about ½ inch and no larger than about 1 inch.

Preliminary Calculations: From Table A-1 in Appendix A, the following values are obtained

$$j = 0$$

$$\nu = 2$$

$$\eta = 1$$

$$S^*_{\nu\eta} = (3.14)\ (0.972) = 3.06$$

The dimensional angular frequency is then calculated from Eq. (A-24 and 40)

$$\omega^* = \bar{c}_{Ia}\left(S^*_{\nu\eta} + \omega'\right) r_0$$

where

$$\omega' = \mathcal{E}_I / A_j \ell_e - \lambda' \lambda^* \mathcal{L}_I / \tilde{\omega} + \bar{M}_e n \sin \omega^* \tau^* / A_j \ell_e$$

For all cases of optimum design, $\mathcal{L}_I = 0$ since the liner operates in resonance, and furthermore

$$\omega^* = \frac{(2)(10^3)}{(1)}\left[3.06 + \frac{0.1}{(2)(2)} - 0 + \frac{(0.2)(0.6)\sin\omega^* t^*}{(2)(2)}\right]$$

The corrections due to the nozzle and combustion response are thus seen to be negligible, so that only the pure acoustic frequency need be considered. Thus

$$\omega^* = (2)(10^3)(3.06) = 6.12 \times 10^3 \text{ radians/sec.}$$

$$f = \omega^*/2\pi = (6.12)(10^3)/6.28 = 975 \text{ Hz.}$$

$$\lambda = \bar{c}_{Ia}/f = (2)(10^3)/975 = 2.05 \text{ ft.}$$

Condition I: The liner geometry must be such that

$$A\lambda/V = 2\pi \tan(2\pi L/\lambda)$$

The limits on L/λ are such that

$$2.04 \times 10^{-2} = 1/(2)(12)(2.05) \leq L/\lambda \leq 1/(12)(2.05) = 4.07 \times 10^{-2}$$

Less liner surface area will be required for the larger value (see the previous section and Condition 2 below). Thus, we choose L = 1 inch and

$$A/V = 2\pi \tan(2\pi L/\lambda)/\lambda$$

$$= 6.28 \tan(6.28 \cdot 4.07 \cdot 10^{-2})/2.05$$

$$= 0.815 \text{ ft}^{-1}$$

Condition 2: The liner geometry must be such that

$$f_L \sigma > \frac{\epsilon_0 \bar{c}_{IL}}{2\gamma_{Ia}\bar{c}_{Ia} C_1 C_2 M}\left[1 - \left(\frac{v}{S^*_{v_2}}\right)^2\right] G$$

In the problem at hand,

$$\bar{c}_{IL} = 1500 \text{ ft./sec.}$$

$$\bar{c}_{Ia} = 2000 \text{ ft./sec.}$$

$$\gamma_{Ia} = 1.2$$

$$C_1 = 0.65$$
$$C_2 = 1.0$$
$$\nu = 2$$
$$S_{D_3}^* = 3.06$$

We choose $\epsilon_o = 0.3$ as a maximum chamber amplitude permissible.* Also

$$M = \left\{ 3C_0^2 \pi / [2\gamma_{z_1}(1 + |\cos^3 2\pi L/\lambda|)] \right\}^{1/2}$$

The larger value for L/λ is chosen since this value will give a larger value for the above M and, in turn, a smaller value for the product $f_L\sigma$. For this value of L/λ ($= 0.0407 < 0.1$), the orifice flow should be assumed to operate in a quasi-steady manner, so that handbook values for C_D should be used. Values for C_D depend upon the ratio L/D where D is the orifice diameter. If we restrict L/D such that

$$2 \leq L/D \leq 5$$

then the minimum values for C_D (conservative values for liner design) are near 0.75. Assuming that this restriction is permissible, we obtain

$$M = [(3)(0.75)^2(3.14)/(2)(1.3)(1 + 0.903)]^{1/2}$$
$$= 1.03$$

The value for G is obtained from Eqs. (3.2-13 to 15). Substitution gives

$$G = -(1 + 1.2)\cdot 0.2/2\cdot 1 + 0.4/2\cdot 1 + 0$$
$$+ \frac{1.2\cdot 0.2\cdot 0.6\cdot(1 - \cos 2\cdot\pi\cdot 970\cdot 5\cdot 10^{-4})(1 - e^{-2})}{2\cdot 1(1 - e^{-2})(1 + 0)}$$
$$- \frac{0.1\cdot 0.2[(e^2 - 1)(1 + 1) - 2\cdot 1(1 + 1)]}{2\cdot 2\cdot 1\cdot 0.1\cdot 2(e^2 - 1)} - 0$$
$$= -0.22 + 0.2 + 0 + 0.144 - 0.0343 - 0$$
$$= 0.09$$

*Such a value corresponds to a 9% pressure amplitude.

we then obtain

$$f_L \sigma > \frac{0.3 \cdot 1500}{2 \cdot 1.2 \cdot 2000 \cdot 0.65 \cdot 1.0 \cdot 1.03} \left[1 - \left(\frac{2}{3.06}\right)^2\right] 0.09$$

$$> 0.00724$$

Condition 3: Place the lined surface at or very near the injector-wall corner of the chamber.

Optimum Designs: Up until now, the following requirements have been placed on the liner geometry

$$L = 1 \text{ inch}$$
$$A/V = 0.815 \text{ ft}^{-1}$$
$$f_L \sigma > 0.00724$$
$$2 \leq L/D \leq 5$$

We note that the above restriction on L/D was made for concreteness, and that, for a different chosen range, the minimum value of $f_L\sigma$ would change slightly. There are an infinite number of ways to satisfy these requirements. One particular example is the following

$$L = 1 \text{ inch}$$
$$D = 3/8 \text{ inch}$$
$$A = 7.65 \times 10^{-4} \text{ ft}^2$$
$$V = 9.4 \times 10^{-4} \text{ ft}^3$$
$$f_L = 1/10$$
$$\sigma = 7.25\%$$

Further specifications as to the shape of the backing volume, the geometry, and spacing of the holes, as well as other particular choices for D, f_L, and σ should be dictated in specific applications.

CHAPTER 4

Special Considerations

The previous chapter was concerned with the problem of optimum design in which there are no significant constraints imposed on the design. In this chapter we deal with certain other problems that are expected to occur in practice. The first of these problems will be to evaluate the performance of a given liner with a given position in the combustion chamber. Another problem is that, in some applications, there will be some uncertainty in the quantities that must be known in order that the methods of the previous chapter be applied. Also, there will be cases in which certain constraints are imposed on the design (i.e., volume limitations, liner placement restrictions, etc). Suggestions for handling those latter problems are also provided here. It is also expected that a particular application may contain a mixture of various problems. It is hoped that the designer can utilize the knowledge in handling specific problems in these more complicated situations.

4.1 Evaluating the Performance of a Given Liner Design

In order to determine whether or not a given liner design will provide chamber stability, the designer must know the chamber geometry, the specific instability mode, the

position of the liner in the chamber, the quantities listed in Sec. (3.2) (the comments provided after this list should be useful here), the parameter $\mathcal{K} = A\,\lambda/V$, the parameter $\omega = 2\pi\, L/\lambda$, the fraction of lined surface area f_L, the percent open area ratio of the liner σ, the orifice mean flow velocity parameter $\bar{u}$, the local values for the chamber flow components $\bar{U}_I$, e, g, and the local value of the angle ψ. These last five quantities can be calculated by use of the methods presented in Appendix A.

In order to calculate the parameters $\bar{u}$, $\bar{U}_I$, e, g, one must know the nondimensional chamber oscillatory amplitude $a^2\epsilon^2$. If, however, there is no orifice mean flow, and the position of the liner is near pressure antinodal positions (maximum pressure amplitudes), these quantities need not be calculated since their effects are negligible. If, on the other hand, there is substantial orifice mean flow, and/or the position of the liner is near a pressure node, one must evaluate the design for particular values of ϵ_p.* For validity of the underlying theory, ϵ should be a number small compared to unity. For spontaneous instability, ϵ_p will be ralatively small, whereas for triggered instability ϵ_p will be relatively large. It is suggested that the calculations of this section be done for a few values of ϵ_p, ranging from a value near the noise level of smooth combustion to a value equal to the largest permissible (before damage occurs) or to a value $\epsilon_p \approx 0.3$, whichever is smaller. The liner configuration tested will provide stability is it is stable for all values of ϵ_p.

*We can choose a = 1 here.

The liner performance evaluation is then accomplished by

(1) Solve for the constants M and N by one of the following methods.

(a) for no liner-mean-through flow, solve Eqs. (2.2-9 and 10)

(b) if there is a liner-mean-through flow, solve Eqs. (2.2-6 and 7) together with the auxiliary equations given in Appendix B.

Method (b) can, of course, be used if the liner-mean-through flow is zero, although Method (a) is then much simpler. A computer program for the solution of the necessary equations for (a) & (b) and instructions for its use are given in Appendix D.

(2) Check to see that the instability frequency of the combined chamber-liner configuration is close to the initial instability frequency; i.e., make sure that

$$f_\ell \sigma N \lambda^* \lambda' / \epsilon_p \tilde{\omega}^2 \quad < \quad \text{about } 0.1 \tag{4.1-1}$$

If this condition is not fulfilled, proceed to Step (3). If it is fulfilled, proceed to Step (6). Note that, if the liner geometry is the resonant geometry, N = 0, and this condition will be satisfied.

(3) Calculate a new instability frequency from

$$(\tilde{\omega})_{new} = (\tilde{\omega})_{original} + f_\ell \sigma N \lambda^* \lambda' / \epsilon_p (\tilde{\omega})_{original} \tag{4.1-2}$$

and then re-do Step (1) with the new frequency $\tilde{\omega}_{new}$. New values for M and N will be obtained (M_{new}, N_{new}). The previous

values for M and N are called M_{old} and N_{old}.

(4) Check to see if

$$|N_{new} - N_{old}| / N_{old} < \text{about } 0.1$$

of if Condition (4.1-1) is fulfilled. If either are fulfilled, retain the values of $\tilde{\omega}_{new}$, M_{new} and N_{new}, and proceed to Step (6). If neither are fulfilled, proceed to Step (5).

(5) Calculate a new instability frequency from Eq. (4.1-2), where $\tilde{\omega}_{original}$ is the <u>same</u> value as it was in that step. Call the present values of M_{new} and N_{new}, M_{old} and N_{old} respectively. Re-do Step (1) with the value $\tilde{\omega}_{new}$ and obtain new values for M_{new} and N_{new}. Go to Step (4).

(6) Check to see if Condition (I-2) of Section (3.2) is satisfied, using the value for M_{new}, and not that value given by Eq. (3.2-10). If this condition is satisfied, the liner should provide chamber stability for that value of ϵ_p.

4.2 Uncertainties in the Chamber Speed of Sound and the Instability Frequency

If the liner design is such that the orifice length L is very small compared to the wavelength λ (L/λ < about 0.1) uncertainties in the chamber speed of sound $\bar{c}_I$ and the instability angular frequency ω^*, and consequently the wavelength of oscillation ($\lambda = 2\pi\bar{c}_I/\omega^*$) will not be very consequential provided the liner-mean-through-flow velocity is not excessively large ($\bar{u}$ less than about 0.3), and any one of Conditions A-1 to A-4 of Section (2.2) is satisfied. Such results are due to the resulting large band-widths. In other cases, such uncertainties

may be consequential. It is then suggested that any calculations performed be done for a minimum, maximum and intermediate value of λ, making sure, of course, that any criteria to be satisfied be satisfied for all cases.

The above comments concerning uncertainties in λ also apply to uncertainties in any other quantity (L, A, etc.)

4.3 Optimization in Volume-Limited Situations

In many design problems, the volume occupied by the liner must be held to a bare minimum. Important in relation to these problems are the facts that 1) the quarter-wave geometry will possess the smallest resonant volume possible (in comparison to the sum of the orifice volume and cavity volume for the Helmholtz resonator), and 2) the quarter-wave (or some multiple quarter-wave) geometry possesses maximum response. Such results follow from the solution to the liner response given in Sec. (2.2). In view of such results, it would be highly desirable to incorporate quarter-wave tubes in the design. Although it is true that the band-width of such devices is relatively small, one might overcome this difficulty by incorporating tubes of various lengths that vary about (only up to about 5%) of the resonant length of 1/4 wavelength. With the knowledge of the quantities listed in Sec. (3.1) (the discussion of the entire section should also be useful here), since the length L is now determined, the design could be accomplished for these devices by simply

1) Choosing f_L and σ (or A) such that Condition (I-2) of Sec. (3.2) is satisfied.

2) Satisfying Conditions (I-3) of Sec. (3.2).

In some cases, merely minimizing the volume is not a sufficient design solution, and 1/4 wave tubes connot be employed. Such cases may occur when the length of such tubes is prohibitive, or if the resulting band-width is too narrow; e.g. if errors in the knowledge of λ overshadows any attempt to increase the liner band-width by utilizing several tubes of slightly different length. One may then want to utilize Helmholtz resonators, but yet still keep the backing volume V to a minimum. We assume here that the value of V is given, and in most cases, this means that the fraction of lined surface area f_L will also be given. The problem considered here then is to find the values of A and L and the corresponding optimum value of σ. In all cases, this method will provide for an off-resonant design, so that the difference between the instability frequency of the chamber-liner configuration and the instability frequency of the chamber alone might be significant. If the chamber flow effects are significant (the liner is placed in regions of pressure nodes), we caution that proceeding to a design even slightly off resonance may be dangerous. The reason for this danger is that uncertainties in λ, A, L, etc., may result in actual designs that operate in regions where the real part of the liner admittance is negative (see Sect. 2.2).

The method of approach is described as follows. For chamber stability, the objective is to make the product $\sigma f_L M$ large enough (see Condition II-2, Sec. (3.2)). As already

mentioned, if the backing-volume V is given, then f_L will usually be given so that these quantities can be considered fixed. For a given instability frequency and a given volume V, as one varies A, the quantity M passes through a maximum. This maximum occurs at a point which is essentially the resonant point for that frequency (Sec. 2.2). On the other hand, for fixed volume V (and f_L), the quantity σ will increase linearly as A increases. Thus, the product σ M will always become a maximum at a value of A that is larger than the resonant value and thus at a frequency that is larger than the liner resonant frequency. The difference between the liner resonant frequency and the relative-optimum frequency will increase as the peak of M vs. A becomes broader (i.e., as ϵ increases). Calculations will be necessary in order to find out where the product σ M maximizes.

In order to carry out the method, the designer must know the quantities discussed in Section (3.1) (the discussion of the entire section should also be useful here), and the backing volume V (from which f_L can usually be found). As in the previous sections, the calculations must be done for particular values of ϵ, say ϵ_o. Also, if velocity effects are important (the liner placement is near a pressure node), and if the liner-mean-flow is sufficiently large ($|\bar{u}|$ > about 0.3), the proper flow parameters must also be specified. The previous sections of this chapter and Chapter 3 contain information that will guide one in calculating the flow parameters $\bar{U}_I$ e, g, and $\bar{U}_{II}$, the liner-mean-flow parameter $\bar{u}$, as well as in choosing the amplitude ϵ_o.

The procedure for this section then becomes

1. Choose a convenient value of $\omega = 2\pi L/\lambda$, and solve for M and N for various values of A in the parameter $\mathcal{H} = A\lambda/V$ (both λ and V are fixed). This solution can be accomplished by one of the following methods:

(a) for no liner-mean-through flow, solve Eqs. (2.2-9 and 10),

(b) if there is a liner-mean-through flow, solve Eqs. (2.2-6 and 7) together with the auxiliary equations given in Appendix B.

Method (b) can be used if the liner-mean-through flow is zero, although Method (a) is then simpler. A computer program for the solution of the equations necessary for (a) and (b) and instructions for its use are given in Appendix D.

2. Calculate the corresponding values of σ as a function of A from

$$\sigma = A/A_L \qquad (4.3\text{-}1)$$

where A_L is the total lined surface area (perforated area plus non-perforated area).

3. Plot the product σM vs A and choose the value of A where the product is maximum. Call this value A_{op} and the corresponding values σ_{op}, M_{op}, N_{op}.

4. Evaluate the above liner geometry by the procedure presented in Sec. (4.1). Step (1) of that procedure has already been performed here. If the liner does not provide stability, choose another permissible value for $\omega = 2\pi L/\lambda$ and repeat this entire procedure. If a value of ω cannot

be chosen such that the liner provides stability, the designer must allow for more backing-volume, and consequently, larger values of f_L if an effective acoustic liner is to be employed.

APPENDIX A

Acoustic Modes

This appendix contains the solutions for the acoustic modes in rectangular, circular-cylindrical, and annular-cylindrical chambers. These results were taken from Reference (8). The effect of an acoustic liner on the frequency of any acoustic mode is given at the end of this appendix.

Rectangular Combustors

The coordinate system for this geometry is illustrated in Fig. (A-1). In what follows, all lengths are nondimensionalized with respect to the chamber width w, velocity with

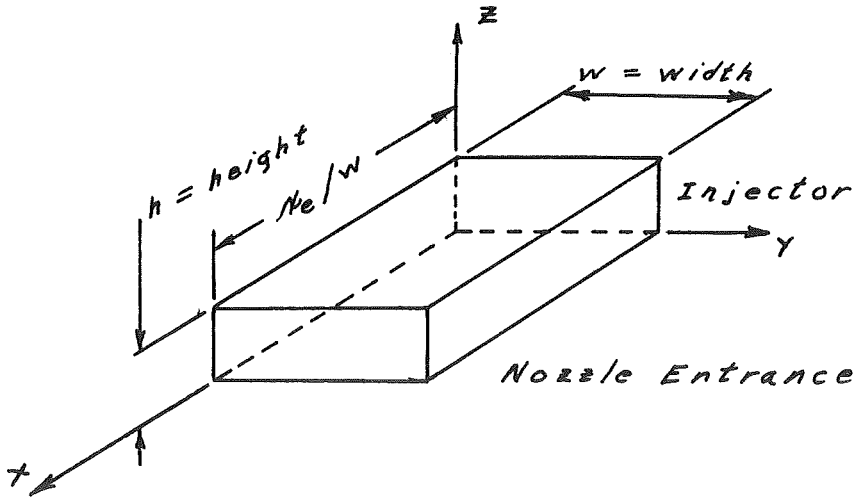

Figure (A-1)

respect to the average chamber-mean-speed of sound $\bar{c}_{Ia}$, and thermodynamic properties with respect to their chamber-mean-static values. Nondimensional time equals physical time multiplied by $\bar{c}_{Ia}/w$.

The nondimensional pressure is given by

$$p_I = 1 + P \cos j\pi \frac{x}{\kappa_e} \cos m^* y \cos n^* z \cos \omega t \qquad \text{(A-1)}$$

where

$$\kappa_e = \text{chamber length/chamber width} \qquad \text{(A-2)}$$

The nondimensional velocities in the x, y, and z directions are given respectively below

$$u = \bar{u}_I + P \frac{j\pi}{\gamma \tilde{\omega} \kappa_e} \sin j\pi \frac{x}{\kappa_e} \cos m^* y \cos n^* z \sin \omega t \qquad \text{(A-3)}$$

$$v = P \frac{m^*}{\gamma \tilde{\omega}} \cos j\pi \frac{x}{\kappa_e} \sin m^* y \cos n^* z \sin \omega t \qquad \text{(A-4)}$$

$$w = P \frac{n^*}{\gamma \tilde{\omega}} \cos j\pi \frac{x}{\kappa_e} \cos m^* y \sin n^* z \sin \omega t \qquad \text{(A-5)}$$

The nondimensional chamber angular frequency $\tilde{\omega}$ is given by

$$\tilde{\omega} = \sqrt{\lambda^{*2} + \frac{j^2 \pi^2}{\kappa_e^2}} \qquad \text{(A-6)}$$

where

$$\lambda^{*2} = m^{*2} + n^{*2} \qquad \text{(A-7)}$$

From the nondimensional scheme, the dimensional angular frequency ω^* is related to $\tilde{\omega}$ in the following way

$$\omega^* = \bar{c}_I \tilde{\omega} / w \qquad \text{(A-8)}$$

In the above, j is an integer:

$$j = 0, 1, 2, \ldots \tag{A-9}$$

When j = 0, it can be seen from Eqs. (A-3 to 5) that the mode is purely transverse, and when j is nonzero, the mode is either purely longitudinal or mixed longitudinal-transverse. If one knows the particular instability mode, j will also be known. The number m* is zero or any integer multiple of π.

$$m^* = i\pi \,, \quad i = 0, 1, 2, \ldots \tag{A-10}$$

The number n* is such that

$$n^* \zeta = l\pi \,, \quad l = 0, 1, 2, \ldots \tag{A-11}$$

where

ζ = chamber height/chamber width (A-12)

Longitudinal modes occur when m* = n* = 0. The constant P is an amplitude that cannot be determined from a linear analysis. This quantity must be estimated when specific numerical results are needed. Suggestions for this estimate are given, where needed, in the main sections of this manual.

The notation of Sec. (2.1) can now be expressed in the following way (dropping the subscript ℓ of Sec. 2.1).

$$\epsilon = p^{1/2} \tag{A-13a}$$

$$a = \left(\cos j\pi \frac{x}{x_e} \cos m^* y \cos n^* z \right)^{1/2} \tag{A-13b}$$

$$\bar{v}_z = \bar{a}_z / \epsilon \tag{A-14}$$

$$e = 0 \tag{A-15}$$

$$q = \frac{p}{\gamma \tilde{\omega} \epsilon} \left\{ \left(\frac{j\pi}{x_e} \sin j\pi \frac{x}{x_e} \cos m^* y \cos n^* z \right)^2 + \left(m^* \cos j\pi \frac{x}{x_e} \sin m^* y \cos n^* z \right)^2 + \left(n^* \cos j\pi \frac{x}{x_e} \cos m^* y \sin n^* z \right)^2 \right\}^{1/2} \quad \text{(A-16)}$$

$$\omega = \angle \tilde{\omega} / w \quad \text{(A-17)}$$

$$\psi = \text{Arctan}\left[(\omega^2 + \nu^2)^{1/2} / (u - \bar{u}_x) \right] + k'\pi \quad \text{(A-18)}$$

where

$$k' = \begin{cases} 0, & u - \bar{u}_x \geq 0 \\ 1, & u - \bar{u}_x < 0 \end{cases} \quad \text{(A-19)}$$

From Eq. (A-15) we notice that only standing modes are permitted in such chambers and the chamber pressure is always 90° out of phase with the chamber velocity. From Eq. (A-18), we notice that, for transverse modes (j = 0). $\psi = \pi/2$, for longitudinal modes (j ≠ 0). $\psi = 0$, and for mixed transverse-longitudinal modes (j ≠ 0) the angle ψ will, in general, oscillate with time.

Circular-Cylindrical and Annular-Cylindrical Combustors

The coordinate system for the annular-cylindrical geometry is illustrated in Fig. (A-2). For this geometry, all physical

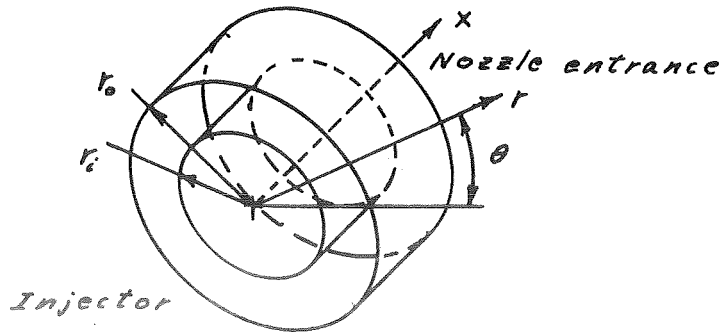

Figure A-2

lengths are nondimensionalized with respect to the outside chamber radius, r_o, velocity with respect to the chamber-mean speed of sound $\bar{c}_I$, and thermodynamic properties with respect to their chamber-mean-static values. Nondimensional time equals the physical time multiplied by $\bar{c}_I/r_o$. The case of a circular-cylindrical combustor arises in the special case when the inner wall radius r_i equals zero.

The nondimensional pressure is now

$$p_z = 1 + \cos j\pi \frac{x}{\kappa_e} \psi_{\nu j}(r)\left[P\cos(\omega t + \nu\theta) + Q\cos(\omega t - \nu\theta) \right] \tag{A-20}$$

where κ_e is the ratio of chamber length to chamber outer radius. The nondimensional velocities in the x, r, and θ directions are then respectively

$$u = \bar{u}_I + \frac{1}{\gamma\tilde{\omega}} \frac{j\pi}{\kappa_e} \sin j\pi \frac{x}{\kappa_e} \psi_{\nu j}(r)\left[P\sin(\omega t + \nu\theta) + Q\sin(\omega t - \nu\theta) \right] \tag{A-21}$$

$$v = -\frac{S^*_{\nu j}}{\gamma\tilde{\omega}} \cos j\pi \frac{x}{\kappa_e} \frac{d}{d(S^*_{\nu j} r)} \psi_{\nu j}(r)\left[P\sin(\omega t + \nu\theta) + Q\sin(\omega t - \nu\theta) \right] \tag{A-22}$$

$$w = -\frac{\nu}{\gamma\tilde{\omega}} \cos j\pi \frac{x}{\kappa_e} \frac{1}{r} \psi_{\nu j}(r)\left[P\cos(\omega t + \nu\theta) - Q\cos(\omega t - \nu\theta) \right] \tag{A-23}$$

The nondimensional-chamber-angular frequency, $\tilde{\omega}$, is given by

$$\tilde{\omega} = \sqrt{\lambda^{*2} + \frac{j^2\pi^2}{\kappa_e^2}} \tag{A-24}$$

where

$$\lambda^{*2} = S^{*2}_{\nu j} \tag{A-25}$$

From the nondimensional scheme, the dimensional angular frequency, ω^*, is related to $\tilde{\omega}$ in the following way

$$\omega^* = \bar{c}_I \tilde{\omega} / r_o \qquad \text{(A-26)}$$

where r_o is the radius of the outer chamber wall.

In these expressions, j and ν are either zero or an integer:

$$j = 0, 1, 2, \ldots \qquad \text{(A-27)}$$

$$\nu = 0, 1, 2, \ldots \qquad \text{(A-28)}$$

Thus, when $j = 0$, the mode is transverse, when $j \neq 0$, the mode is either longitudinal or mixed transverse-longitudinal. When both j and ν are zero, the mode is purely radial. If the particular instability mode is known, both j and ν will be determined. See Tables (A-1 and 2) for further explanation.

The function $\psi_{\nu\eta}(r)$ is a linear combustion of Bessel functions; namely,

$$\psi_{\nu j}(r) = J_\nu(\lambda^* r) + B^* Y_\nu(\lambda^* r) \qquad \text{(A-29a)}$$

where $\lambda^* = S^*_{\nu\eta}$ and B* are determined from

$$\frac{d}{dr} J_\nu(r)\Big|_{r = S^*_{\nu j}} \frac{d}{dr} Y_\nu(r)\Big|_{r = S^*_{\nu j}} - \frac{d}{dr} J_\nu(r)\Big|_{r = S^*_{\nu j}} \frac{d}{dr} Y_\nu(r)\Big|_{r = S^*_{\nu j}} = 0 \qquad \text{(A-30a)}$$

and

$$B^* = - \frac{d}{dr} J_\nu(r)\Big|_{r = S^*_{\nu j}} \Big/ \frac{d}{dr} Y_\nu(r)\Big|_{r = S^*_{\nu j}} \qquad \text{(A-31)}$$

where

ξ = chamber inner radius/chamber outer radius (A-32)

For full chambers ($\xi = 0$), Eqs. (A-29a and 30a) specialize to

$$\psi_{\nu j}(r) = J_\nu(\lambda^* r) \tag{A-29b}$$

$$\frac{d}{dr} J_\nu(r)\Big|_{r = S^*_{\nu j}} = 0 \tag{A-30b}$$

so that B* is then zero.

Roots of Eq. (A-30b) are given in Table (A-1), and were obtained from Ref. (12). Roots of Eq. (A-30a) are given in Table (A-2), and additional values can be found in Ref. (13).

The amplitudes P and Q are constants that must be estimated. Only in certain special cases will this estimation be necessary for design work. In particular, for spinning modes, Q = 0. For standing modes in which there exists nodal points, P = Q. In other cases of standing modes, two measurements can serve to determine P and Q: at the point where the pressure oscillations are maximum ($(p')_{max}$), $P + Q = (p')_{max} / \cos j\pi \frac{x}{x_e} \psi_{\nu\eta}(r)$, and where the pressure oscillations are minimum ($(p')_{min}$), $P - Q = (p')_{min} / \cos j\pi \frac{x}{x_e} \psi_{\nu\eta}(r)$. Further suggestions are provided, where necessary, in the main section of this manual.

The notation of Sec. (2.1) can now be expressed as

$$\epsilon = \left[\sqrt{P^2 + Q^2}\right]^{1/2} \tag{A-33a}$$

$$a = \left[\cos j\pi \frac{x}{x_e} \psi_{\nu j}(r)\right]^{1/2} \tag{A-33b}$$

Table A-1

ACOUSTIC MODES IN CIRCULAR-CYLINDRICAL CHAMBERS

1. Roots of $J'_\nu(\pi\alpha) = 0$

$\alpha_{\nu\eta}$ is the η^{th} root of $J'_\nu(\pi\alpha) = 0$

$S^*_{\nu\eta}$ is obtained by multiplying the corresponding values of $\alpha_{\nu\eta}$ by π

$\alpha_{\nu\eta} = \frac{1}{\pi} S^*_{\nu\eta}$	$\eta = 1$	$\eta = 2$	$\eta = 3$	$\eta = 4$	$\eta = 5$
$\nu = 0$	0.000	1.220	2.233	3.238	4.241
$\nu = 1$	0.586	1.697	2.714	3.726	4.731
$\nu = 2$	0.972	2.135	3.173	4.192	5.204
$\nu = 3$	1.337	2.551	3.612	4.643	5.662
$\nu = 4$	1.693	2.955	4.037	5.082	6.110

2. Meaning of ν, η, amd j

Both ν and η give the transverse character of the mode. The value of ν gives the tangential number of the mode, and $\nu = 0$ means the transverse character can only be radial. The value of $(\eta - 1)$ gives the radial number of the mode, and $\eta = 1$ means the transverse character can only be tangential. The value of j gives the longitudinal character of the mode, and $j = 0$ means the mode can only be transverse.

Examples: $j = 0$, $\nu = 0$, $\eta = 2$ means 1^{st} radial
$j = 0$, $\nu = 1$, $\eta = 1$ means 1^{st} tangential
$j = 0$, $\nu = 2$, $\eta = 3$ means combined 2^{nd} tangential, 2^{nd} radial
$j = 1$, $\nu = 0$, $\eta = 2$ means mixed first longitudinal, first radial

The acoustic frequency is given by $f = \frac{\bar{c}}{2\pi r_o} Ia \sqrt{S^{*2}_{\nu\eta} + \frac{\pi^2 j^2}{x_e^2}}$

TABLE A-2

ACOUSTIC MODES IN ANNULAR-CYLINDRICAL CHAMBERS

Values of $\hat{S}^*_{\nu\eta}$ in $J'_\nu(\hat{S}^*_{\nu\eta})\, Y'_\nu(\xi\, \hat{S}^*_{\nu\eta}) - J'_\nu(\xi\, \hat{S}^*_{\nu\eta})\, Y'_\nu(\hat{S}^*_{\nu\eta}) = 0$, where $S^*_{\nu\eta} = \frac{1}{\xi}\hat{S}^*_{\nu\eta}$

$\xi = \frac{1}{1.1}$	ν / η	1	2	3	4	5	6	7	8	9	10	11	12
	1	0.953	1.905	2.858	3.811	4.764	5.716	6.669	7.621	8.574	9.526	10.478	11.430
	2	31.441	31.485	31.560	31.658	31.787	31.944	32.129	32.341	32.580	32.845	33.135	33.450

$\xi = \frac{1}{1.2}$	ν / η	1	2	3	4	5	6	7	8	9	10	11	12
	1	0.910	1.820	2.731	3.640	4.550	5.458	6.367	7.274	8.181	9.087	9.992	10.896
	2	16.754	15.834	15.966	16.150	16.382	16.663	16.988	17.356	17.765	18.210	18.692	19.206
	3	31.439	31.478	31.545	31.638	31.756	31.901	32.070	32.265	32.485	32.728	33.995	33.285

$\xi = \frac{1}{1.5}$	ν / η	1	2	3	4	5	6	7	8	9	10	11	12
	1	0.805	1.608	2.407	3.200	3.981	4.760	5.525	6.280	7.025	7.760	8.486	9.205
	2	6.377	6.538	6.800	7.153	7.587	8.090	8.653	9.266	9.921	10.610	11.327	12.065
	3	12.613	12.693	12.825	13.008	13.240	13.519	13.842	14.206	14.610	15.050	15.523	16.028
	4	18.881	18.934	19.022	19.145	19.302	19.492	19.715	19.969	20.254	20.568	20.910	21.278
	5	25.156	25.196	25.262	25.355	25.473	25.617	25.786	25.981	26.199	26.441	26.706	26.994
	6	31.435	31.466	31.519	31.593	31.688	31.804	31.941	32.097	32.274	32.470	32.686	32.921
	7	37.715	37.741	37.785	37.847	37.926	38.023	38.137	38.268	38.416	38.581	38.763	38.961

The meaning of ν, η, and j for annular-cylindrical chamber is the same as that for circular-cylindrical chambers. See Table (A-1).

The acoustic frequency is given by $f = \frac{c_{Ia}}{2\pi r_o}\sqrt{S^{*2}_{\nu\eta} + \frac{\pi^2 j^2}{x_e^2}}$ where r_o is the outer radius.

$$\bar{U}_I = \bar{a}_I / \epsilon \tag{A-34}$$

$$e = -\frac{\sqrt{P^2+Q^2}}{\epsilon}\,\frac{\nu}{\gamma\tilde{\omega}}\cos j\pi\frac{x}{x_e}\,\frac{1}{r}\,\psi_{\nu\eta}(r) \tag{A-35}$$

$$q = \left\{\frac{\sqrt{P^2+Q^2}}{\epsilon}\,\frac{1}{\gamma\tilde{\omega}}\left[\left(\frac{j\pi}{x_e}\sin j\pi\frac{x}{x_e}\,\psi_{\nu\eta}(r)\right)^2 + \left(S^*_{\nu\eta}\cos j\pi\frac{x}{x_e}\,\psi'_{\nu\eta}(r)\right)^2\right]\right\}^{1/2} \tag{A-36}$$

$$\omega = \angle\tilde{\omega}/r_0 \tag{A-37}$$

and

$$\psi = \text{Arctan}\left[(\nu^2+\omega^2)^{1/2}/(u-\bar{u})\right] + k'\pi \tag{A-38}$$

where

$$k' = \begin{cases} 0\,, & u-\bar{u} \geq 0 \\ 1\,, & u-\bar{u} < 0 \end{cases} \tag{A-39}$$

Thus, for mixed longitudinal-transverse modes ($j \neq 0$), the angle ψ will, in general, oscillate with time. For purely transverse modes ($j = 0$), $\psi = \pi/2$, and for purely longitudinal modes, ($\nu = S^*_{\nu\eta} = 0$), $\psi = 0$.

Frequency Corrections

In an actual combustor, the instability frequencies differ slightly from the acoustic-mode frequencies given above. Certain effects not present in the acoustic-mode solution account for this difference. The effects of a nozzle, liner, and combustion response have been considered in Ref. (8), and we present these results here. The liner considered is a full-length liner with uniform admittance and with no liner-mean-through flow. The results can be expressed by a correction ω' to the above values of $\tilde{\omega}$ as follows

$$\tilde{\omega}' = \tilde{\omega} + \omega' \tag{A-40}$$

where $\tilde{\omega}'$ is the corrected frequency. The results are

$$\omega' = \mathcal{E}_I / A_j \kappa_e - \lambda^* \lambda' \mathcal{L}_I / \tilde{\omega} + \bar{M}_e n \sin \omega^* \tau^* / A_j \kappa_e \tag{A-41}$$

See the Table of Nomenclature for the definitions of these quantities. $\mathcal{E}_I$ is the imaginary part of the nozzle admittance. If $\mathcal{E}_I$ is not known, one might exclude the first term of the above equation and consider the dimensional chamber length x_e^* as the actual chamber length plus 2/3 of the nozzle contraction section. One could consider partial-length liners in an approximate way by considering the imaginary part of the liner admittance $\mathcal{L}_I$ appearing above as

$$\mathcal{L}_I = f_L \mathcal{L}_{Ip} \tag{A-42}$$

where p denotes the value for the partial-length liner and f_L is defined in Chapter 3.

If the mean flow Mach number at the nozzle entrance $\bar{M}_e$ is large, one could approximately account for its effect on the longitudinal "component" of the frequency by correcting the $(j\pi/x_e)^2$ term in Eqs. (A-6 and 24) in the following way

$$\left[(j\pi/\kappa_e)^2\right]_{flow} = \left[(j\pi/\kappa_e)^2\right]_{\substack{no \\ flow}} (1 - \bar{M}_e^2)^2 \tag{A-43}$$

APPENDIX B

Definition of Constants and Auxiliary Equations

The constants in Eqs. (2.2-6,7) are:

$$A_{2,0} = [\alpha_1(\phi_1^c - \phi_1^A) + \beta_1 \Delta\tau_1 + \delta_1(\phi_1^A + 2\pi - \phi_1^c - \Delta\tau_1)]/2\pi + [(\alpha_5 - \beta_5)(\sin\phi_1^c - \sin\phi_1^A) + (\alpha_4 - \beta_4)(\cos\phi_1^A - \cos\phi_1^c) + (\alpha_3 - \beta_3)(\sin 2\phi_1^c - \sin 2\phi_1^A)/2 + (\alpha_2 - \beta_2)(\cos 2\phi_1^A - \cos 2\phi_1^c)/2]/\pi \quad \text{(B-1)}$$

$$A_{1,1} = 1/\gamma + [(\alpha_1 - \beta_1)\sin\phi_1^c + (\delta_1 - \alpha_1)\sin\phi_1^A + (\beta_1 - \delta_1)\sin(\phi_1^c + \Delta\tau_1) + (\alpha_2 - \beta_2)(\cos\phi_1^A + \cos 3\phi_1^A/3 - \cos\phi_1^c - \cos 3\phi_1^c/3)/2 + (\alpha_3 - \beta_3)(-\sin\phi_1^A - \sin 3\phi_1^A/3 + \sin\phi_1^c + \sin 3\phi_1^c/3)/2 + (\alpha_4 - \beta_4)(\cos 2\phi_1^A - \cos 2\phi_1^c)/4 + (\alpha_5 - \beta_5)(\sin 2\phi_1^c - \sin 2\phi_1^A)/4 + \alpha_5\phi_1^B/2 + \beta_5(2\pi - \phi_1^B)/2]/\pi \quad \text{(B-2)}$$

$$A_{2,0} = [\phi_2^A(\delta_6 - \beta_6) + \phi_2^c(\beta_6 - \delta_6) + \Delta\tau_2(\alpha_6 - \beta_6) + 2\pi\delta_6]/2\pi + [\delta_{10}(\sin\phi_2^A - \sin\phi_2^c) + \delta_9(\cos\phi_2^c - \cos\phi_2^A) + \delta_8($$

$$\sin 2\phi_2^A - \sin 2\phi_2^C)/2 + \delta_7(\cos 2\phi_2^C - \cos 2\phi_2^A)/2]/\pi \quad \text{(B-3)}$$

$$A_{2,1} = [\alpha_6(\sin(\phi_2^A + \Delta\tau_2) - \sin\phi_2^A) + \beta_6(\sin\phi_2^C - \sin(\phi_2^A + \Delta\tau_2)) + \delta_6(\sin\phi_2^A - \sin\phi_2^C) + \delta_7(\cos\phi_2^C + \cos 3\phi_2^C/3 - \cos\phi_2^A - \cos 3\phi_2^A/3)/2 + \delta_8(\sin\phi_2^A + \sin 3\phi_2^A/3 - \sin\phi_2^C - \sin 3\phi_2^C/3)/2 + \delta_9(\cos 2\phi_2^C - \cos 2\phi_2^A)/4 + \delta_{10}(\sin 2\phi_2^A - \sin 2\phi_2^C)/4 + \delta_{10}(2\pi - \phi_2^B)/2]/\pi \quad \text{(B-4)}$$

$$B_{1,1} = [(\alpha_1 - \beta_1)(\cos\phi_1^A - \cos\phi_1^C) + (\delta_1 - \beta_1)(\cos(\phi_1^C + \Delta\tau_1)) + (\alpha_2 - \beta_2)(-\sin\phi_1^A + \sin 3\phi_1^A/3 + \sin\phi_1^C - \sin 3\phi_1^C/3)/2 + (\alpha_3 - \beta_3)(-\cos\phi_1^A + \cos 3\phi_1^A/3 + \cos\phi_1^C - \cos 3\phi_1^C/3)/2 + (\alpha_4 - \beta_4)(\sin 2\phi_1^A - \sin 2\phi_1^C)/4 + (\alpha_5 - \beta_5)(\cos 2\phi_1^A - \cos 2\phi_1^C)/4 + \alpha_4\phi_1^B/2 + \beta_4(2\pi - \phi_1^B)/2]/\pi \quad \text{(B-5)}$$

$$B_{2,1} = [\alpha_6 (\cos\phi_2^A - \cos(\phi_2^A + \Delta\tau_2)) + \beta_6 (\cos(\phi_2^A + \Delta\tau_2) - \cos\phi_2^C) + \delta_6 (\cos\phi_2^C - \cos\phi_2^A) + \delta_7 (\sin\phi_2^A - \sin 3\phi_2^A/3 - \sin\phi_2^C + \sin 3\phi_2^C/3)/2 + \delta_8 (\cos\phi_2^A - \cos 3\phi_2^A/3 - \cos\phi_2^C + \cos 3\phi_2^C/3)/2 + \delta_{10} (\cos 2\phi_2^C - \cos 2\phi_2^A)/4 + \delta_9 (\sin 2\phi_2^C - \sin 2\phi_2^A)/4 + \delta_9 (2\pi - \phi_2^B)/2] / \pi \quad \text{(B-6)}$$

where

$$\alpha_1 = -R^2/4C_D^2 - \bar{u}^2/2C_D^2 + (2\bar{U}_I^2 + e^2 + g^2)/4 \quad \text{(B-7)}$$

$$\alpha_2 = MN/2C_D^2 + eg/2 \quad \text{(B-8)}$$

$$\alpha_3 = -(M^2 - N^2)/4C_D^2 + (e^2 - g^2)/4 \quad \text{(B-9)}$$

$$\alpha_4 = \bar{U}_I g \cos\psi + \bar{u} N/C_D^2 \quad \text{(B-10)}$$

$$\alpha_5 = \bar{U}_I e \cos\psi - \bar{u} M/C_D^2 \quad \text{(B-11)}$$

$$\alpha_6 = \bar{C}_{pII} \bar{U}_{II}^2/2 + (\bar{\eta}_T - \bar{\alpha})/(\gamma_I - 1) \quad \text{(B-12)}$$

$$\beta_1 = \bar{C}_{pI} (2\bar{U}_I^2 + e^2 + g^2)/4 \quad \text{(B-13)}$$

$$\beta_2 = \bar{C}_{pI} eg/2 \quad \text{(B-14)}$$

$$\beta_3 = \bar{C}_{pI} (e^2 - g^2)/4 \quad \text{(B-15)}$$

$$\beta_4 = \bar{C}_{pI} \bar{U}_I g \cos\psi \quad \text{(B-16)}$$

$$\beta_5 = \bar{C}_{pI} \bar{U}_I e \cos\psi \quad \text{(B-17)}$$

$$\delta_6 = -\bar{u}^2/2C_D^2 - R^2\cos^2\omega/4C_D^2 + \bar{U}_{II}^2/2 + (\bar{z}_T - \bar{\alpha})/(\gamma_I - 1) \quad \text{(B-18)}$$

$$\delta_7 = MN\cos^2\omega/2C_D^2 \quad \text{(B-19)}$$

$$\delta_8 = -(M^2 - N^2)\cos^2\omega/4C_D^2 \quad \text{(B-20)}$$

$$\delta_9 = \bar{u}N\cos\omega/C_D^2 \quad \text{(B-21)}$$

$$\delta_{10} = -\bar{u}M\cos\omega/C_D^2 \quad \text{(B-22)}$$

If $\bar{u} = 0$ or if Eqs. (B-31a and 32b) can be satisfied:

$$\delta_1 = -\bar{\alpha}/\gamma_I + \bar{C}_{pI}(2\bar{U}_I^2 + e^2 + g^2)/4 \quad \text{(B-23a)}$$

$$\beta_6 = \bar{C}_{pII}\bar{U}_{II}^2/2 + (\gamma_I\bar{z}_T - \bar{\alpha})/\gamma_I(\gamma_I - 1) \quad \text{(B-24b)}$$

If $\bar{u} < 0$ and Eq. (B-32a) cannot be satisfied:

$$\delta_1 = -\bar{\alpha}/\gamma_I + \bar{C}_{pI}(2\bar{U}_I^2 + e^2 + g^2)/4 \quad \text{(B-23b)}$$

$$\beta_6 = \alpha_6 = \bar{C}_{pII}\bar{U}_{II}^2/2 + (\bar{z}_T - \bar{\alpha})/(\gamma_I - 1) \quad \text{(B-24b)}$$

If $\bar{u} > 0$ and Eq. (B-31a) cannot be satisfied:

$$\delta_1 = \beta_1 = \bar{C}_{pI}(2\bar{U}_I^2 + e^2 + g^2)/4 \quad \text{(B-23c)}$$

$$\beta_6 = \bar{C}_{pII}\bar{U}_{II}^2/2 + (\gamma_I\bar{z}_T - \bar{\alpha})/\gamma_I(\gamma_I - 1) \quad \text{(B-24c)}$$

In addition

$$\varphi_1^A = -\text{Arccos}(-\bar{u}/R) - \text{Arctan}(N/M) - k\pi \quad \text{(B-25)}$$

$$\varphi_1^B = 2\,\text{Arccos}(-\bar{u}/R) \quad \text{(B-26)}$$

If $\cos\omega > 0$:

$$\varphi_2^A = -\text{Arccos}(-\bar{u}/R\cos\omega) - \text{Arctan}(N/M) - k\pi \quad \text{(B-27a)}$$

$$\varphi_2^B = 2\,\text{Arccos}(-\bar{u}/R\cos\omega) \quad \text{(B-28a)}$$

If $\cos \omega < 0$:

$$\phi_2^A = \text{Arccos}(-\bar{u}/R\cos\omega) - \text{Arctan}(N/M) - k\pi \quad \text{(B-27b)}$$

$$\phi_2^B = 2\,\text{Arccos}(\bar{u}/R\cos\omega) \quad \text{(B-28b)}$$

also,

$$\phi_1^C = \phi_1^A + \phi_1^B \,, \quad \phi_2^C = \phi_2^A + \phi_2^B \quad \text{(B-29)}$$

$$k = 0 \text{ if } M \geq 0 \,, \text{ or } = 1 \text{ if } M < 0 \quad \text{(B-30)}$$

The following equations can serve as implicit definitions for $\Delta\tau_1$ and $\Delta\tau_2$. Such equations are necessary only when $\bar{u} \neq 0$. If $\bar{u} = 0$, the correct result can be obtained by setting $\Delta\tau_1 = \Delta\tau_2 = 0$ in the above expressions. In all of the following three sets of equations, one must consider $\omega \ll 1$. If a solution exists for the first set of two equations, then that is the proper solution.

$$\omega - \epsilon\left[-\Delta\tau_1\,\bar{u} + R(1 - \cos\Delta\tau_1)\right] = 0 \quad \text{(B-31a)}$$

$$\omega - \epsilon\left[\Delta\tau_2\,\bar{u} + R(1 - \cos\Delta\tau_2)\right] = 0 \quad \text{(B-32a)}$$

For $\bar{u} < 0$, if ω is so large (but still $\omega \ll 1$) that a solution to Eq. (B-32a) does not exist, then the proper set is

$$2\bar{u}\,\text{Arccos}(-\bar{u}/R) + \bar{u}\Delta\tau_1 + \sqrt{R^2 - \bar{u}^2}\,(\cos\Delta\tau_1 + 1) - \bar{u}\sin\Delta\tau_1 = 0 \quad \text{(B-31b)}$$

$$\Delta\tau_2 = 0 \quad \text{(B-32b)}$$

For $\bar{u}>0$, if ω is so large (but still $\omega\ll 1$) that a solution to Eq. (B-31a) does not exist, then the proper set is

$$\Delta\tau_1 = 0 \tag{B-31c}$$

$$2\bar{a}\,\mathrm{Arccos}(-\bar{a}/R) - \bar{a}\Delta\tau_2 + \sqrt{R^2-\bar{a}^2}\,(\cos\Delta\tau_2 + 1) + \bar{a}\sin\Delta\tau_2 - 2\pi\bar{a} = 0 \tag{B-32c}$$

The constants for Eqs. (2.2-9,10) are

$$F_1 = [\bar{U}_I^2 + (e^2+g^2)/2](1-\bar{C}_{PI}) + \bar{U}_{II}^2|\cos\omega|(1-\bar{C}_{PII}) \tag{B-33}$$

$$F_2 = (e^2-g^2)(1-\bar{C}_{PI})/3 \tag{B-34}$$

$$F_3 = 2eg(1-\bar{C}_{PI})/3 \tag{B-35}$$

$$F_4 = \pi\bar{U}_I g\cos\psi(\bar{C}_{PI}+1)/2 \tag{B-36}$$

$$F_5 = \pi\bar{U}_I e\cos\psi(\bar{C}_{PI}+1)/2 \tag{B-37}$$

APPENDIX C

Local Liner Effects

In this appendix, we obtain, by a method similar to that used by Cantrell and Hart[11], an expression for the acoustic growth coefficient for a volume V enclosed by a surface S. The difference between the approach here and the one in the reference is that the ordering assumed in the flow quantities is consistent with that presented in Chapter 2. It will thus be necessary to proceed to third order for the surface flow quantities.

The basic assumptions here are that volume-loss (or gain) mechanisms are omitted, and that the flow field is irrotational and isentropic. The basic equations can be found in the reference, and the energy equation can be written as follows (analogous to Eq. (14) of the reference).

$$
\begin{aligned}
&\left\langle \frac{d}{dt}\int_V dV \left\{ \left[\rho \left(c_v T + v^2/2 \right) \right]_2 \right\} \right\rangle = \\
&- \left\langle \int_S d\vec{s} \cdot \left\{ \vec{m}_1 \left(h + v^2/2 \right)_1 + \vec{m}_1 \left(h + v^2/2 \right)_2 \right.\right. \\
&+ \vec{m}_2 \left(h + v^2/2 \right)_0 + \vec{m}_2 \left(h + v^2/2 \right)_1 \\
&+ \vec{m}_0 \left(h + v^2/2 \right)_2 + \vec{m}_0 \left(h + v^2/2 \right)_3 \\
&\left.\left. + \vec{m}_3 \left(h + v^2/2 \right)_0 \right\} \right\rangle
\end{aligned}
\qquad \text{(C-1)}
$$

where the symbols of the flow quantities are dimensional and have their conventional meanings, subscripts denote the order of the perturbation (e.g. $\vec{v} = \vec{v}_o + \vec{v}_1$, etc.) and $< >$ denotes a time average much larger than a period of oscillation but yet much smaller than any transient time. Utilizing the continuity and momentum equations, the above can be rearranged to (analogous to Eq. (15) of the reference).

$$< \frac{d}{dt} \int_v dV \{ [\rho (c_v T + v^2/2)]_2 - \rho_2 (h + v^2/2)_o - \vec{m}_o \cdot \vec{v}_2 \} > = - < \int_s d\vec{s} \cdot \{ \vec{m}_1 (h + v^2/2)_1 + \vec{m}_1 (h + v^2/2)_2 + \vec{m}_2 (h + v^2/2)_1 \} > \quad \text{(C-2)}$$

Performing the indicated expansions, utilizing the equation of state and the isentropic relation, considering that p_1, ρ_1, v_o, v_1^2 are all of the same order at the surface but that p_1, ρ_1, v_o, v_1 are all of the same order in the volume, with $p_2 \ll p_1$, $\rho_2 \ll \rho_1$, $v_2 \ll v_1$ everywhere, the above becomes (analogous to Eq. (16) of the reference).

$$< \frac{d}{dt} \int_v dV \{ p_1^2/2\rho_o c_o^2 + \rho_o v_1^2/2 \} > = - < \int_s d\vec{s} \cdot \{ p_1 \vec{v}_1 + \rho_o \vec{v}_1 (\vec{v}_o \cdot \vec{v}_1) + \rho_o \vec{v}_1 v_1^2/2 \} > \quad \text{(C-3)}$$

Assuming that any first-perturbation flow quantity $g_1 \sim e^{\alpha^* t^*}$, the above becomes (analogous to Eq. (17) of the reference).

$$2\alpha^* = - \frac{< \int_s ds \{ p_1 v_{1n} + \rho_o v_{1n} (\vec{v}_o \cdot \vec{v}_1) + \rho_o v_{1n} v^2/2 \} >}{< \int_v dV \{ p_1^2/2\rho_o c_o^2 + \rho_o v_1^2/2 \} >} \quad \text{(C-4)}$$

where subscript n denotes normal component.

In the notation of Chapter 2, we have at the surface

$$p_1 = (a\epsilon)^2 \bar{p}_x \cos \omega t \tag{C-5}$$

$$p_0 = \bar{p}_1 \tag{C-6}$$

$$v_{0n} = \sigma \epsilon \bar{c}_x \bar{u} \tag{C-7}$$

$$v_{0t} = \epsilon \bar{c}_x \bar{v}_x \tag{C-8}$$

$$v_{1n} = \sigma \epsilon \bar{c}_x (M \cos \omega t - N \sin \omega t) \tag{C-9}$$

$$v_{1t} = \epsilon \bar{c}_x (e \cos \omega t + g \sin \omega t) \tag{C-10}$$

where the coefficient a is a function of position and is of order unity or less. In the volume, we can say that

$$p_2 = O(\epsilon^2) \tag{C-11}$$

$$v_1 = O(\epsilon^2) \tag{C-12}$$

Substitution of Expressions (C-5 to 12) in Eq. (C-4), and performing the time averages gives

$$2\alpha^* = -\int_S ds \{ \sigma a^2 \epsilon^3 \bar{p}_x \bar{c}_x M/2 + \sigma (\epsilon \bar{c}_x)^3 \bar{p}_x \bar{v}_x (Me - Ng)/2 + \sigma^3 (\epsilon \bar{c}_x)^3 \bar{p}_x \bar{u} (M^2 + N^2)/2 \} / G \tag{C-13}$$

where G is a positive constant of $O(\epsilon^4)$. Thus we can write

$$\alpha^* = -K \int_S ds \{ (\sigma/\epsilon) [a^2 M/\gamma_x + \bar{v}_x (Me - Ng) + \sigma^2 \bar{u} (M^2 + N^2)] \} \tag{C-14}$$

where K is a positive constant of order unity.

APPENDIX D

Computer Program

This appendix contains a computer program written in Fortran 4, that calculates the liner response by means of the theoretical results presented in Sect. 2.2. The construction of the program is such that it is convenient only for Helmholtz resonators of finite cavity volume V and for half-wave or multiple half-wave tubes. For quarter or multi-quarter wave tubes (V = 0), a different programming technique would be required.

The main program is set up in such a way that caculations will proceed with $\mathcal{K} = A\lambda/V$ as the running variable; i.e., the results will contain information for a plot similar to those presented in Sect. 2.2. Subroutine RNEWT1 solves Equations (2.2-6 and 7) together with any necessary auxiliary equations presented in Appendix B by means of a Newton-Raphson interaction method. This subroutine is used when the orifice-mean-flow velocity ($\bar{u}$) is non-zero, and is restricted to values of $\omega = 2\pi L/\lambda$ less than 0.3. The theory is not valid for larger values. Subroutine RNEWT2 solves Equations (2.2-9) and 10) by a Newton-Raphson method and is used when the orifice-mean-flow velocity is zero. There is no restriction on the value of ω in this program. Subroutine CRAMER merely evaluates a determinant and is necessary for the calculations in subroutine RNEWT1.

Required Inputs

The required input data is the following:

MGUESS - the value of M that will serve as the initial guess for the iteration method at the starting value of the running parameter $\mathcal{K} = A\lambda/V$. For succeeding values of $\mathcal{K}$, the value of MGUESS is chosen as the value of M that is the solution for the previous value of $\mathcal{K}$. If no solution is obtained, then MGUESS is not changed. The value of MGUESS should be fairly close to the solution for M in order that convergence be obtained. For instance, if the solution for M is 2.0, experience indicates that reasonable values for MGUESS would range from about 1.0 to 3.0.

NGUESS - has the same relation to the solution for N as does MGUESS have to the solution for M.

ALPBGU - has the same relation to the solution for $\bar{\alpha}$ as does MGUESS have to the solution for M. This parameter is important only when the orifice-mean-flow velocity ($\bar{u}$) is non-zero (it appears in the auxiliary equation in Appendix B). If $\bar{u} = 0$, one could choose ALPBGU = 1.0. In all cases thus far, a value of 1.0 was found to be sufficiently close to the solution (when $\bar{u} \neq 0$) for convergence to be obtained.

DTAUIG - has the same relation to the solution for $\Delta \tau_1$ as does ALPBGU have to the solution for $\bar{\alpha}$. This parameter also appears in the auxiliary equations presented in Appendix B and is important only when $\bar{u} \neq 0$. If $\bar{u} = 0$, choose DTAUIG = 0.0. In other cases, the proper value will depend on the problem, although it is always true that $0 \leq$ DTAUIG $\leq \pi$. Choosing DTAUIG near unity appears to be good for many cases.

DTAU2G - has the same relation to the solution for $\Delta\tau_2$ as does DTAUIG have to the solution for $\Delta\tau_1$.

ALOVES - the starting value of the running parameter $\mathcal{K} = A\lambda/V$.

DALAMO - the increment of $\mathcal{K} = A\lambda/V$ at which the calculations proceed.

UCZB - the value of $\bar{U}_I$ for which the calculation is desired.

EU - the value of e for which the calculation is desired.

GU - the value of g for which the calculation is desired.

SY - the value of ψ for which the calculation is desired.

CPCB - the value of $\overline{C}_{pI}$ for which the calculation is desired.

UCAZB - the value of $\overline{U}_I$ for which the calculation is desired.

CPCAB - the value of $\overline{C}_{pII}$ for which the calculation is desired.

UZB - the value of $\overline{u}$ for which the calculation is desired.

CD - the value of C_D for which the calculation is desired

PAMP - the value of the local non dimensional chamber pressure amplitude ϵ_ℓ^2 for which the calculation is desired.

W - the value of $\omega = 2\pi\ L/\lambda$ for which the calculation is desired.

ETAB - the value of $\overline{\eta}_T$ for which the calculation is desired. This parameter is important only when $\overline{u} \neq 0$. See Nomenclature for its definition.

GAM - the value of γ for which the calculation is desired.

NUMPTS - the number of values of $\mathcal{K} = A\lambda/V$ for which calculations are desired.

ICASE - a parameter important only when $\overline{u} \neq 0$, and instructs the program on what set of equations to solve. If ICASE = 1, the contact surface in the orifice flow is assumed to pass completely through the orifice. If ICASE = 2, the contact surface is assumed not to pass completely through the orifice. When the solution for ICASE = 1 exists, it is the proper solution. See the example calculations of Sect. 2.2 for further understanding of this aspect of the problem. for most problems, near the resonant point of operation, the proper value of ICASE is 1.

In order to feed in the above input values, one must write the proper values on data cards in the order given above. The parameters MGUESS to GAM must be written in floating point notation (a decimal point must be present) and

the field alloted to each parameter is 10 characters. Since a data card contains space for 80 characters, the first 8 parameters MGUESS to UCZB must be written in the first data card, the next 8 parameters EU to CD must be written on the next data card, and the last 4 parameters must be written on the third data card. Only the first 40 spaces will be utilized on the third data card. The last two parameters NUMPTS and ICASE are integer values (no decimal point) and must be written on the fourth data card. The number of spaces alloted to these parameters is 10 each and both numbers must be right justified; i.e., the integer value of NUMPTS must end at the 10^{th} space, and the integer value of ICASE must end at the 20^{th} space of the fourth data card.

Output

The program output first consists of a presentation of pertinent information characterizing the run. Most of the above input values will be printed out. The calculated results then appear for each value of the parameter κ, written as ALAMOV. Results of each iteration are printed along with the final answer.

When $\bar{u} = 0$, the final answer contains the only two variables M and N, since two simultaneous equations are solved (appearing in the output as F1 = 0 and F2 = 0). When $\bar{u} \neq 0$, the variables M, N. $\bar{\alpha}$ (ALPB), $\Delta\tau$, (DTAU1), and $\Delta\tau_2$ (DTAU2) appear in the calculated results. In general, five simultaneous equations are solved (F1 = 0, F2 = 0, F3 = 0, F4 = 0, and F5 = 0). When the word ANSWER appears before the final

result, that result is considered as a proper solution.

Possible Print-out for Troubled Programs

When difficulty occurs, one or more of the following print-outs will occur.

FOR NONZERO ORIFICE-MEAN-THROUGH-FLOW, W MUST BE SUFFICIENTLY SMALL FOR VALIDITY. VALUE OF W GIVEN IS TOO LARGE.

The underlying theory is restricted to values of w small compared to unity. The program will not run if ω (written as W) is greater than 0.3.

JACOBIAN TOO SMALL, ITERATION WAS STOPPED, BUT LAST RESULTS ARE PRINTED BELOW.

The mathematical technique employed cannot converge if the jacobian is zero. This will happen when there is no solution to the stated problem or when the values of MGUESS, NGUESS, etc. are too far from the solution. When values for M become too largely negative, it has been observed that no solution to the programmed equations exists. This is believed to occur because of certain approximations made in the theory. These regions appear to be too far from resonance to be of practical concern in the optimization problem.

TOO MUCH ITERATION, ITERATION WAS STOPPED, BUT LAST RESULTS ARE PRINTED BELOW

This print-out will occur when there is no solution to the stated problem (M becomes too largely negative), the wrong value for ICASE was chosen (solution of an improper set of equations is attempted), or the values of MGUESS, NGUESS, etc. are too far from the solution.

There are also certain comments concerning the parameter UWIG ($= \tilde{u}_1 = \tilde{u}_2 = \bar{u}/R$). The reason for these comments is that, in the solution, the arc cos of UWIG must be taken. If the magnitude of the orifice mean velocity $\bar{u}$ is too large, UWIG will be greater than unity. Even though the solution for R may be larger than $\bar{u}$, for intermediate values within the iteration, UWIG will be re-defined if a wild point predicts too small a value for R. In the final step of the iteration, no interference is made with UWIG, and if R is then too small, this is interpreted as that a solution for R does not exist that is larger than $\bar{u}$. The theory is not valid in this case. Only smaller values of $\bar{u}$ could be allowed.

Program Listing

At the end of this appendix is presented a listing of the program.

```
      $JOB            TONON
 1          REAL M, N, M2, N2, MGUESS, NGUESS
 2          COMMON MGUESS, NGUESS, ALPBGU, DTAU1G, DTAU2G
 3          COMMON CD, UZB, UCZB, UCAZB, EU, GU, SY, W, PY, APAR, ETAB, GAM
 4          COMMON EPSB, SIG, CPCB, CPCAB
 5          COMMON ICASE
 6          READ(5,101) MGUESS,NGUESS,ALPBGU,DTAU1G,DTAU2G,ALOVES,DALAMO,UCZB
 7          READ(5,101) EU,GU,SY,CPCB,UCAZB,CPCAB,UZB,CD
 8          READ(5,101) PAMP,W,ETAB,GAM
 9        101 FORMAT(8F10.4)
10          READ(5,102) NUMPTS,ICASE
11        102 FORMAT(2I10)
12          PY = 3.1415926536
13          EPSB = PAMP**0.5
      C PRINT-OUT OF GENERAL INFORMATION
14          8 CONTINUE
15            WRITE(6,9)
16          9 FORMAT(/111H ************************************************
             1**********************************************/)
17            WRITE(6,10) UCZB, EU, GU, SY, CPCB
18         10 FORMAT(8H UCZB = ,F10.4,5X, 5HEU = ,F10.4, 5X,5HGU = ,F10.4, 5X,
             1 5HSY = ,F10.4, 5X, 7HCPCB = ,F10.4)
19            WRITE (6,11) UCAZB, CPCAB
20         11 FORMAT (9H UCAZB = ,F10.4, 5X, 8HCPCAB = ,F10.4)
21            WRITE(6,12) CD
22         12 FORMAT(6H CD = ,F10.4,40H, WHAT IS THE ORIFICE FLOW REALLY DOING?)
23            WRITE( 6,13) PAMP, EPSB, GAM,W, ETAB
24         13 FORMAT(8H PAMP = ,F10.4, 5X, 7HEPSB = ,F10.4,5X,6HGAM = ,F10.4,
             1 5X, 4HW = ,F10.4,5X,7HETAB = ,F10.4)
25            IF(UZB) 115,113,115
26        113 WRITE(6,114) UZB
27        114 FORMAT(7H UZB = ,F10.4)
28            GO TO 120
29        115 GO TO (116,118), ICASE
30        116 WRITE(6,117) UZB,ICASE
31        117 FORMAT(7H UZB = ,F10.4,2X,8HICASE = ,I1,64H,  CONTACT SURFACE IS A
             1SSUMED TO PASS COMPLETELY THROUGH ORIFICE)
32            GO TO 120
33        118 WRITE(6,119) UZB,ICASE
34        119 FORMAT(7H UZB = ,F10.4,2X,8HICASE = ,I1,68H,  CONTACT SURFACE IS A
             1SSUMED NOT TO PASS COMPLETELY THROUGH ORIFICE)
35        120 CONTINUE
      C DOING THE DOG-WORK
36         21 CONTINUE
37            ALAMOV = ALOVES
38            NUM = 1
39        821 CONTINUE
40            WRITE(6,921) ALAMOV
41        921 FORMAT(/10H ALAMOV = ,F10.4)
42            IF(UZB) 822,826,822
43        822 IF(W-0.3 ) 825,825,823
44        823 WRITE (6,824)
45        824 FORMAT(105H FOR NONZERO ORIFICE-MEAN-THROUGH-FLOW, W CAN'T BE TOO
             1LARGE FOR VALIDITY. VALUE OF W GIVEN IS TOO LARGE.)
46            GO TO 32
47        825 CALL RNEWT1(M,N,ALPB,DTAU1,DTAU2,ALAMOV,JACOSM,ITERLG,NEAT)
48            GO TO 827
49        826 CALL RNEWT2(M,N,ALAMOV,JACOSM,ITERLG,NEAT)
50        827 CONTINUE
51            IF(JACOSM) 24,24,22
```

```
      22 WRITE(6,23)
      23 FORMAT(87H JACOBIAN TOO SMALL, ITERATION WAS STOPPED, BUT LAST RES
        1ULTS ARE PRINTED DIRECTLY BELOW)
      24 CONTINUE
         IF(ITERLG) 27,27,25
      25 WRITE(6,26)
      26 FORMAT(87H TOO MUCH ITERATION, ITERATION WAS STOPPED, BUT LAST RES
        1ULTS ARE PRINTED DIRECTLY BELOW)
      27 CONTINUE
         IF (NEAT) 728,928,728
     728 MGUESS = M
         NGUESS = N
         IF(UZB) 528,529,528
     528 CONTINUE
         ALPBGU = ALPB
         DTAU1G = DTAU1
         DTAU2G = DTAU2
     529 CONTINUE
         GO TO 929
     928 CONTINUE
         WRITE (6,729)
     729 FORMAT(/80H SOMETHING'S WRONG. SEE ABOVE COMMENT(S). QUANTITIES BE
        1LOW SHOULD NOT BE TRUSTED/)
     929 CONTINUE
C PRINT-OUT OF SPECIFICS
         IF(NEAT) 532,532,530
     530 WRITE(6,531)
     531 FORMAT(8H ANSWER:)
     532 CONTINUE
         IF(UZB) 18,628,18
      18 CONTINUE
         WRITE(6,28) M,N,ALPB,DTAU1,DTAU2
      28 FORMAT(5H M = ,F10.4,5X, 4HN = ,F10.4,5X, 7HALPB = ,F10.4, 5X,
        1 8HDTAU1 = ,F10.4, 5X, 8HDTAU2 = ,F10.4)
         GO TO 30
     628 WRITE(6,629) M,N
     629 FORMAT(5H M = ,F10.4,5X,4HN = ,F10.4)
      30 CONTINUE
         IF(NUM-NUMPTS) 31,32,32
      31 CONTINUE
         ALAMOV = ALAMOV + DALAMO
         NUM = NUM +1
         GO TO 821
      32 CONTINUE
         WRITE(6,9)
      35 RETURN
         END

         SUBROUTINE RNEWT1(M,N,ALPB,DTAU1,DTAU2,ALAMOV,JACOSM,ITERLG,NEAT)
         REAL M, N, M2, N2, MGUESS, NGUESS
         DIMENSION A(5,5)
         DIMENSION ALP1D(2), ALP2D(2), ALP3D(2), ALP4D(2), ALP5D(2),
        1 ALP6D(2), BET1D(2), BET2D(2), BET3D(2), BET4D(2), BET5D(2),
        2 BET6D(2),DEL1D(2), DEL6D(2), DEL7D(2), DEL8D(2), DEL9D(2),
        3 DEL10D(2)
         DIMENSION PHEAD(2), PHEBD(2), PHECD(2)
         DIMENSION G11D(2), G12D(2),G21D(2), G22D(2), XJ1D(2), XJ2D(2)
         DIMENSION RHS(5), DELVAR(5), ASTORE(5)
         COMMON MGUESS, NGUESS, ALPBGU, DTAU1G, DTAU2G
         COMMON CD, UZB, UCZB, UCAZB, EU, GU, SY, W, PY, APAR, ETAB, GAM
```

```
103         COMMON EPSB, SIG, CPCB, CPCAB
104         COMMON ICASE
105         JWIG = 0
106         NEAT = 0
      C INITIAL GUESS
107       1 M = MGUESS
108         N = NGUESS
109         ALPB = ALPBGU
110         DTAU1 = DTAU1G
111         DTAU2 = DTAU2G
      C CALCULATIONS NOT DEPENDING UPON M,N,ALPB,DTAU1,DTAU2
112       2 CONTINUE
113         CD2 = CD*CD
114         UZB2 = UZB*UZB
115         UCZB2 = UCZB*UCZB
116         EU2 = EU*EU
117         GU2 = GU*GU
118         CSY = COS(SY)
119         UCAZB2 = UCAZB*UCAZB
120         SW = W
121         CW = 1.0
122         CW2 = CW*CW
123         SW2 = SW*SW
      C CALCULATIONS IN SOME WAY RELEVANT TO M,N,ALPB,DTAU1,DTAU2
      CC CALCULATION OF VALUES
124         ICOUNT = 0
125         WRITE(6,103)
126     103 FORMAT(102H ITERATION BEGINS WITH POSSIBLE INTERFERENCE WITH UWIG.
           1 PRINT-OUT WILL OCCUR WHEN INTERFERENCE IS MADE)
127       3 CONTINUE
128         IF(ICOUNT-10) 804,804,803
129     803 ITERLG = 1
130         RETURN
131     804 ITERLG = 0
132         M2 = M*M
133         N2 = N*N
134         R = (M2+N2)**0.5
135         R2 = M2+N2
136         R3 = R2*R
137         ALP1 = - R2/(4.0*CD2) - UZB2/(2.0*CD2) + UCZB2/2.0 + (EU2+GU2)/4.0
138         ALP2 = M*N/(2.0*CD2) + EU*GU/2.0
139         ALP3 = -(M2-N2)/(4.0*CD2) +(EU2-GU2)/4.0
140         ALP4 = UCZB*CSY*GU + UZB*N/CD2
141         ALP5 = UCZB*CSY*EU - UZB*M/CD2
142         ALP6 = CPCAB*UCAZB2/2.0 + (ETAB-ALPB)/(GAM-1.0)
143         BET1 = (UCZB2/2.0+(EU2+GU2)/4.0)*CPCB
144         BET2 = EU*GU*CPCB/2.0
145         BET3 = (EU2-GU2)*CPCB/4.0
146         BET4 = UCZB*CSY*GU*CPCB
147         BET5 = UCZB*CSY*EU*CPCB
148         GO TO (704,705), ICASE
149     704 BET6 = UCAZB2*CPCAB/2.0 + (ETAB-ALPB/GAM)/(GAM-1.0)
150         DEL1 = - ALPB/GAM + BET1
151         GO TO 708
152     705 IF(UZB) 706,706,707
153     706 BET6 = ALP6
154         DEL1 = -ALPB/GAM + BET1
155         GO TO 708
156     707 BET6 = UCAZB2*CPCAB/2.0 + (ETAB-ALPB/GAM)/(GAM-1.0)
157         DEL1 = BET1
```

```
158     708 CONTINUE
159         DEL6 = - UZB2/(2.0*CD2) - R2*CW2/(4.0*CD2) + UCAZB2/2.0 +
           1 (ETAB-ALPB)/(GAM-1.0)
160         DEL7 = M*N*CW2/(2.0*CD2)
161         DEL8 = - (M2-N2)*CW2/(4.0*CD2)
162         DEL9 = UZB*N*CW/CD2
163         DEL10 = - UZB*M*CW/CD2
164         UWIG = UZB/R
      CCC KEEPING UWIG<1.0 FOR WILD POINTS
165         IF(JWIG) 904,904,907
166     904 IF(ABS(UWIG)-1.0) 907,905,905
167     905 CONTINUE
168         UWIG = 0.99999999
169         RUF = 0.0001
170         INTERF = 1
171         GO TO 610
172     907 CONTINUE
173         INTERF = 0
174         IF(ABS(UWIG)-1.0) 504,502,502
175     502 WRITE(6,503)
176     503 FORMAT (115H IT SEEMS THAT UZB IS SO LARGE THAT THE TOTAL ORIFICE
           1MOTION IS NON-OSCILLATORY. THEORY IS NOT VALID FOR THIS CASE.)
177         NEAT = 0
178         RETURN
179     504 CONTINUE
180         RUF = (R2-UZB2)**0.5
181     610 CONTINUE
182         IF(M) 4,5,5
183       4 XK = 1.0
184         GO TO 6
185       5 XK = 0.0
186       6 CONTINUE
187         ACMUW = ARCOS(-UWIG)
188         PHEB = 2.0*ACMUW
189         PHEA = - PHEB/2.0 - ATAN(N/M) - XK*PY
190         PHEC = PHEA + PHEB
191         CPHEA = COS(PHEA)
192         CPHEB = COS(PHEB)
193         CPHEC = COS(PHEC)
194         C3PHEA = COS(3.0*PHEA)
195         C3PHEC = COS(3.0*PHEC)
196         C2PHEA = COS(2.0*PHEA)
197         C2PHEC = COS(2.0*PHEC)
198         SPHEA = SIN(PHEA)
199         SPHEB = SIN(PHEB)
200         SPHEC = SIN(PHEC)
201         S3PHEA = SIN(3.0*PHEA)
202         S3PHEC = SIN(3.0*PHEC)
203         S2PHEA = SIN(2.0*PHEA)
204         S2PHEC = SIN(2.0*PHEC)
205         CPCPT1 = COS(PHEC + DTAU1)
206         SPCPT1 = SIN(PHEC + DTAU1)
207         CPAPT2 = COS(PHEA + DTAU2)
208         SPAPT2 = SIN(PHEA + DTAU2)
209         G11 = ( (ALP1-BET1)*SPHEC + (DEL1-ALP1)*SPHEA + (BET1-DEL1)*SPCPT1
           1 + (ALP2-BET2)*(CPHEA/2.0+C3PHEA/6.0-CPHEC/2.0-C3PHEC/6.0) +
           2 (ALP3-BET3)*(-SPHEA/2.0-S3PHEA/6.0+SPHEC/2.0+S3PHEC/6.0) +
           3 (ALP4-BET4)*(C2PHEA-C2PHEC)/4.0 + (ALP5-BET5)*(-S2PHEA+S2PHEC)/4.
           4 + ALP5*PHEB/2.0 + (2.0*PY-PHEB)*BET5/2.0 )/PY
210         G12 = ( -(ALP1-BET1)*CPHEC + (ALP1-DEL1)*CPHEA + (DEL1 -BET1)*
```

```
     1 CPCPT1 + (ALP2-BET2)*(-SPHEA/2.0 +S3PHEA/6.0 + SPHEC/2.0 -S3PHEC/
     2 6.0) + (ALP3-BET3)*(-CPHEA/2.0+C3PHEA/6.0+CPHEC/2.0-C3PHEC/6.0) +
     3 (ALP4-BET4)*(S2PHEA-S2PHEC)/4.0 + (ALP5-BET5)*(C2PHEA-C2PHEC)/4.0
     4 + ALP4*PHEB/2.0 + (2.0*PY-PHEB)*BET4/2.0  )/PY
211   G21 = (  (SPAPT2-SPHEA)*ALP6 + (SPHEC-SPAPT2)*BET6 + (SPHEA-SPHEC)
     1 *DEL6 + (CPHEC/2.0+C3PHEC/6.0-CPHEA/2.0-C3PHEA/6.0)*DEL7 + (SPHEA
     2 /2.0+S3PHEA/6.0-SPHEC/2.0-S3PHEC/6.0)*DEL8 + (C2PHEC-C2PHEA)*
     3 DEL9/4.0 + ( (2.0*PY-PHEB)/2.0 + (S2PHEA-S2PHEC)/4.0)* DEL10  )/
     4 PY
212   G22 = (  (CPHEA -CPAPT2)*ALP6 + (CPAPT2-CPHEC)*BET6 + (CPHEC-CPHEA
     1 )*DEL6 + (SPHEA/2.0-S3PHEA/6.0-SPHEC/2.0+S3PHEC/6.0)*DEL7 +
     2 (CPHEA/2.0-C3PHEA/6.0-CPHEC/2.0+C3PHEC/6.0)*DEL8 + ( (2.0*PY-PHEB
     3 )/2.0 + (S2PHEC-S2PHEA)/4.0 )*DEL9 + (C2PHEC-C2PHEA)*DEL10/4.0  )
     4 /PY
213   XJ1 = (  (DEL1-ALP1)*(PHEA-PHEC) + (BET1-DEL1)*DTAU1 + 2.0*PY*DEL1
     1 + (SPHEA-SPHEC)*(BET5-ALP5)*2.0 + (CPHEA-CPHEC)*(ALP4-BET4)*2.0 +
     2 (S2PHEA-S2PHEC)*(BET3-ALP3) + (C2PHEA-C2PHEC)*(ALP2-BET2)  )/(
     3 2.0*PY)
214   XJ2 = (  (DEL6-BET6)*(PHEA-PHEC) + (ALP6-BET6)*DTAU2 + 2.0*PY*DEL6
     1 + (SPHEA-SPHEC)*DEL10*2.0 + (CPHEC-CPHEA)*DEL9*2.0 + (S2PHEA-
     2 S2PHEC)*DEL8 + (C2PHEC-C2PHEA)*DEL7  )/(2.0*PY)
215    7 CONTINUE
216   F1 = EPSB*G12 - EPSB*G22*CW - EPSB*SW2*N*UZB - (ALAMOV*CW/(2.0*PY)
     1 - SW)*M*CW
217   F2 = - EPSB*(G11 + 1.0/GAM) + EPSB*G21*CW - EPSB*SW2*M*UZB +
     1 (ALAMOV*CW/(2.0*PY)-SW)*N*CW
218   F3 = XJ1 - XJ2 + (GAM-1.0)*SW2*R2/4.0
219  808 CONTINUE
220   GO TO (8,9), ICASE
221    8 CONTINUE
222   F4 = W + EPSB*UZB*DTAU1 - EPSB*R*(1.0-COS(DTAU1))
223   F5 = W - EPSB*UZB*DTAU2 - EPSB*R*(1.0-COS(DTAU2))
224   GO TO 10
225    9 IF(UZB) 909,909,910
226  909 F4 = 2.0*UZB*ACMUW + UZB*DTAU1 + RUF*(1.0+COS(DTAU1)) - UZB*
     1 SIN(DTAU1)
227   F5 = DTAU2
228   GO TO 10
229  910 F4 = DTAU1
230   F5 = 2.0*UZB*ACMUW - UZB*DTAU2 + RUF*(1.0+COS(DTAU2)) + UZB*
     1 SIN(DTAU2) - 2.0*PY*UZB
231   10 CONTINUE
CC CALCULATION OF DERIVATIVES
232   ALP1D(1) = - M/(2.0*CD2)
233   ALP1D(2) = - N/(2.0*CD2)
234   ALP1AB = 0.0
235   ALP2D(1) = N/(2.0*CD2)
236   ALP2D(2) = M/(2.0*CD2)
237   ALP2AB = 0.0
238   ALP3D(1) = ALP1D(1)
239   ALP3D(2) = - ALP1D(2)
240   ALP3AB = 0.0
241   ALP4D(1) = 0.0
242   ALP4D(2) = UZB/CD2
243   ALP4AB = 0.0
244   ALP5D(1) = - UZB/CD2
245   ALP5D(2) = 0.0
246   ALP5AB = 0.0
247   ALP6D(1) = 0.0
248   ALP6D(2)  = 0.0
```

```
      ALP6AB = - 1.0/(GAM-1.0)
      BET1D(1) = 0.0
      BET1D(2) = 0.0
      BET1AB = 0.0
      BET2D(1) = 0.0
      BET2D(2) = 0.0
      BET2AB = 0.0
      BET3D(1) = 0.0
      BET3D(2) = 0.0
      BET3AB = 0.0
      BET4D(1) = 0.0
      BET4D(2) = 0.0
      BET4AB = 0.0
      BET5D(1) = 0.0
      BET5D(2) = 0.0
      BET5AB = 0.0
      GO TO (710,711), ICASE
  710 BET6D(1) = 0.0
      BET6D(2) = 0.0
      BET6AB = - 1.0/(GAM*(GAM-1.0))
      DEL1D(1) = 0.0
      DEL1D(2) = 0.0
      DEL1AB  = - 1.0/GAM
      GO TO 714
  711 IF(UZB) 712,712,713
  712 BET6D(1) = ALP6D(1)
      BET6D(2) = ALP6D(2)
      BET6AB = ALP6AB
      DEL1D(1) = 0.0
      DEL1D(2) = 0.0
      DEL1AB = -1.0/GAM
      GO TO 714
  713 BET6D(1) = 0.0
      BET6D(2) = 0.0
      BET6AB = -1.0/(GAM*(GAM-1.0))
      DEL1D(1) = BET1D(1)
      DEL1D(2) = BET1D(2)
      DEL1AB = BET1AB
  714 CONTINUE
      DEL6D(1) = ALP1D(1)*CW2
      DEL6D(2) = ALP1D(2)*CW2
      DEL6AB = ALP6AB
      DEL7D(1)  = ALP2D(1)*CW2
      DEL7D(2) = ALP2D(2)*CW2
      DEL7AB = 0.0
      DEL8D(1) = ALP3D(1)*CW2
      DEL8D(2) = ALP3D(2)*CW2
      DEL8AB = 0.0
      DEL9D(1) = 0.0
      DEL9D(2) = ALP4D(2)*CW
      DEL9AB = 0.0
      DEL10D(1) = ALP5D(1)*CW
      DEL10D(2) = 0.0
      DEL10A = 0.0
      RM = M/R
      RN = N/R
      UWIGM = -UZB*RM/R2
      UWIGN = - UZB*RN/R2
      PHEBD(1) = 2.0*UWIGM*R/RUP
      PHEBD(2)  = 2.0*UWIGN*R/RUP
```

```
309          PHEAD(1) = - PHEBD(1)/2.0 + N/R2
310          PHEAD(2) = - PHEBD(2)/2.0 - M/R2
311          PHECD(1) = PHEAD(1) + PHEBD(1)
312          PHECD(2) = PHEAD(2) + PHEBD(2)
313       11 CONTINUE
314          G11AB = (DEL1AB*SPHEA - DEL1AB*SPCPT1)/PY
315          G11DT1 = (  (BET1-DEL1)*CPCPT1)/PY
316          G11DT2 = 0.0
317          G12AB = (-DEL1AB*CPHEA + DEL1AB*CPCPT1)/PY
318          G12DT1 = (-(DEL1-BET1)*SPCPT1)/PY
319          G12DT2 = 0.0
320          G21AB = (ALP6AB*(SPAPT2-SPHEA) + BET6AB*(SPHEC-SPAPT2) + DEL6AB*
          1  (SPHEA-SPHEC) )/PY
321          G21DT1 = 0.0
322          G21DT2 = (ALP6-BET6)*CPAPT2/PY
323          G22AB = (ALP6AB*(CPHEA-CPAPT2) + BET6AB*(CPAPT2-CPHEC) + DEL6AB*
          1 (CPHEC-CPHEA)  )/PY
324          G22DT1 = 0.0
325          G22DT2 = (ALP6*SPAPT2 - BET6*SPAPT2 )/PY
326          XJ1AB = (  (PHEA-PHEC-DTAU1+2.0*PY)*DEL1AB  )/(2.0*PY)
327          XJ1DT1 = ( BET1-DEL1)/(2.0*PY)
328          XJ1DT2 = 0.0
329          XJ2AB = ( PHEA*(DEL6AB-BET6AB) + PHEC*(BET6AB-DEL6AB) + DTAU2*(
          1 ALP6AB-BET6AB) + 2.0*PY*DEL6AB)/(2.0*PY)
330          XJ2DT1 = 0.0
331          XJ2DT2 = (ALP6-BET6)/(2.0*PY)
332          J = 1
333       12 CONTINUE
334          G11DA =     (  (ALP1D(J)-BET1D(J))*SPHEC + (ALP1-BET1)*CPHEC*
          1 PHECD(J) + (DEL1D(J)-ALP1D(J))*SPHEA + (DEL1-ALP1)*CPHEA*PHEAD(J)
          2 + (BET1D(J)-DEL1D(J))*SPCPT1 + (BET1-DEL1)*CPCPT1*PHECD(J) +
          3 (ALP2D(J)-BET2D(J))*(CPHEA/2.0+C3PHEA/6.0-CPHEC/2.0-C3PHEC/6.0) +
          4 (ALP2-BET2)*(-SPHEA*PHEAD(J)/2.0-3.0*S3PHEA*PHEAD(J)/6.0+SPHEC*
          5 PHECD(J)/2.0 +3.0*S3PHEC*PHECD(J)/6.0) + (ALP3D(J)-BET3D(J))*(-
          6 SPHEA/2.0-S3PHEA/6.0+SPHEC/2.0+S3PHEC/6.0)  )/PY
335          G11DB =     (  (ALP3-BET3)*(-CPHEA*PHEAD(J)/2.0-3.0*C3PHEA*PHEAD(J)
          1 /6.0 + CPHEC*PHECD(J)/2.0+3.0*C3PHEC*PHECD(J)/6.0) + (ALP4D(J)-
          2 BET4D(J))*(C2PHEA-C2PHEC)/4.0 + (ALP4-BET4)*(-2.0*S2PHEA*PHEAD(J)
          3 +2.0*S2PHEC*PHECD(J))/4.0 + (ALP5D(J)-BET5D(J))*(-S2PHEA+S2PHEC)
          4 /4.0 + (ALP5-BET5)*(-2.0*C2PHEA*PHEAD(J) + 2.0*C2PHEC*PHECD(J))
          5 /4.0 + ALP5D(J)*PHEB/2.0+ALP5*PHEBD(J)/2.0 +BET5D(J)*PY-BET5D(J)*
          6 PHEB/2.0 - BET5*PHEBD(J)/2.0  )/PY
336          G11D(J) = G11DA + G11DB
337          G12DA = (  (BET1D(J)-ALP1D(J))*CPHEC - (BET1-ALP1)*SPHEC*PHECD(J)
          1 + (ALP1D(J)-DEL1D(J))*CPHEA-(ALP1-DEL1)*SPHEA*PHEAD(J) + (DEL1D(J
          2 )-BET1D(J))*CPCPT1 - (DEL1-BET1)*SPCPT1*PHECD(J) +(ALP2D(J)-BET2D
          3 (J))*(-SPHEA/2.0+S3PHEA/6.0+SPHEC/2.0-S3PHEC/6.0) + (ALP2-BET2)*
          4 (-CPHEA*PHEAD(J)/2.0+3.0*C3PHEA*PHEAD(J)/6.0 +CPHEC*PHECD(J)/2.0
          5 - 3.0*C3PHEC*PHECD(J)/6.0) + (ALP3D(J)-BET3D(J))*(-CPHEA/2.0+
          6 C3PHEA/6.0 +CPHEC/2.0-C3PHEC/6.0)  )/PY
338          G12DB = (  ( ALP3-BET3)*(SPHEA*PHEAD(J)/2.0-3.*S3PHEA*PHEAD(J)/6.0
          1 - SPHEC*PHECD(J)/2.0+3.0*S3PHEC*PHECD(J)/6.0)+(ALP4D(J)-BET4D(J))
          2 *(S2PHEA-S2PHEC)/4.0+(ALP4-BET4)*(2.0*C2PHEA*PHEAD(J)-2.0*C2PHEC*
          3 PHECD(J))/4.0 + (ALP5D(J)-BET5D(J))*(C2PHEA-C2PHEC )/4.0 +(ALP5-
          4 BET5)*(-2.0*S2PHEA*PHEAD(J)+2.0*S2PHEC*PHECD(J))/4.0 + ALP4D(J)*
          5 PHEB/2.0 + ALP4*PHEBD(J)/2.0 + BET4D(J)*PY- BET4D(J)*PHEB/2.0 -
          6 BET4*PHEBD(J)/2.0  )/PY
339          G12D(J) = G12DA + G12DB
340          G21DA = (  ALP6D(J)*(SPAPT2-SPHEA) + ALP6*(CPAPT2*PHEAD(J)-CPHEA*
          1 PHEAD(J)) + BET6D(J)*(SPHEC-SPAPT2) + BET6*(CPHEC*PHECD(J)-CPAPT2
```

```
     2 *PHEAD(J)) + DEL6D(J)*(SPHEA-SPHEC) + DEL6*(CPHEA*PHEAD(J)-CPHEC*
     3 PHECD(J)) + DEL7D(J)*(CPHEC/2.0+C3PHEC/6.0-CPHEA/2.0-C3PHEA/6.0)
     4 + DEL7*(-SPHEC*PHECD(J)/2.0-3.0*S3PHEC*PHECD(J)/6.0+SPHEA*PHEAD
     5(J)/2.0 + 3.0*S3PHEA*PHEAD(J)/6.0)  )/PY
341   G21DB = (  DEL8D(J)*(SPHEA/2.0+S3PHEA/6.0-SPHEC/2.0-S3PHEC/6.0)+
     1 DEL8*(CPHEA*PHEAD(J)/2.0+3.0*CPHEA*PHEAD(J)/6.0-CPHEC*PHECD(J)/2.
     2 - 3.0*C3PHEC*PHECD(J)/6.0) + DEL9D(J)*(C2PHEC-C2PHEA)/4.0 + DEL9*
     3 (-2.0*S2PHEC*PHECD(J) +2.0*S2PHEA*PHEAD(J))/4.0 + DEL10D(J)*( (
     4 2.0*PY-PHEB)/2.0 + (S2PHEA-S2PHEC)/4.0) + DEL10*(-PHEBD(J)/2.0 +
     5 (2.0*C2PHEA*PHEAD(J)-2.0*C2PHEC*PHECD(J))/4.0) )/PY
342    G21D(J) = G21DA + G21DB
343    G22DA = (  ALP6D(J)*(CPHEA-CPAPT2) + ALP6*(-SPHEA+SPAPT2)*PHEAD(J)
     1 + BET6D(J)*(CPAPT2-CPHEC) + BET6*(-SPAPT2*PHEAD(J)+SPHEC*PHECD(J)
     2 ) + DEL6D(J)*(CPHEC-CPHEA) + DEL6*(-SPHEC*PHECD(J) +SPHEA*PHEAD(J
     3 )) +DEL7D(J)*( SPHEA/2.0-S3PHEA/6.0-SPHEC/2.0 +S3PHEC/6.0) + DEL7
     4 *(CPHEA*PHEAD(J)/2.0-3.0*C3PHEA*PHEAD(J)/6.0-CPHEC*PHECD(J)/2.0+
     5 3.0*C3PHEC*PHECD(J)/6.0) + DEL8D(J)*(CPHEA/2.0-C3PHEA/6.0-CPHEC/
     6 2.0+C3PHEC/6.0)  )/PY
344    G22DB = (  DEL8*(-SPHEA*PHEAD(J)/2.0+3.0*S3PHEA*PHEAD(J)/6.0+SPHEC
     1 *PHECD(J)/2.0-3.0*S3PHEC*PHECD(J)/6.0) + DEL9D(J)*( (2.0*PY-PHEB)
     2 /2.0 + (S2PHEC-S2PHEA)/4.0) + DEL9*(-PHEBD(J)/2.0 +(2.0*C2PHEC*
     3 PHECD(J)-2.0*C2PHEA*PHEAD(J))/4.0)+  DEL10D(J)*(C2PHEC-C2PHEA)/4.
     4 + DEL10*(-2.0*S2PHEC*PHECD(J) + 2.0*S2PHEA*PHEAD(J))/4.0  )/PY
345    G22D(J) = G22DA + G22DB
346    XJ1DA =  (   PHEAD(J)*(DEL1-ALP1) + PHEA*(DEL1D(J)-ALP1D(J)) +
     1 PHECD(J)*(ALP1-DEL1) + PHEC*(ALP1D(J)-DEL1D(J)) + DTAU1*(BET1D(J)
     2 -DEL1D(J))+ 2.0*PY*DEL1D(J) + 2.0*(CPHEA*PHEAD(J)-CPHEC*PHECD(J))
     3*(BET5-ALP5) + 2.0*(SPHEA-SPHEC)*(BET5D(J)-ALP5D(J)) + 2.0*(-SPHEA
     4 *PHEAD(J) +SPHEC*PHECD(J))*(ALP4-BET4) + 2.0*(CPHEA-CPHEC)*(
     5 ALP4D(J)-BET4D(J))   )/(2.0*PY)
347    XJ1DB = (   2.0*(C2PHEA*PHEAD(J)-C2PHEC*PHECD(J))*(BET3-ALP3) + (
     1 S2PHEA-S2PHEC)*(BET3D(J)-ALP3D(J)) + 2.0*(-S2PHEA*PHEAD(J)+S2PHEC
     2 *PHECD(J))*(ALP2-BET2) + (C2PHEA-C2PHEC)*(ALP2D(J)-BET2D(J))   )/
     3 (2.0*PY)
348    XJ1D(J) = XJ1DA + XJ1DB
349    XJ2DA = (   PHEAD(J)*(DEL6-BET6) + PHEA*(DEL6D(J)-BET6D(J)) +
     1 PHECD(J)*(BET6-DEL6) + PHEC*(BET6D(J)-DEL6D(J)) + DTAU2*(ALP6D(J)
     2 -BET6D(J)) + 2.0*PY*DEL6D(J) + 2.0*(CPHEA*PHEAD(J)-CPHEC*PHECD(J)
     3 )*DEL10 + 2.0*(SPHEA-SPHEC)*DEL10D(J)   )/(2.0*PY)
350    XJ2DB = (   -2.0*(-SPHEA*PHEAD(J) + SPHEC*PHECD(J))*DEL9 - 2.0*(
     1 CPHEA-CPHEC)*DEL9D(J) + 2.0*(C2PHEA*PHEAD(J) - C2PHEC*PHECD(J))*
     2 DEL8 + (S2PHEA-S2PHEC)*DEL8D(J) + 2.0*(-S2PHEC*PHECD(J) + S2PHEA*
     3 PHEAD(J))*DEL7 + (C2PHEC-C2PHEA)*DEL7D(J)   )/(2.0*PY)
351    XJ2D(J) = XJ2DA + XJ2DB
352    IF(J-1) 13,13,14
353   13 CONTINUE
354      G11M = G11D(J)
355      G12M = G12D(J)
356      G21M = G21D(J)
357      G22M = G22D(J)
358      XJ1M = XJ1D(J)
359      XJ2M = XJ2D(J)
360      J = 2
361      GO TO 12
362   14 CONTINUE
363      G11N = G11D(J)
364      G12N = G12D(J)
365      G21N = G21D(J)
366      G22N = G22D(J)
367      XJ1N = XJ1D(J)
```

```
      XJ2N = XJ2D(J)
   15 CONTINUE
      F1M = EPSB*G12M- EPSB*G22M*CW - (ALAMOV*CW/(2.0*PY)-SW)*CW
      F1N = EPSB*G12N - EPSB*G22N*CW - EPSB*SW2*UZB
      F1AB = EPSB*G12AB - EPSB*G22AB*CW
      F1DT1 = EPSB*G12DT1 - EPSB*G22DT1*CW
      F1DT2 = EPSB*G12DT2 - EPSB*G22DT2*CW
      F2M = - EPSB*G11M + EPSB*G21M*CW - EPSB*SW2*UZB
      F2N = - EPSB*G11N + EPSB*G21N*CW + (ALAMOV*CW/(2.0*PY)-SW)*CW
      F2AB = - EPSB*G11AB + EPSB*G21AB*CW
      F2DT1 = - EPSB*G11DT1 + EPSB*G21DT1*CW
      F2DT2 = - EPSB*G11DT2 + EPSB*G21DT2*CW
      F3M = XJ1M - XJ2M + (GAM-1.0)*SW2*2.0*M/4.0
      F3N = XJ1N - XJ2N + (GAM-1.0)*SW2*2.0*N/4.0
      F3AB = XJ1AB - XJ2AB
      F3DT1 = XJ1DT1 - XJ2DT1
      F3DT2 = XJ1DT2 - XJ2DT2
  817 CONTINUE
      GO TO (16,17), ICASE
   16 CONTINUE
      F4M = -EPSB*RM*(1.0-COS(DTAU1))
      F4N = -EPSB*RN*(1.0-COS(DTAU1))
      F4AB = 0.0
      F4DT1 = EPSB*UZB - EPSB*R*SIN(DTAU1)
      F4DT2 = 0.0
      F5M = -EPSB*RM*(1.0-COS(DTAU2))
      F5N = -EPSB*RN*(1.0-COS(DTAU2))
      F5AB = 0.0
      F5DT1 = 0.0
      F5DT2 = -EPSB*UZB - EPSB*R*SIN(DTAU2)
      GO TO 18
   17 IF(UZB) 917,917,918
  917 F4M = 2.0*UZB*UWIGM*R/RUF                    + R*RM*(1.0+COS(DTAU1))
     1 /RUF
      F4N = 2.0*UZB*UWIGN*R/RUF                    + R*RN*(1.0+COS(DTAU1))
     1 /RUF
      F4AB = 0.0
      F4DT1 = UZB-RUF*SIN(DTAU1) - UZB*COS(DTAU1)
      F4DT2 = 0.0
      F5M = 0.0
      F5N = 0.0
      F5AB = 0.0
      F5DT1 = 0.0
      F5DT2 = 1.0
      GO TO 18
  918 F4M = 0.0
      F4N = 0.0
      F4AB = 0.0
      F4DT1 = 1.0
      F4DT2 = 0.0
      F5M = 2.0*UZB*UWIGM*R/RUF                    + R*RM*(1.0+COS(DTAU2))
     1 /RUF
      F5N = 2.0*UZB*UWIGN*R/RUF                    + R*RN*(1.0+COS(DTAU2))
     1 /RUF
      F5AB = 0.0
      F5DT1 = 0.0
      F5DT2 = -UZB - RUF*SIN(DTAU2) + UZB*COS(DTAU2)
   18 CONTINUE
      A(1,1) = F1M
      A(1,2) = F1N
```

```
424           A(1,3) = F1AB
425           A(1,4) = F1DT1
426           A(1,5) = F1DT2
427           A(2,1) = F2M
428           A(2,2) = F2N
429           A(2,3) = F2AB
430           A(2,4) = F2DT1
431           A(2,5) = F2DT2
432           A(3,1) = F3M
433           A(3,2) = F3N
434           A(3,3) = F3AB
435           A(3,4) = F3DT1
436           A(3,5) = F3DT2
437           A(4,1) = F4M
438           A(4,2) = F4N
439           A(4,3) = F4AB
440           A(4,4) = F4DT1
441           A(4,5) = F4DT2
442           A(5,1) = F5M
443           A(5,2) = F5N
444           A(5,3) = F5AB
445           A(5,4) = F5DT1
446           A(5,5) = F5DT2
447           RHS(1) = - F1
448           RHS(2) = - F2
449           RHS(3) = - F3
450           RHS(4) = - F4
451           RHS(5) = - F5
452           WRITE(6,818) ICOUNT,M,N,ALPB,DTAU1,DTAU2
453       818 FORMAT(11H ITERATION-,I2,7H:   M = ,E13.6,2X,4HN = ,E13.6,2X,
              1 7HALPB = ,E13.6,2X,8HDTAU1 = ,E13.6,2X,8HDTAU2 = ,E13.6)
454           WRITE (6,819) F1,F2,F3,F4,F5
455       819 FORMAT(6H F1 = ,E13.6,2X,5HF2 = ,E13.6,2X,5HF3 = ,E13.6,2X,5HF4 =
              1,E13.6,2X,5HF5 = ,E13.6)
456           IF(INTERF) 119,120,119
457       119 WRITE (6,906) UWIG
458       906 FORMAT(53H VALUE OF UWIG PREDICTED FROM PREVIOUS ITERATION WAS ,
              1 E13.6,36H, BUT VALUE USED HERE WAS 0.99999999)
459       120 CONTINUE
460           CALL CRAMER(A,DETERM)
461           XJACO = DETERM
462           WRITE (6,919) XJACO
463       919 FORMAT(12H JACOBIAN = ,E13.6)
464           IF(ABS(XJACO) - 0.0000000001) 19,19,20
465        19 JACOSM = 1
466           RETURN
467        20 JACOSM = 0
468           DO 922 J = 1,5
469           DO 21 I = 1,5
470           ASTORE(I) = A(I,J)
471           A(I,J) = RHS(I)
472        21 CONTINUE
473           CALL CRAMER(A,DETERM)
474           DELVAR(J) = DETERM/XJACO
475           DO 921 I = 1,5
476           A(I,J) = ASTORE(I)
477       921 CONTINUE
478       922 CONTINUE
479           M = M + DELVAR(1)
480           N = N + DELVAR(2)
```

```
481          ALPB = ALPB + DELVAR(3)
482          DTAU1 =  DTAU1 + DELVAR(4)
483          DTAU2 = DTAU2 + DELVAR(5)
484       22 CONTINUE
485          IF(ABS(F1)-0.0001)  23,23,27
486       23 IF(ABS(F2)-0.0001)  24,24,27
487       24 IF(ABS(F3)-0.0001)  25,25,27
488       25 IF(ABS(F4)-0.0001)  26,26,27
489       26 IF(ABS(F5)-0.0001)  28,28,27
490       27 CONTINUE
491          ICOUNT = ICOUNT + 1
492          GO TO 3
      C CHECKING SMOOTH CONVERGENCE
493       28 IF(ABS(M) - 0.000001) 30,29,29
494       29 IF(ABS(DELVAR(1)/M) - 0.01) 30,30,38
495       30 IF(ABS(N) - 0.000001) 32,31,31
496       31 IF(ABS(DELVAR(2)/N) - 0.01) 32,32,38
497       32 IF(ABS(ALPB) - 0.000001) 34,33,33
498       33 IF(ABS(DELVAR(3)/ALPB) - 0.01) 34,34,38
499       34 IF(ABS(DTAU1) - 0.000001) 36,35,35
500       35 IF(ABS(DELVAR(4)/DTAU1) - 0.01) 36,36,38
501       36 IF(ABS(DTAU2) - 0.000001) 40,37,37
502       37 IF(ABS(DELVAR(5)/DTAU2) - 0.01) 40,40,38
503       38 WRITE (6,39)
504       39 FORMAT(50H CONVERGENCE TOO RAPID FOR ONE VARIABLE, TRY AGAIN)
505          ICOUNT = ICOUNT + 1
506          GO TO 3
507       40 CONTINUE
508          IF(JWIG) 41,41,42
509       41 JWIG = 1
510          ICOUNT = 0
511          WRITE(6,141)
512      141 FORMAT(95H ITERATION STARTED AGAIN USING PREVIOUS VALUES, THERE IS
            1 NOW NO POSSIBLE INTERFERENCE WITH UWIG)
513          GO TO 3
514       42 CONTINUE
515       43 IF(DTAU1) 47,44,44
516       44 IF(DTAU2) 47,45,45
517       45 IF(DTAU1-PY) 46,46,47
518       46 IF(DTAU2-PY) 49,49,47
519       47 NEAT = 0
520          WRITE(6,48)
521       48 FORMAT( 83H AT LEAST ONE VARIABLE IS OUTSIDE OF ALLOWABLE RANGE, B
            1UT CALCULATIONS APPEAR BELOW)
522          GO TO 50
523       49 NEAT = 1
524       50 CONTINUE
525          RETURN
526          END

527          SUBROUTINE RNEWT2 (M,N,ALAMOV,JACOSM,ITERLG,NEAT)
528          REAL M, N, M2, N2, MGUESS, NGUESS
529          COMMON MGUESS, NGUESS, ALPBGU, DTAU1G, DTAU2G
530          COMMON CD, UZB, UCZB, UCAZB, EU, GU, SY, W, PY, APAR, ETAB, GAM
531          COMMON EPSB, SIG, CPCB, CPCAB
532          COMMON ICASE
533          NEAT = 0
      C INITIAL GUESS
534        1 CONTINUE
535          M = MGUESS
```

```
536         N = NGUESS
      C CALCULATIONS NOT DEPENDING UPON M,N
537       2 CONTINUE
538         CD2 = CD*CD
539         UCZB2  = UCZB*UCZB
540         EU2 = EU*EU
541         GU2 = GU*GU
542         CSY = COS(SY)
543         UCAZB2 = UCAZB*UCAZB
544         SW = SIN(W)
545         CW = COS(W)
546         CPCBF = 1.0-CPCB
547         CPCABF = 1.0-CPCAB
548         XF1 = (UCZB2 + (EU2+GU2)/2.0)*CPCBF + UCAZB2*(ABS(CW))*CPCABF
549         XF2 = (EU2-GU2)*CPCBF/3.0
550         XF3 = 2.0*EU*GU*CPCBF/3.0
551         XF4 = PY*UCZB*GU*CSY*(CPCB+1.0)/2.0
552         XF5 = PY*UCZB*EU*CSY*(CPCB+1.0)/2.0
      C CALCULATIONS IN SOME WAY RELEVANT TO M,N
      CC CALCULATION OF VALUES
553         ICOUNT = 0
554       3 CONTINUE
555         IF(ICOUNT-10)5,5,4
556       4 ITERLG = 1
557         RETURN
558       5 ITERLG  = 0
559         M2 = M*M
560         N2 = N*N
561         R2 = M2+N2
562         R = R2**0.5
563         M3 = M*M2
564         N3 = N*N2
565         R3 = R*R2
566         R4 = R2*R2
567         CWF = 1.0 + (ABS(CW))**3
568         ALAMOF = ALAMOV*CW - 2.0*PY*SW
569         F1 = EPSB*2.0*CWF*N*R/(3.0*CD2) - EPSB*N*XF1/R + EPSB*(3.0*N/(2.0*
           1 R) - N3/R3)*XF2 + EPSB*M3*XF3/R3 + EPSB*XF4 - 0.5*ALAMOF*CW*M
570         F2 = EPSB*2.0*CWF*M*R/(3.0*CD2) - EPSB*M*XF1/R - EPSB*(3.0*M/(2.0*
           1 R) - M3/R3)*XF2 + EPSB*N3*XF3/R3 - EPSB*XF5 - EPSB*PY/GAM + 0.5*
           2 ALAMOF*CW*N
      CC CALCULATION OF DERIVATIVES
571     104 CONTINUE
572         RM = M/R
573         RN = N/R
574         F1M = EPSB*2.0*CWF*N*RM/(3.0*CD2) + EPSB*N*XF1*RM/R2 + EPSB*(-3.0*
           1 N*RM/(2.0*R2) + 3.0*N3*RM/R4)*XF2 + EPSB*3.0*M2*XF3/R3 - EPSB*3.0
           2 *M3*RM*XF3/R4 - 0.5*(ALAMOF)*CW
575         F1N = EPSB*2.0*CWF*(R+N*RN)/(3.0*CD2) - EPSB*XF1/R + EPSB*N*XF1*RN
           1 /R2 + EPSB*(3.0/(2.0*R) - 3.0*N*RN/(2.0*R2) - 3.0*N2/R3 + 3.0*N3*
           2 RN/R4)*XF2 - EPSB*3.0*M3*RN*XF3/R4
576         F2M = EPSB*2.0*CWF*(R+M*RM)/(3.0*CD2) - EPSB*XF1/R + EPSB*M*RM*XF1
           1 /R2 - EPSB*(3.0/(2.0*R) - 3.0*M*RM/(2.0*R2) - 3.0*M2/R3 + 3.0*M3*
           2 RM/R4)*XF2-EPSB*3.0*N3*RM*XF3/R4
577         F2N = EPSB*2.0*CWF*M*RN/(3.0*CD2) + EPSB*M*RN*XF1/R2 - EPSB*(-3.0*
           1 M*RN/(2.0*R2) + 3.0*M3*RN/R4)*XF2 + EPSB*3.0*N2*XF3/R3 - EPSB*3.0
           2 *N3*RN*XF3/R4 + 0.5*ALAMOF*CW
578         WRITE (6,105) ICOUNT,M,N
579     105 FORMAT(11H ITERATION-,I2,9H:     M = ,E13.6,2X,4HN = ,E13.6)
580         WRITE(6,6) F1,F2
```

```
581       6 FORMAT(6H F1 = ,E13.6,2X,5HF2 = ,E13.6)
      C CHECKING JACOBIAN
582       7 CONTINUE
583         XJACO = F1M*F2N - F1N*F2M
584         WRITE (6,8) XJACO
585       8 FORMAT(12H JACOBIAN = ,E13.6)
586         IF(ABS(XJACO) - 0.0000000001) 9,9,10
587       9 JACOSM = 1
588         RETURN
589      10 JACOSM = 0
590         DELM = (F2*F1N - F1*F2N)/XJACO
591         DELN = (F1*F2M - F2*F1M)/XJACO
592         M = M + DELM
593         N = N + DELN
594      11 CONTINUE
595         IF(ABS(F1) - 0.0001) 12,12,13
596      12 IF(ABS(F2) - 0.0001) 14,14,13
597      13 CONTINUE
598         ICOUNT = ICOUNT + 1
599         GO TO 3
      C CHECKING SMOOTH CONVERGENCE
600      14 CONTINUE
601         IF(ABS(M) - 0.000001) 16,15,15
602      15 IF(ABS(DELM/M) - 0.01) 16,16,18
603      16 IF(ABS(N) - 0.000001) 20,17,17
604      17 IF(ABS(DELN/N) - 0.01) 20,20,18
605      18 CONTINUE
606         WRITE(6,19)
607      19 FORMAT(50H CONVERGENCE TOO RAPID FOR ONE VARIABLE, TRY AGAIN)
608         ICOUNT = ICOUNT + 1
609         GO TO 3
610      20 CONTINUE
611         NEAT = 1
612         RETURN
613         END

614         SUBROUTINE CRAMER(A,DETERM)
615         REAL M, N, M2, N2, MGUESS, NGUESS
616         DIMENSION A(5,5)
617         COMMON MGUESS, NGUESS, ALPBGU, DTAU1G, DTAU2G
618         COMMON CD, UZB, UCZB, UCAZB, EU, GU, SY, W, PY, APAR, ETAB, GAM
619         COMMON EPSB, SIG, CPCB, CPCAB
620         COMMON ICASE
621         JIG1 = 0
622         SUM1 = 0.0
623         DO 100 I1 = 1,5
624         JIG2 = 0
625         SUM2 = 0.0
626         DO 90 I2 = 1,5
627         IF(I2 - I1) 50,90,50
628      50 JIG3 = 0
629         SUM3 = 0.0
630         DO 80 I3 = 1,5
631         IF(I3 - I1) 51,80,51
632      51 IF(I3 - I2) 52,80,52
633      52 JIG4 = 0
634         SUM4 = 0.0
635         DO 70 I4 = 1,5
636         IF(I4 - I1) 53,70,53
637      53 IF(I4 - I2) 54,70,54
```

```
638       54 IF(I4 - I3) 55, 70,55
639       55 DO 60 I5 = 1,5
640          IF(I5 - I1) 56,60,56
641       56 IF(I5 - I2) 57, 60, 57
642       57 IF(I5 - I3) 58,60,58
643       58 IF(I5 - I4) 59,60,59
644       59 SUM5 = A(I5,5)
645       60 CONTINUE
646          IF(JIG4) 62,61,62
647       61 SIGN = 1.0
648          JIG4 = 1
649          GO TO 63
650       62 SIGN = - 1.0
651          JIG4 = 0
652       63 SUM4 = SUM4 + SIGN*A(I4,4)*SUM5
653       70 CONTINUE
654          IF (JIG3) 72,71,72
655       71 SIGN = 1.0
656          JIG3 = 1
657          GO TO 73
658       72 SIGN = - 1.0
659          JIG3 = 0
660       73 SUM3 = SUM3 + SIGN*A(I3,3)*SUM4
661       80 CONTINUE
662          IF(JIG2) 82,81,82
663       81 SIGN = 1.0
664          JIG2 = 1
665          GO TO 83
666       82 SIGN = - 1.0
667          JIG2 = 0
668       83 SUM2 = SUM2 + SIGN*A(I2,2)*SUM3
669       90 CONTINUE
670          IF(JIG1) 92,91,92
671       91 SIGN = 1.0
672          JIG1 = 1
673          GO TO 93
674       92 SIGN = - 1.0
675          JIG1 = 0
676       93 SUM1 = SUM1 + SIGN*A(I1,1)*SUM2
677      100 CONTINUE
678          DETERM = SUM1
679          RETURN
680          END

      $ENTRY
```

REFERENCES

1. Sirignano, W. A., "Nonlinear Dissipation in Acoustic Liners," Section III C in "Nonlinear Aspects of Combustion Instability in Liquid Propellant Rocket Motors," Princeton University Department of Aerospace and Mechanical Sciences Report No. 553-f, June 1966.

2. Tonon, T. S. B., and Sirignano, W. A., "The Nonlinearity of Acoustic Liners with Flow Effects," AIAA 8th Aerospace Sciences Meeting, preprint No. 70-128, January 1970.

3. Tonon, T. S. B., and Sirignano, W. A., "Nonlinear Theories on Acoustic Liner Operation with Flow Effects," Princeton University, Department of Aerospace and Mechanical Sciences, Report No. 885.

4. Sirignano, W. A., "The Nonlinearity of Acoustic Liners," to be published

5. Tonon, T. S. B., and Sirignano, W. A., "Near-resonance, Nonlinear, Harmonic Theories on the Operation of Acoustic Liners," to be published.

6a. Bradbury, L. J. S., and Wood, M. N., "The Static Pressure Distribution Around a Circular Jet Exhausting Normally from a Plane Wall into an Airstream," RAE Tech. Note 2978, 1964.

6b Gelb, G. H., and Martin, W. A., "An Experimental Investigation of the Flow Field About a Subsonic Jet Exhausting into a Quiescent and a Low Velocity Air Stream," Canadian Aeronautics and Space Journal, October, 1966, p. 333.

7. Stinger, W. A., "Theoretical Studies of Flow Behavior with Acoustic Liners," Section IV A, in "Nonlinear Aspects of Combustion Instability in Liquid Propellant Rocket Motors," Princeton University, Department of Aerospace and Mechanical Sciences, Report No. SR-553g, June 1967.

8. Sirignano, W. A., Chapter 3 in Reference Book on Liquid Propellant Rocket Combustion Instability, Harrje, D. T. and Reardon, F. H., editors, NASA SP- in preparation, 1971.

9. "Design Guide for Stable H_2/O_2 Combustors," Volume I, Design Application, George Marshall Space Flight Center NASA, Report 20672-P2D, May 1970.

10. Bracco, F. V., "The 'Direct' Method as Applied to Liquid Rocket Engine Combustion and Explosion Problems," Princeton University, Department of Aerospace and Mechanical Sciences, Ph.D. Thesis, June 1970.

11. Cantrell, R. H., and Hart, R. W., "Interaction between Sound and Flow in Acoustic Cavities: Mass, Momentum, and Energy Considerations," J. Acoustical Soc. Amer., Vol. 36, No. 4, April 1964, p. 697.

12. Morse, P. M., and Feshback, H., Methods of Theoretical Physics, Part II, McGraw-Hill Book Co., Inc. 1953, p. 1565.

13. Bridge, J. F., and Angrist, S. W., "An Extended Table of Roots of $J_n'(x)\ Y_n'(\beta x) - J_n'(\beta x)\ Y_n'(x) = 0$, Mathematics of Computation, No. 16-17, 1962-63, p. 198.

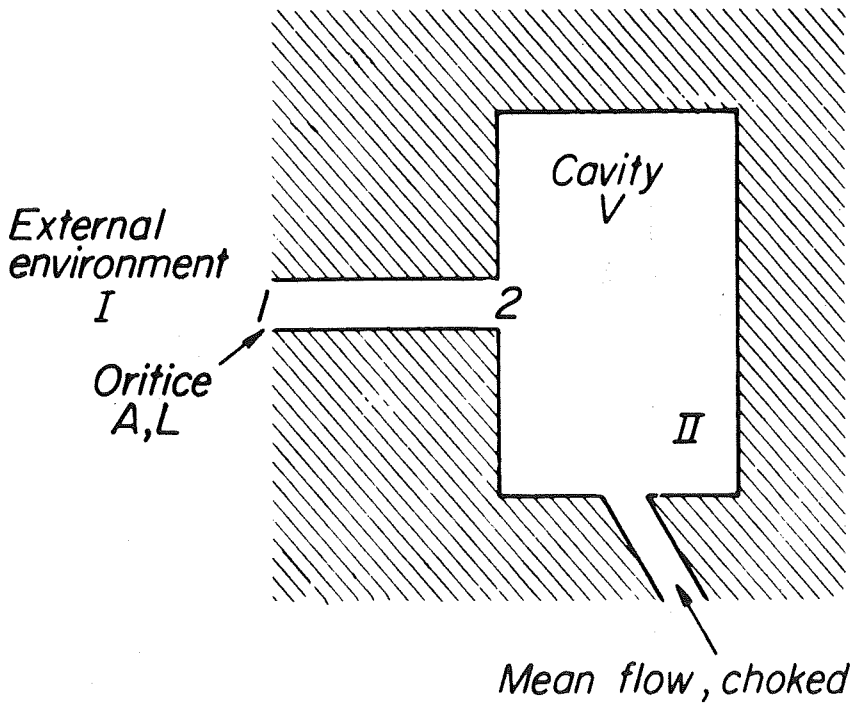

Figure 1 · Problem description

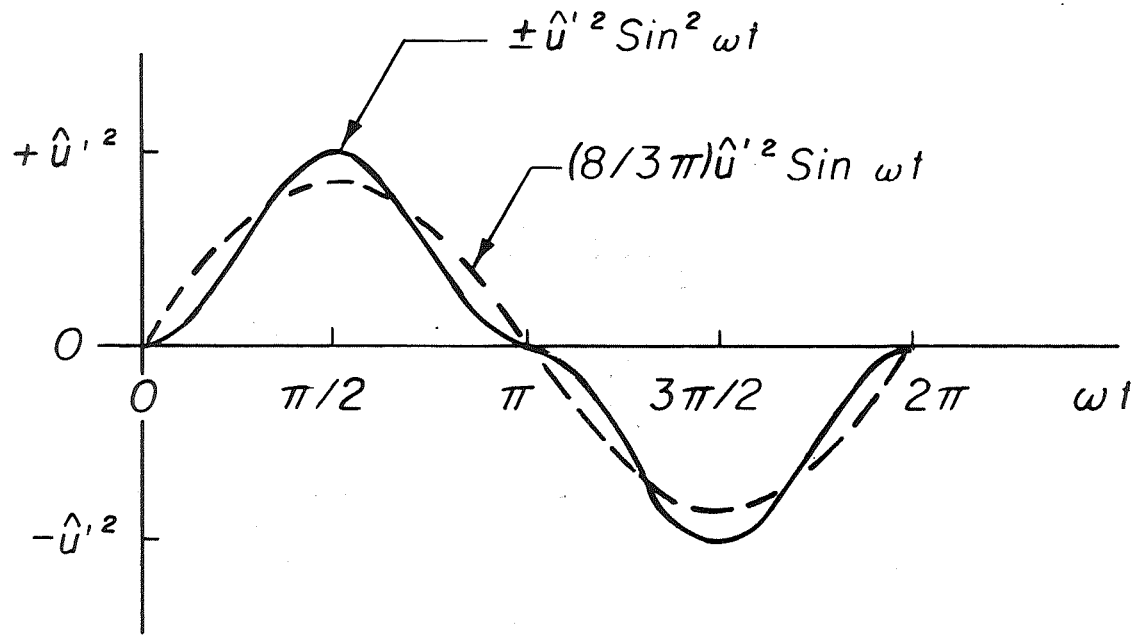

FIGURE 2. Contradiction obtained when orifice velocity is assumed harmonic in the quasi-steady case when flow effects are absent

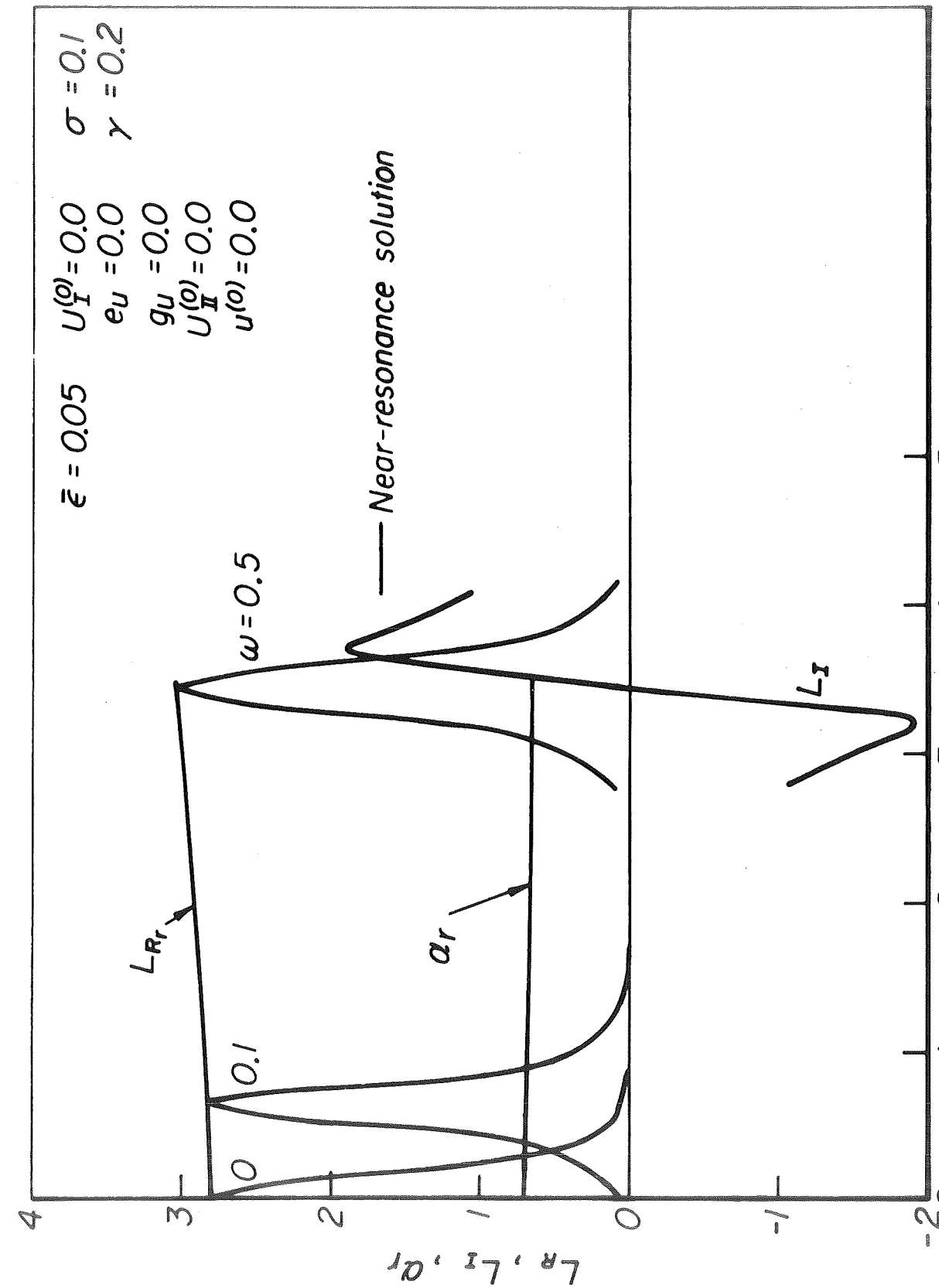

Figure 3a · Smaller amplitude

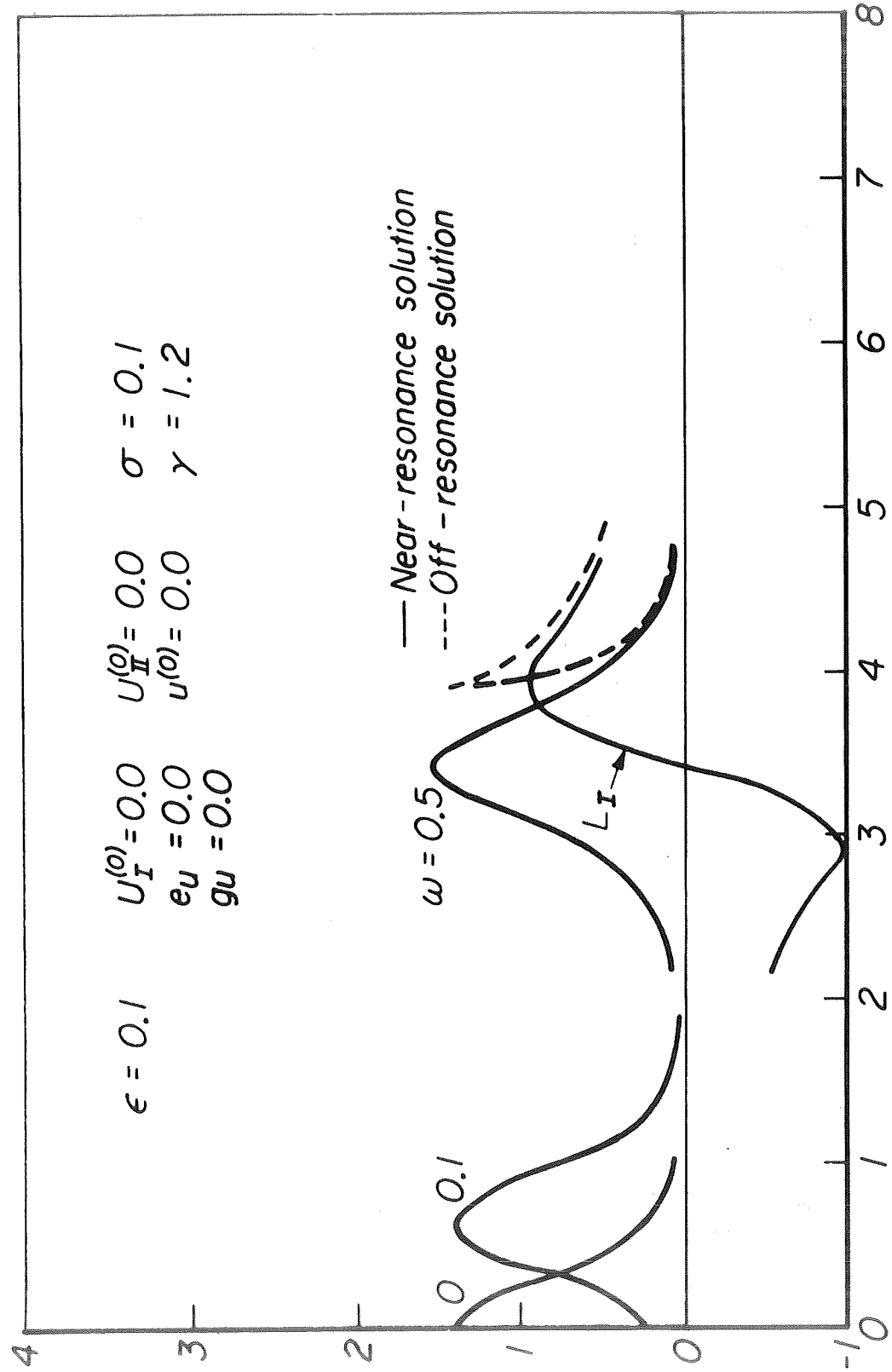

Figure 3b · Larger amplitude

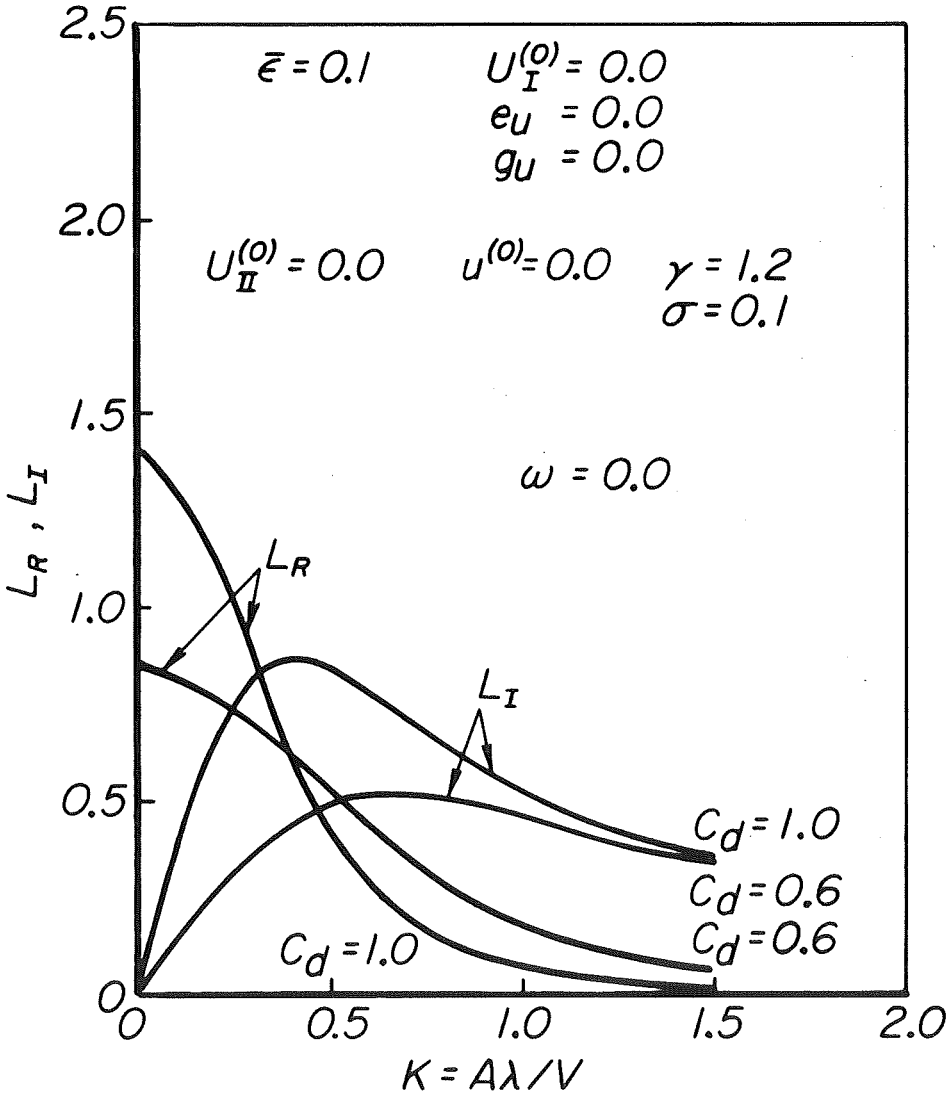

Figure 4 · Effect of discharge coefficient on liner behavior

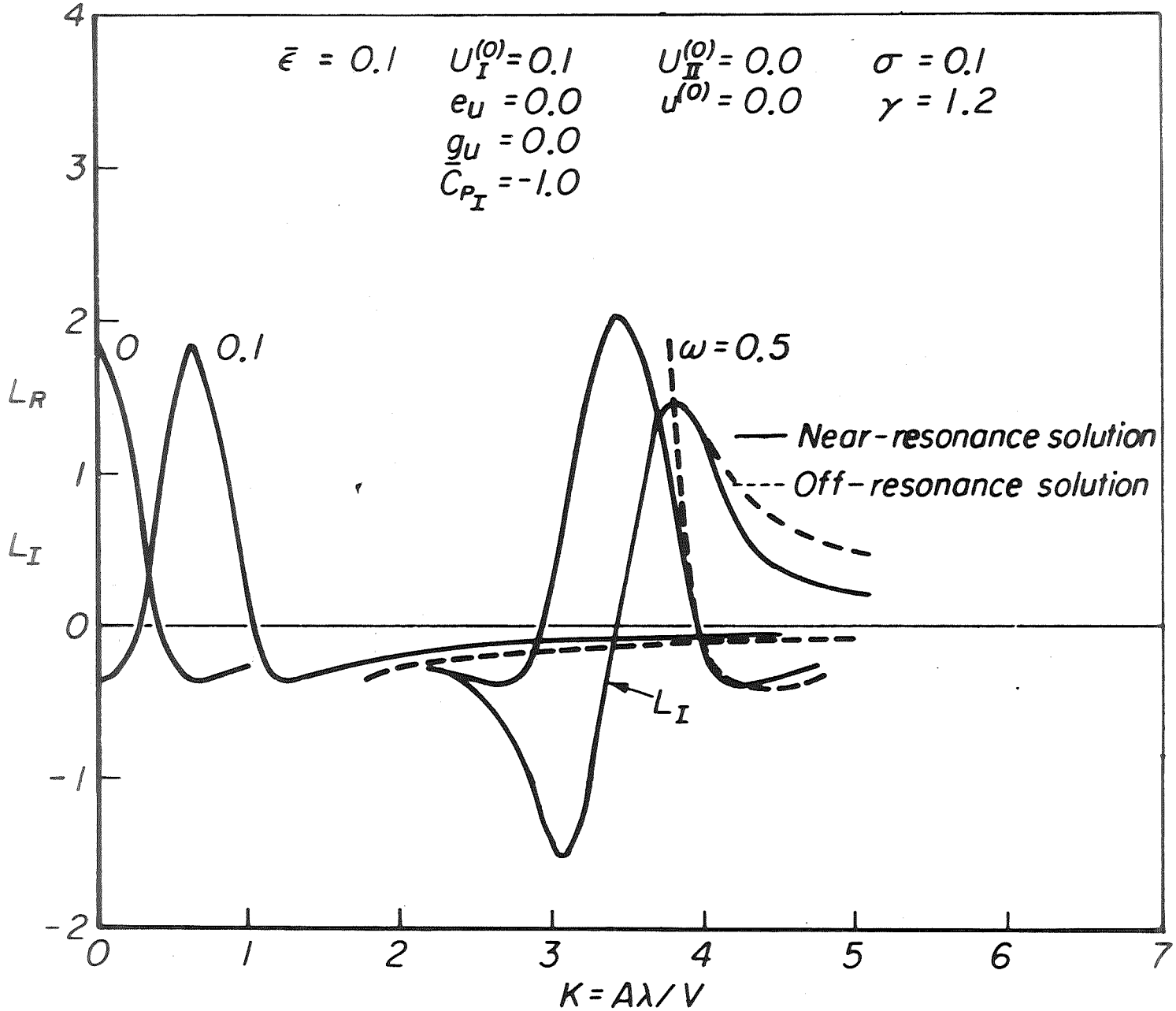

Figure 5a · External mean flow and smaller $[-C_{P_I}]$

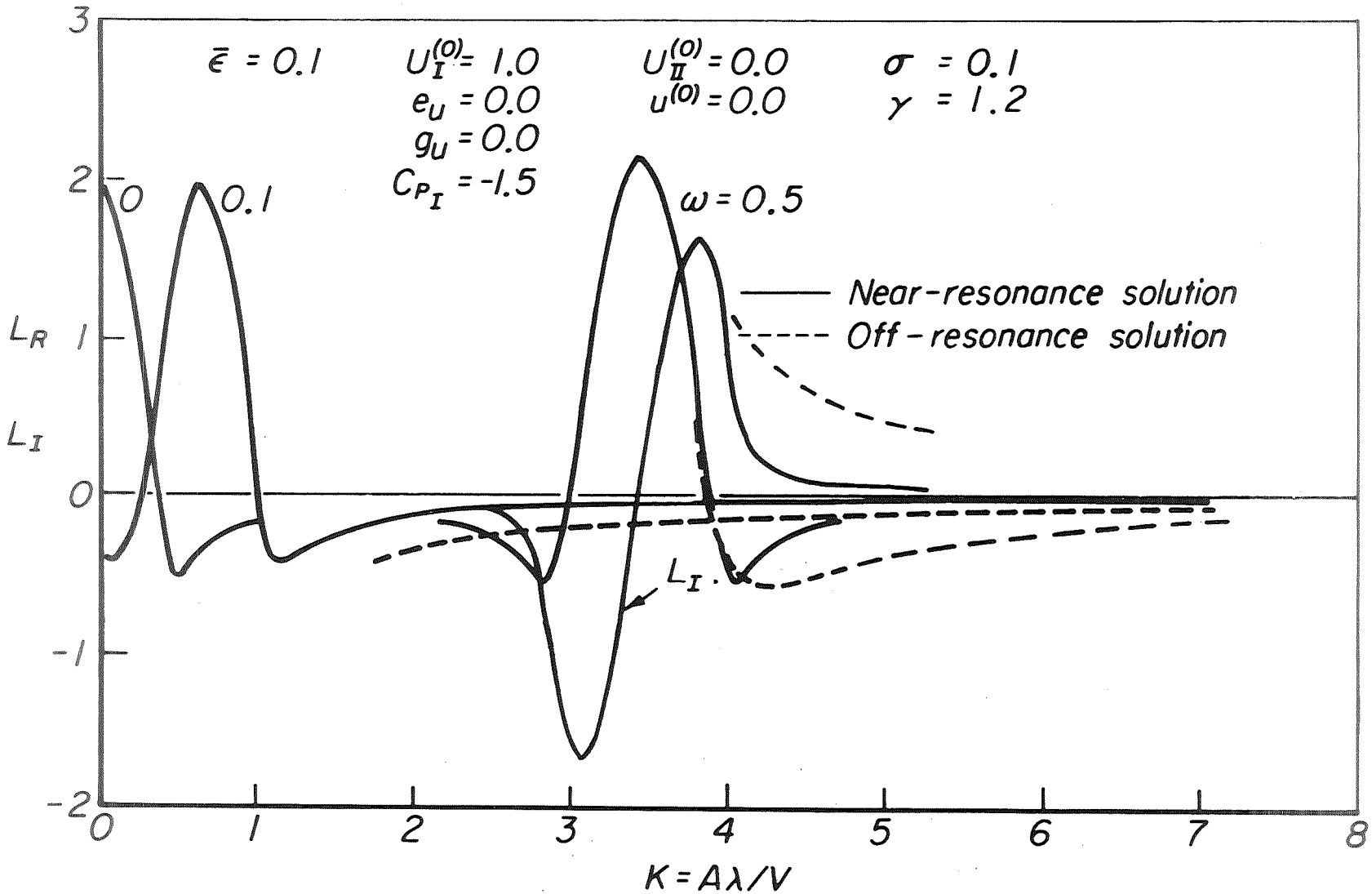

Figure 5b · External mean flow and larger $[-\bar{C}_{P_I}]$

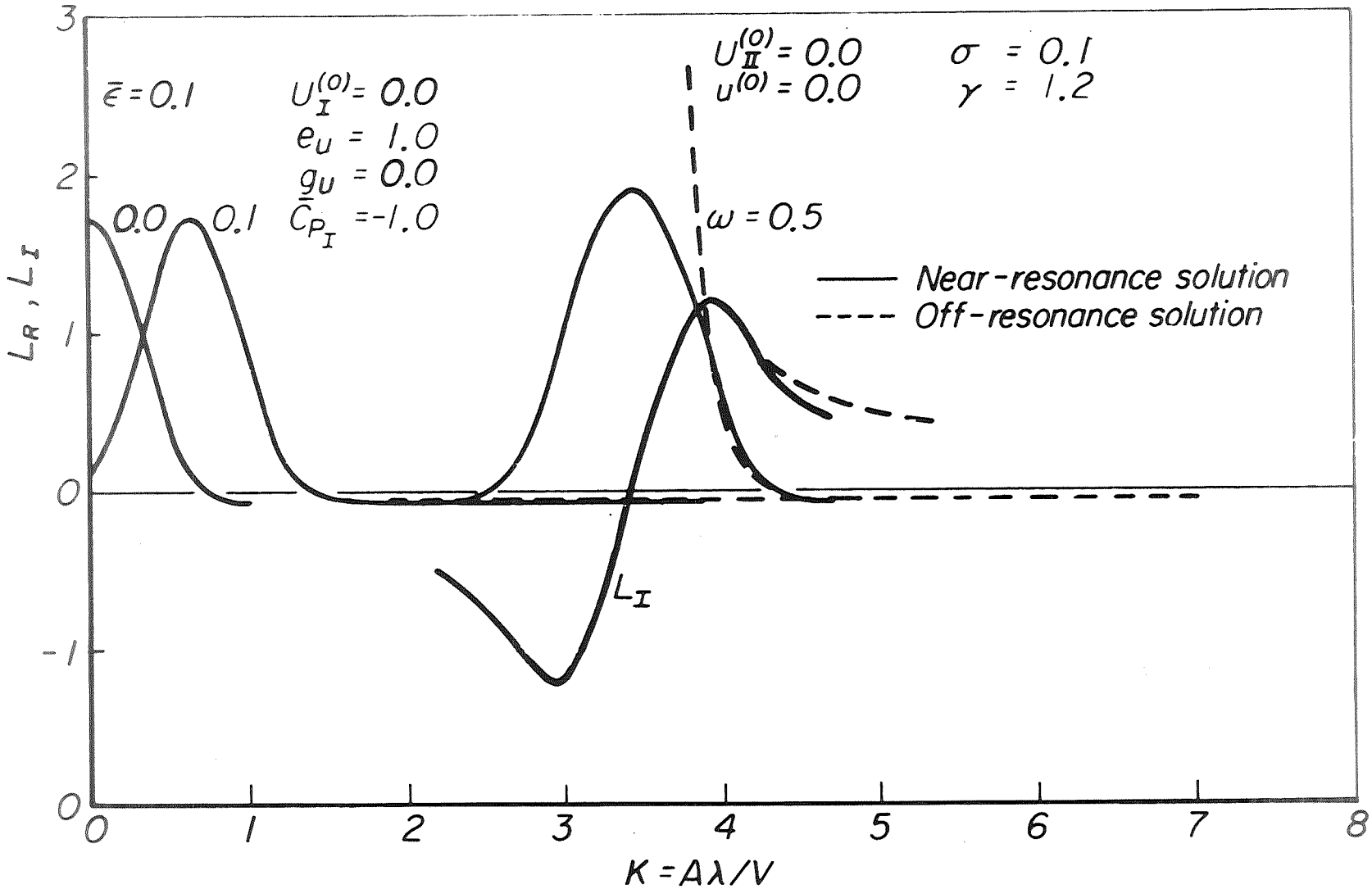

Figure 5c · External oscillatory flow in phase with the pressure

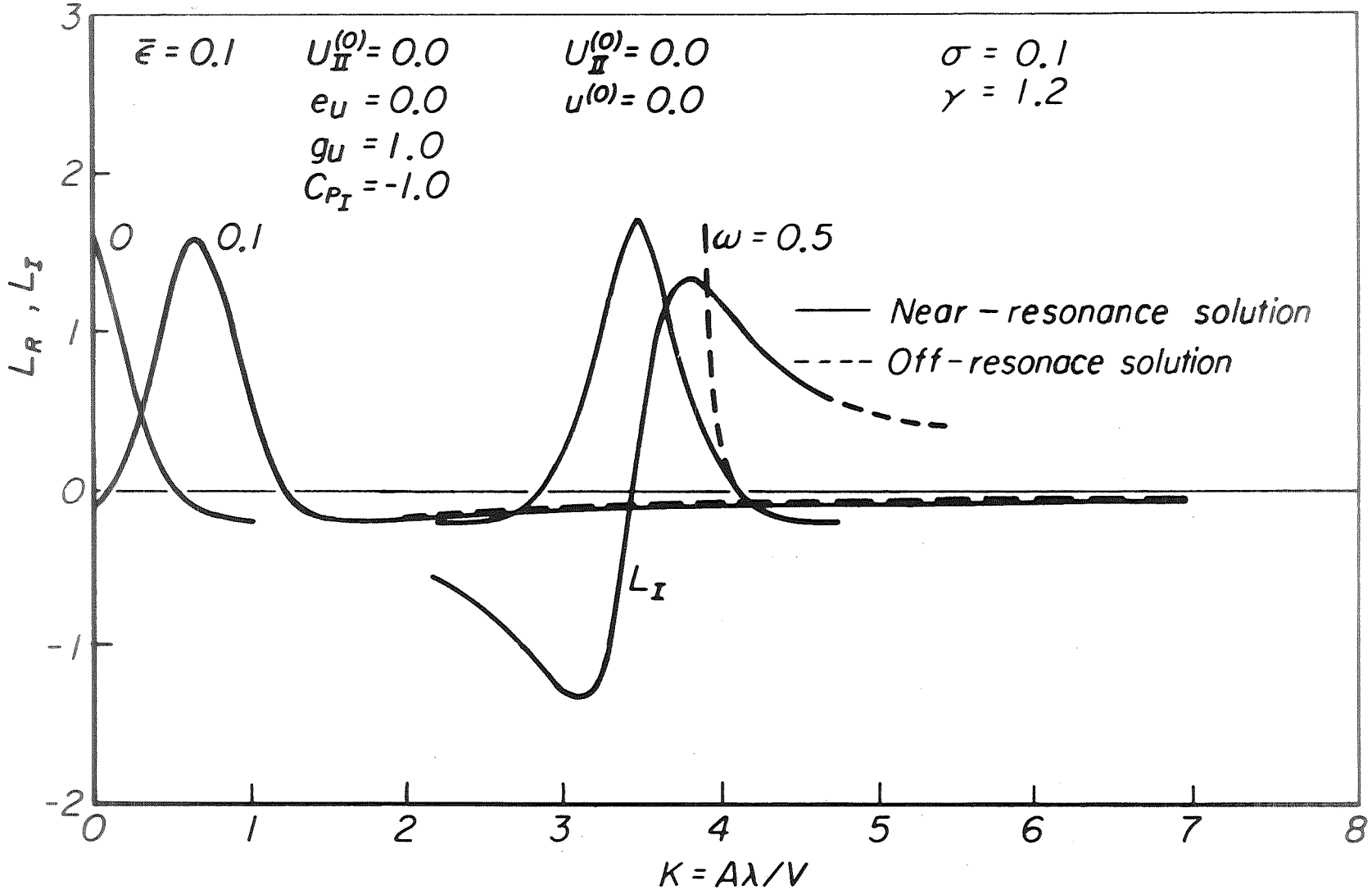

Figure 5d · External oscillatory flow 90° out of phase with the pressure

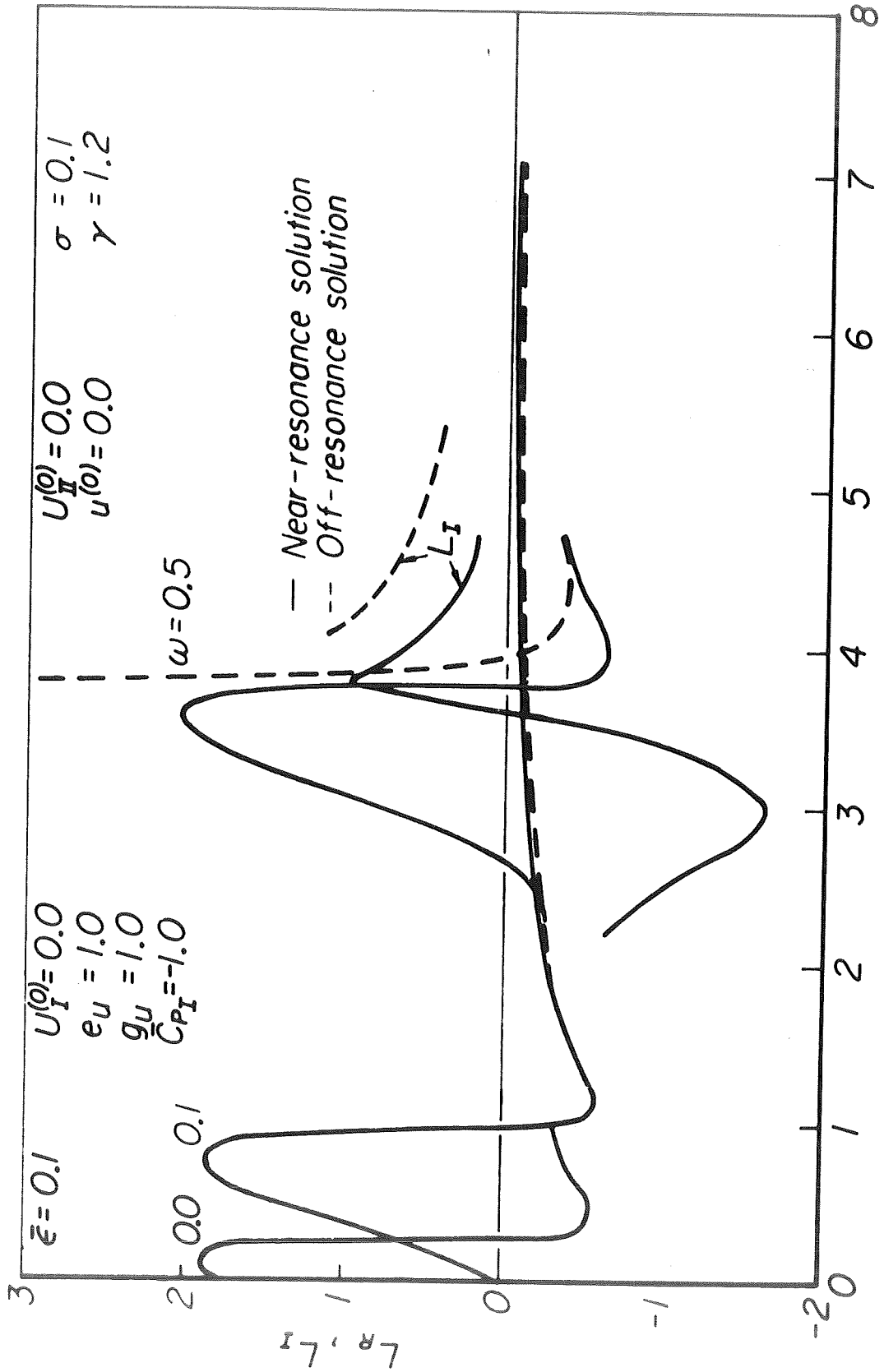

Figure 5e · External oscillatory flow 45° out of phase with the pressure

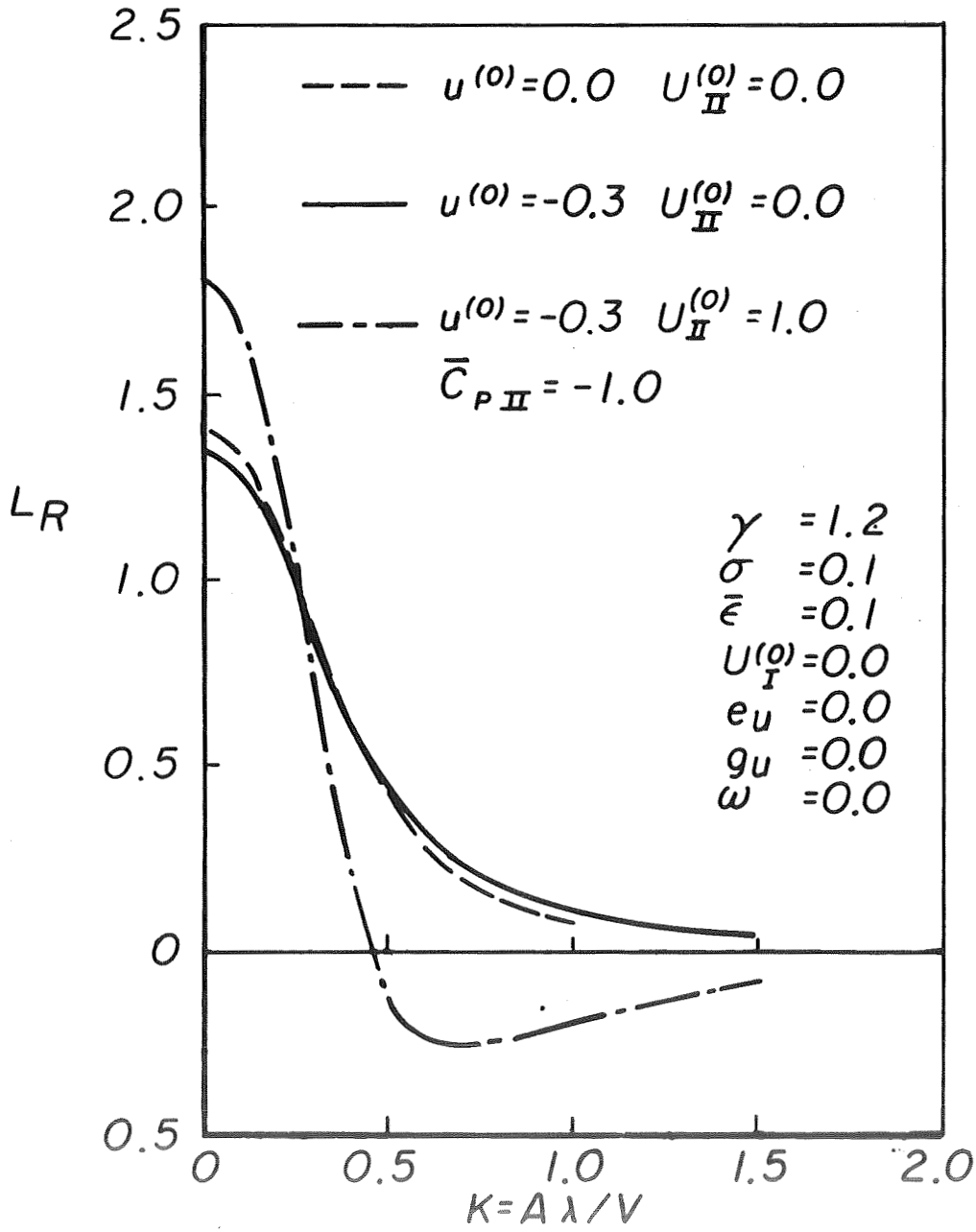

FIGURE 6a. Quasi-steady case, contact surface passes completely thru orifice in zero time

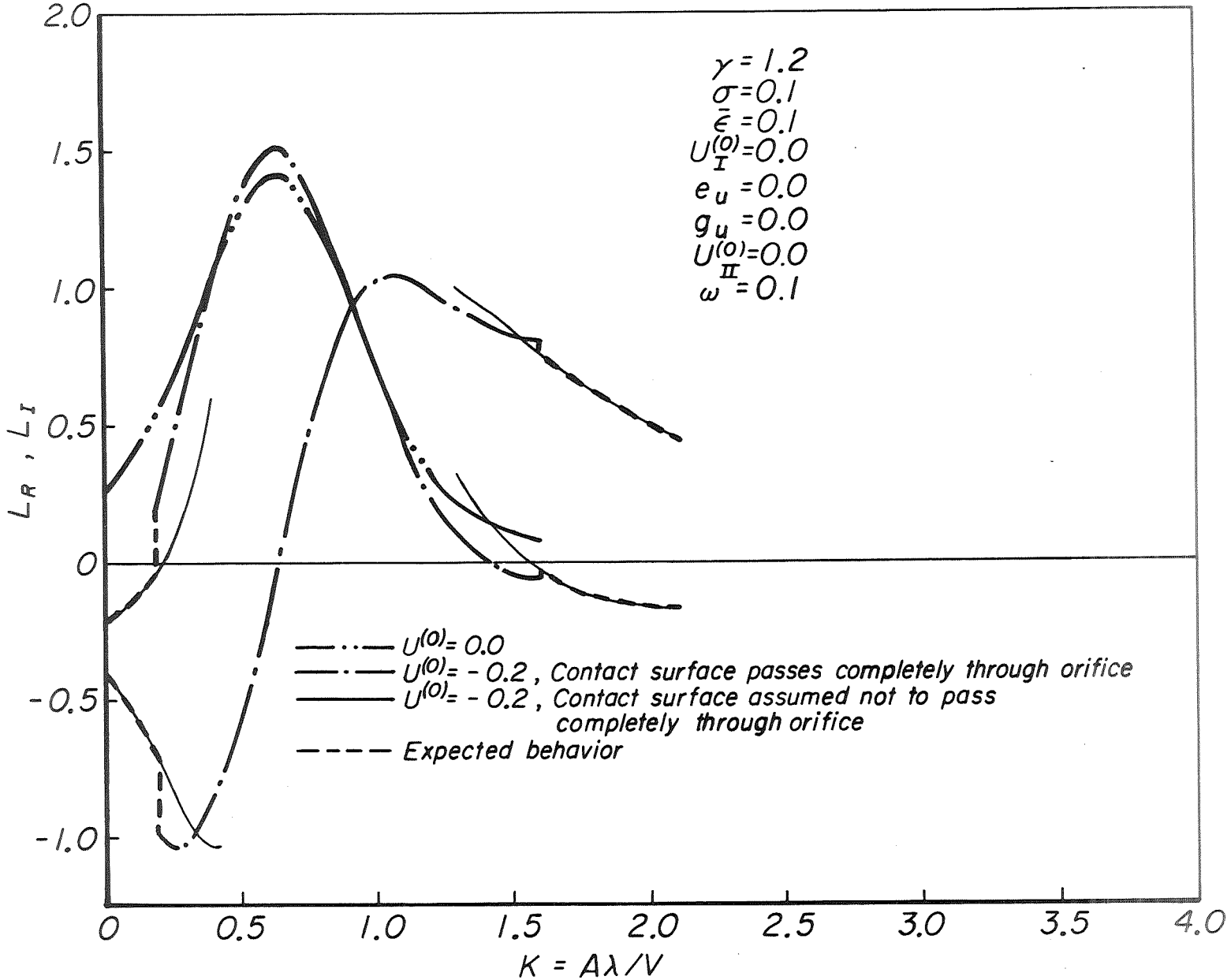

Figure 6b · Unsteady case with no cavity flow

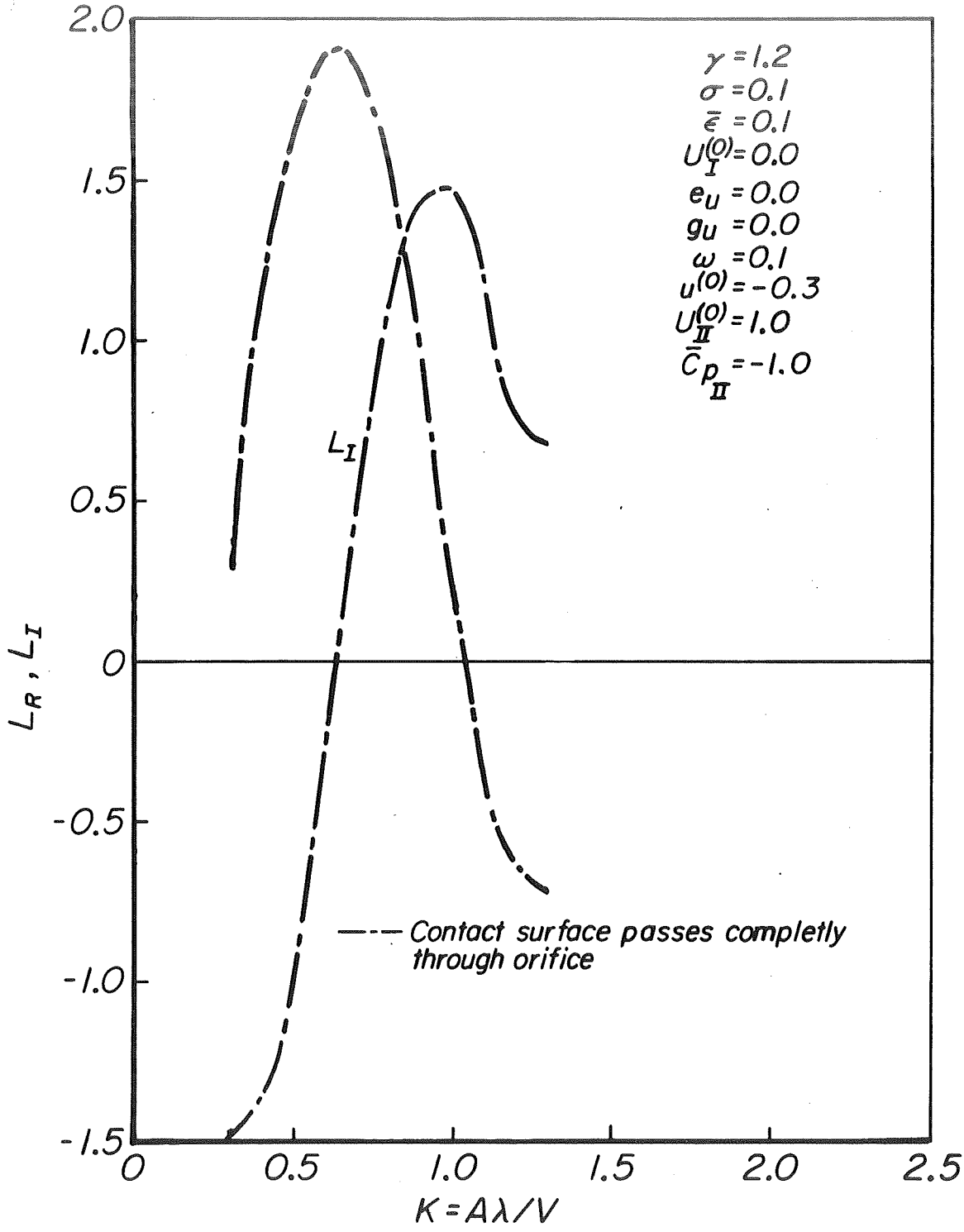

Figure 6c · Unsteady case with cavity flow

1970 DISTRIBUTION LIST

Dr. R. J. Priem MS 500-204
NASA Lewis Research Center
21000 Brookpark Road
Cleveland, Ohio 44135 (2)

Norman T. Musial
NASA Lewis Research Center
21000 Brookpark Road
Cleveland, Ohio 44135

Library
NASA Lewis Research Center
21000 Brookpark Road
Cleveland, Ohio 44135 (2)

Report Control Office
NASA Lewis Research Center
21000 Brookpark Road
Cleveland, Ohio 44135

NASA Representative
NASA Scientific and Technical Information Facility
P.O. Box 33
College Park, Maryland 20740 (6)

NASA
Universal North Building
Connecticut & Florida Avenues
Washington, D. C. (10)
Attn: Dr. T. L. Smull, Director
Grants & Space Contracts

V. Agosta
Brooklyn Polytechnic Institute
Long Island Graduate Center
Route 110
Farmingdale, New York 11735

B. P. Breen
Dynamic Science, a Division of Marshall Industries
1900 Walker Avenue
Monrovia, California 91016

Thomas J. Chew
AFRPL(RPPZ)
Edwards, California 93523

T. W. Christian
Chemical Propulsion Information Agency
8621 Georgia Avenue
Silver Spring, Maryland 20910

R. M. Clayton
Jet Propulsion Laboratory
California Institute of Technology
4800 Oak Grove Drive
Pasadena, California 91103

E. W. Conrad MS 500-204
NASA Lewis Research Center
21000 Brookpark Road
Cleveland, Ohio 44135

Dr. E. K. Dabora
University of Connecticut
Aerospace Department
Storrs, Connecticut 06268

O. W. Dykema
Aerospace Corporation
P.O. Box 95085
Los Angeles, California 90045

G. W. Elverum
TRW Systems
1 Space Park
Redondo Beach, California 90278

R. Edse
Ohio State University
Dept. of Aeronautical and Astronautical Engineering
Columbus, Ohio 43210

G. M. Faeth
The Pennsylvania State University
Mechanical Engineering Department
207 Mechanical Engineering Blvd.
University Park, Pa. 16802

G. D. Garrison
Pratt and Whitney Aircraft
Florida Research and Development Center
P.O. Box 2691
West Palm Beach, Florida 33402

M. Gerstein
Dept. Mech. Engr.
University of Southern
California
University Park
Los Angeles, California 90007

I. Glassman
Princeton University
Forrestal Campus
Princeton, New Jersey 08540

R. W. Haffner
Air Force Office of Scientific
Research
1400 Wilson Blvd.
Arlington, Virginia 22209

D. Harrje
Princeton University
Forrestal Campus
Princeton, New Jersey 08540

T. Inouye Code 4581
U. S. Naval Weapons Center
China Lake, California 93555

R. D. Jackel, 429
Office of Naval Research
Navy Department
Washington, D. C. 20360

R. B. Lawhead
Rocketdyne
A Division of North American
Aviation
6633 Canoga Avenue
Canoga Park, California 91304

R. S. Levine, Code RPL
NASA Headquarters
6th and Independence Ave., S.W.
Washington, D. C. 20546

Ted Male MS 500-209
NASA Lewis Research Center
21000 Brookpark Road
Cleveland, Ohio 44135

J. M. McBride
Aerojet-General Corporation
P.O. Box 15847
Sacramento, California 95809

P. D. McCormack
Dartmouth University
Hanover, New Hampshire 03755

C. E. Mitchell
Colorado State University
Fort Collins, Colorado 80521

P. S. Myers
University of Wisconsin
Mechanical Engineering Dept.
1513 University Avenue
Madison, Wisconsin 53705

J. A. Nestlerode
Rocketdyne
A Division of North American
Aviation
6633 Canoga Avenue
Canoga Park, California 91304

J. A. Nicholls
University of Michigan
Aerospace Engineering
Ann Arbor, Michigan 48104

J. C. O'Hara
Tulane University
Dept. of Mechanical Engr.
New Orleans, La. 70118

A. K. Oppenhiem
University of California
Dept. of Aeronautical Sciences
6161 Etcheverry Hall
Berkeley, California 94720

J. R. Osborn
Purdue University
School of Mechanical Engr.
Lafayette, Indiana 47907

Dr. K. Ragland
University of Wisconsin
Mechanical Engineering Dept.
Madison, Wisconsin 53705

Dr. A. A. Ranger
Purdue University
School of Aeronautics,
Astronautics and Eng. Sciences
Lafayette, Indiana 47907

F. H. Reardon
Sacramento State College
School of Engineering
6000 J. Street
Sacramento, California 95819

B. A. Reese
Purdue University
School of Mechanical Engr.
Lafayette, Indiana 47907

R. J. Richmond R-P and VE-PA
NASA George C. Marshall Space Flight Center
Huntsville, Alabama 35812

J. H. Rupe
Jet Propulsion Laboratory
California Institute of Tech.
4800 Oak Grove Drive
Pasadena, California 91103

Dr. R. F. Sawyer
University of California
Mechanical Engineering, Thermal Systems
Berkeley, California 94720

K. Scheller
ARL(ARC)
Wright-Patterson AFB
Dayton, Ohio 45433

Roger A. Strehlow
University of Illinois
Aeronautical Engineering Dept.
Urbana, Illinois 61801

J. G. Thibadaux
NASA Manned Spacecraft Center
Houston, Texas 77058

T. P. Torda
Illinois Institute of Tech.
Room 200 M.H.
3300 S. Federal Street
Chicago, Illinois 60616

T. Y. Toong
Massachusetts Institute of Technology
Department of Mechanical Engr.
Cambridge, Massachusetts 02139

R. R. Weiss
AFRPL
Edwards, California 93523

W. W. Wharton AMSMI-RKL
U. S. Army Missile Command
Redstone Arsenal, Alabama 35808

F. A. Williams
University of California
Aerospace Engineering Dept.
P.O. Box 109
LaJolla, California 92038

L. M. Wood
Bell Aerospace Company
P.O. Box 1
Mail Zone J-81
Buffalo, New York 14205

B. T. Zinn
Georgia Institute of Technology
Aerospace School
Atlanta, Georgia 30332

Library
Goddard Space Flight Center (NASA)
Greenbelt, Maryland 20771

Library
NASA John F. Kennedy Space Center
Cocoa Beach, Florida 32931

Library
NASA Langley Research Center
Langley Station
Hamption, Virginia 23365

Library
NASA Manned Spacecraft Center
Houston, Texas 77001

Library
NASA George C. Marshal Space Flight Center
Huntsville, Alabama 35812

Library
Jet Propulsion Laboratory
4800 Oak Grove Drive
Pasadena, California 91103

Library
NASA Flight Research Center
P.O. Box 273
Edwards, California 93523

Library
NASA Ames Research Center
Moffett Field, California 94035

TISIA
Defense Documentation Center
Cameron Station
Building 5
5010 Duke Street
Alexandria, Virginia 22314

Office of Asst. Dir. (Chem. Tech.)
Office of the Director of Defense Research & Engineering
Washington, D. C. 20301

D. E. Mock
Advanced Research Projects Agency
Washington, D. C. 20525

Dr. H. K. Doetsch
Arnold Engineering Development Center
Air Force Systems Command
Tullahoma, Tennessee 37389

Library
Air Force Rocket Propulsion Laboratory (RPR)
Edwards, California 93523

Library
Air Force Rocket Propulsion Laboratory (RPM)
Edwards, California 93523

Library
Bureau of Naval Weapons
Department of the Navy
Washington, D. C.

Library
Director (Code 6180)
U. S. Naval Research Laboratory
Washington, D. C. 20390

APRP (Library)
Air Force Aero-Propulsion Laboratory
Research & Technology Division
Air Force Systems Command
United States Air Force
Wright-Patterson AFB, Ohio 45433

Technical Information Department
Aeronutronic Division of Philco Ford Corp.
Ford Road
Newport Beach, California 92663

Library-Documents
Aerospace Corporation
2400 E. El Segundo Blvd.
Los Angeles, California 90045

Library
Bell Aerospace, Inc.
Box 1
Buffalo, New York 14205

Report Library, Room 6A
Battelle Memorial Institute
505 King Avenue
Columbus, Ohio 43201

D. Suichu
General Electric Company
Flight Propulsion Lab. Department
Cincinnati, Ohio 45215

Library
Ling-Temco-Vought Corp.
P.O. Box 5907
Dallas, Texas 75222

Marquardt Corporation
16555 Saticoy Street
Box 2013 - South Annex
Van Nuys, California 91409

P. F. Winternitz
New York University
University Heights
New York, New York

I. Forsten
Picatinny Arsenal
Dover, New Jersey 07801

R. Stiff
Propulsion Division
Aerojet-General Corporation
P.O. Box 15847
Sacramento, California 95803

Library, Department 596-306
Rocketdyne Division of Rockwell
North American Rockwell Inc.
6633 Canoga Avenue
Canoga Park, California 91304

Library
Stanford Research Institute
333 Ravenswood Avenue
Menlo Park, California 94025

Library
Susquehanna Corporation
Atlantic Research Division
Shirley Highway & Edsall Road
Alexandria, Virginia 22314

STL Tech. Lib. Doc. Acquisitions
TRW System Group
1 Space Park
Redondo Beach, California

Prof. W. A. Sirignano
Princeton University
Forrestal Campus
Princeton, New Jersey 08540

Dr. David Altman
United Aircraft Corporation
United Technology Center
P.O. Box 358
Sunnyvale, California 94088

Library
United Aircraft Corporation
Pratt & Whitney Division
Florida Research & Development Center
P.O. Box 2691
West Palm Beach, Florida 33402

J. B. Large
Institute of Sound and Vibration Research
University of South Hampton
England

A. P. Chervinsky
Dept. of Aeronautical Engineering
Technion Israel Institute of Technology
Haifa, Israel

Dr. W. E. Strahle
Aerospace School
Georgia Institute of Technology
Atlanta 13, Georgia

Prof. F. E. Culick
California Institute of Technology
204 Karman Laboratory
Pasadena, California 91109

Dr. A. E. Fuhs
Chief Scientist
Aero-Propulsion Laboratory (AFSC)
Wright-Patterson Air Force Base
Dayton, Ohio 45433